Copyright

by

Abdulaziz Salem Al-Qasim

2011

Simulation of Asphaltene Deposition During CO_2 Flooding

by

Abdulaziz Salem Al-Qasim

Thesis

Presented to the Faculty of the Graduate School of

The University of Texas at Austin

In Partial Fulfillment

Of the Requirements

For the Degree of

MASTER OF SCIENCE IN ENGINEERING

The University of Texas at Austin

August 2011

The Thesis Committee for Abdulaziz Salem Al-Qasim

Certifies that this is the approved version of the following thesis:

Simulation of Asphaltene Deposition During CO_2 Flooding

APPROVED BY

SUPERVISING COMMITTEE:

Supervisor: _____

Kamy Sepehrnoori

_____

M. Hosein Kalaei

Dedication

To my family

Acknowledgments

I would like to express my sincere gratitude to Allah for giving me strong faith and wonderful moments in my life. Everything I have achieved so far is a gift from Allah.

I would like to take this opportunity to thank my supervisor, Professor Kamy Sepehrnoori for his support, constructive ideas, and extensive discussions which were enlightening. I would also like to thank Dr. M. Hosein Kalaei for his ultimate support, guidance, and valuable advice. Enormous thanks to my wife's family and my family who prayed for me and took care of my two little daughters and provided all kinds of support to me. I am especially grateful to my wife, Arwa Al-Aqil. After the guidance from Allah, my wife was my main supporter. Without her, I would not have achieved this milestone.

I also want to thank my company, Saudi Aramco, for awarding me a scholarship for my Master's degree and continuous financial and logistical support which eliminated all the difficulties I faced. Last but not least, special appreciation to my Saudi counterparts for being such good friends for me during my stay in the U.S. I really enjoyed every moment. Much gratitude is extended to the people that I cannot mention individually, who helped this thesis be completed and delivered in a timely manner.

Abstract

Simulation of Asphaltene Deposition During CO_2 Flooding

by

Abdulaziz Salem Al-Qasim, M.S.E.

The University of Texas at Austin, 2011

Supervisor: Kamy Sepehrnoori

This Thesis presents the results of phase behavior calculations and simulation of asphaltene precipitation, flocculation, and deposition in five Middle-Eastern wells from different fields, based on a reliable experimental data provided for this purpose. The asphaltene precipitation, flocculation, and deposition have been simulated throughout the primary (pressure depletion), secondary (Waterflooding) and tertiary recovery (CO_2 injection) stages. Asphaltene precipitation becomes a serious problem especially when it causes plugging of the formation, wellbore, or production facilities, which will significantly affect the productivity and final recovery of the area. To help preventing asphaltene precipitation a bottomhole pressure higher than the asphaltene onset pressure (AOP) has been applied. Also, water and CO_2 injection has provided enough support for pressure maintenance, which helps in preventing asphaltene. Several scenarios were tested to investigate and identify the cases with lowest asphaltene precipitation and

higher recovery. It has been considered obligatory to have a representative numerical simulation model that can predict the phase behavior of asphaltene precipitation, flocculation, and deposition accurately.

The first part of this thesis includes a comprehensive literature review of asphaltene precipitation flocculation, and deposition that include asphaltene structure, models and prevention techniques. The second part of the thesis includes a detailed study of modeling asphaltene precipitation phase behavior utilizing experimental and real field data obtained from five Middle-Eastern wells from different fields. Experimental data include measurements of asphaltene onset pressure (AOP), saturation pressure, and PVT data. Asphaltene precipitation was modeled by using WinProp (a phase behavior utility from CMG) which uses Nghiem solid model. Saturation pressures, PVT, and AOP data were used to match Peng-Robinson EOS and the precipitation model was matched by the experimental data of AOP. The third part of the thesis includes a one-dimensional simulation comparison study of asphaltene precipitation between three different compositional simulators; UTCOMP, ECLIPSE and CMG/GEM. The last part of the thesis includes a full field scale study based on a heterogeneous three-dimensional cartesian single-well model. The objective of this study was to assess the effect of asphaltene precipitation, flocculation, and deposition in the well productivity and the economic impacts related to it. Different production practices were applied to define the most appropriate and efficient production strategy. This study includes a discussion and comparison of production rates with and without asphaltene precipitation, flocculation,

and deposition and a comparison of asphaltene precipitation, flocculation, and deposition at different times using different bottomhole and production rate constraints. Several cases (i.e., WAG cycles, completion, target layers of injection, etc.) will be tested to come up with the optimum completion and operating strategy in the presences asphaltene.

Despite the work devoted to understanding this subject, asphaltene still represents a challenging and unresolved problem. This thesis will help bridge the gap of this limited understanding in the field of asphaltene.

TABLE OF CONTENTS

LIST OF TABLES

LIST OF FIGURES

Chapter 1: INTRODUCTION

1.1 Research Objectives

This research has two main objectives. The first objective of this research is to investigate asphaltene-related problems in petroleum reservoirs using available precipitation, flocculation, and deposition models in three different compositional simulators (CMG/GEM, ECLIPSE and UTCOMP). This includes phase behavior calculations and simulation of asphaltene precipitation using experimental and field data obtained from five Middle-Eastern wells.

The second objective of this research is to review the effective mechanisms or production strategies to prevent asphaltene precipitation and deposition. The appropriate strategies to prevent asphaltene deposition require understanding and quantifying asphaltene precipitation and deposition in reservoirs and wellbores as well as modeling and studying field cases related to the implementation of flow assurance.

1.2 Review of Chapters

This thesis presents an overview of asphaltene properties, structure, and its impact on oil production operations. It also specifically, discusses different available modeling approaches used to analyze and predict asphaltene precipitation, flocculation, and deposition in oil reservoirs.

Chapter 2 reviews asphaltene in crude oil systems: asphaltene properties and their impact on oil production, including the effects of pressure, temperature, and composition. Asphaltene properties and problems are discussed utilizing Middle-Eastern oil reservoir data. This chapter also includes an important section on the different strategies to prevent/reduce asphaltene precipitation and deposition in the wellbore and its cumulative impact on oil production. The effect of carbon dioxide, which can both induce and prevent asphaltene precipitation, depending on the operating conditions, is investigated. Also, the chapter includes a section that highlights the differences between asphaltene and wax, and related compositions, to enhance our understanding of each component. This in turn leads to improved simulation results. The literature related to asphaltene phase behavior is reviewed and a description of modeling asphaltene deposition, precipitation, and flocculation is presented.

Chapter 3 presents a case study that describes a procedure for modeling the precipitation of asphaltene from an oil reservoir due to pressure depletion. The solid thermodynamic model was used in this case study to describe the precipitation behavior of asphaltene and petroleum reservoir fluid. This chapter includes a CO_2 flooding process in a synthetic reservoir using CMG/GEM, ECLIPSE, and UTCOMP simulators. The

implementation of the model in a simulation tool is described. Their results are compared and main differences between the three simulators are highlighted. The comparison with experimental data and field observations shows good agreement. Finally, we discuss the limitations of the model and discuss the differences between the experimental and field measurements that are needed to enhance the tool.

Chapter 4 presents a case study that includes a CO_2 flooding process in a real three-dimensional heterogeneous reservoir using CMG/GEM simulator. This study highlights the effect of asphaltene precipitation, flocculation, and deposition in the well productivity and the economic impact related to it. Different production practices were applied in this study to define the most appropriate and efficient production strategy

Chapter 4 presents summary, conclusions and suggestions for future work.

Chapter 2: LITERATURE REVIEW

2.1 Introduction

Serious operational problems caused by asphaltene deposition during oil production have driven the ongoing effort to understand this phenomenon. Many studies have focused on related asphaltene precipitation flocculation and deposition in oil reservoirs and flow assurance in the wellbores. Experimental techniques and theoretical models have been developed trying to understand and predict asphaltene behavior. Nevertheless, some ambiguities still remain with regard to the characterization of asphaltene in crude oil and its stability during the primary, secondary, and tertiary recovery stages within the near-wellbore regions. This chapter reviews the literature related to asphaltene precipitation, flocculation, and deposition. Field cases related to asphaltene precipitation are studied and discussed in the chapter. This chapter will also highlight the economic impact of asphaltene on production and maintenance cost.

2.2 Asphaltene

2.2.1 Definition of asphaltene

The classic definition of asphaltenes is based on the solution properties of petroleum residue in various solvents. The word asphaltene was coined by J.B. Boussingault to describe the constituents of bitumens (asphalts), he found in Eastern France and in Peru (Boussingault, 1837). He named the alcohol insoluble solid obtained from the distillation residue, as "asphaltene," since it resembled the original asphalt (Yen and Chilingarian, 1994)

Asphaltenes are impure hydrocarbons often referred to as nitrogen sulfur oxygen (NSO) compounds, because they contain nitrogen, sulfur, and oxygen hetero-atoms. Some of these hetero-atoms substitute for carbon in the aromatic rings. The NSO compounds have the highest molecular weights and are the heaviest components in crude oils (Hutton *et al*., 1994). The NSO compounds are defined also by the standard test method for n-heptane/n-pentane as the crude components that are insoluble in low molecular weight alkanes (*i.e.* n-heptane and n-pentane) and as the most polar fraction of crude oil. The molecular weight of asphaltene ranges between a thousand and several hundred thousands, due to this fact, their molecular weights are usually reported in terms of distribution curves (IPIMS, 2011).

2.2.2 Structure of asphaltene

Our knowledge of the asphaltene structure is very limited. Asphaltenes are composed of fused benzene-ring networks, but contain other atoms and are not true hydrocarbons (IPIMS, 2011). Asphaltenes are not crystallized and cannot be separated individual components or narrow fractions. Thus, the ultimate analysis is not very significant, particularly taking into consideration that the neutral resins are strongly adsorbed by asphaltenes and probably cannot be quantitatively separated from them. Also, not much is known of the chemical properties of asphaltenes. However, analytical chemists have made considerable efforts to characterize the asphaltenes in terms of chemical structure and elemental analysis as well as by carbonaceous sources. A number of investigators have proposed model structures for asphaltenes, resins, and other heavy fractions based on physical and chemical methods (Sanchez and Mansoori, 1998). **Figure 2.1** shows a general structure model of asphaltene.

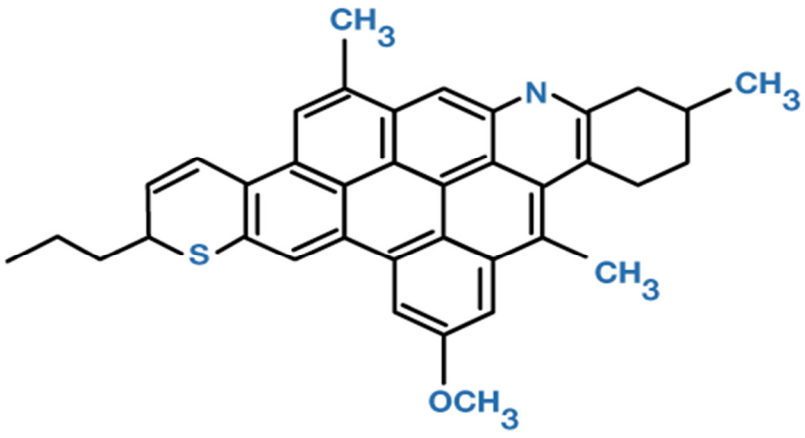

Figure 2.1: General Structure Model of Asphaltene (IPIMS, 2011)

The physical and chemical properties of asphaltenes are different from those of neutral resins. The reported molecular weight of asphaltene varies considerably depending on the method and conditions of measurement. A major concern in reporting asphaltene molecular weight is the association/aggregation of asphaltenes which can exist at the conditions of the method of measurement. Vapor pressure osmometry (VPO) has become the prevalent method for determining asphaltene molecular weights. However, the value of the molecular weight from VPO must be weighed carefully since the measured value of the molecular weight is a function of temperature and solvent molecular properties. Reported molecular weights from ultracentrifuge and electron microscope studies are high, in contrast to those from solution viscometry and cryoscopic methods, which are low (Sanchez and Mansoori, 1998). **Table 2.1** shows the elemental composition of asphaltene fractions precipitated by different solvents.

Table 2.1: Composition of Asphaltene Fractions Precipitated by Different Solvents According to Speight and Moschopedis (1981)

		Composition (*wt %*)					**Atomic Ratios**			
Source	**Precipitating Medium**	***C***	***H***	***N***	***O***	***S***	**H/C**	**N/C**	**O/C**	**S/C**
Canada	*n*-pentane	79.5	8	1.2	3.8	7.5	1.21	0.013	0.036	0.035
	n-heptane	78.4	7.6	1.4	4.6	8	1.16	0.015	0.044	0.038
Iran	*n*-pentane	83.8	7.5	1.4	2.3	5	1.07	0.014	0.021	0.022
	n-heptane	84.2	7	1.6	1.4	5.8	1.0	0.016	0.012	0.026
Iraq	*n*-pentane	81.7	7.9	0.8	1.1	8.5	1.16	0.008	0.01	0.039
	n-heptane	80.7	7.1	0.9	1.5	9.8	1.06	0.01	0.014	0.046
Kuwait	*n*-pentane	82.4	7.9	0.9	1.4	7.4	1.14	0.009	0.014	0.034
	n-heptane	82.0	7.3	1.0	1.9	7.8	1.07	0.01	0.017	0.036

2.3 Oil Characterization

Asphaltene content is an important factor in determining the properties of a crude oil. A convenient laboratory method called SARA has been developed to quantify the asphaltene fraction in this process. This technique separates dead oil (oil with no gaseous components) into saturates, aromatics, resins, and asphaltenes depending on their solubility and polarity. A schematic representation of this method is shown in **Figure 2.2**. The advantage of the SARA method is that it is a simple procedure that can be performed in many laboratories (ASTM, 1980). One type of SARA screening method is the colloidal instability index (*CII*). The *CII* is the ratio of the unfavorable components to the favorable components of the oil as shown in **Equation 2.4.1**.

$$CII = \frac{S + As}{R + Ar}, \qquad (\mathbf{2.4.1})$$

Where *S* is the percentage of saturates, *As* is the percentage of asphaltenes, *R* is the percentage of resins, and *Ar* is the percentage of aromatics in the oil. If the *CII* is greater than one, the amount of unfavorable components exceeds the amount of favorable components in the system. Consequently, the asphaltenes are likely to be unstable. However, the SARA analysis has several disadvantages that become apparent when it is used for purposes beyond its original intent. For example, dead oil lacks the gaseous components that are dissolved in live oils, and so the results are not representative of how the oil would act under reservoir conditions. In addition, laboratory methods may vary greatly, and the solubility of asphaltenes varies with the type of n-alkanes used to precipitate them. This means that single oil could have two or more SARA results

depending on the precipitant used. Because of its simplicity, SARA analysis has become a widespread means for comparing oils, but often, because variations in laboratory technique are not reported, comparisons between laboratories may not be valid. Nevertheless, the SARA method is a reasonable first step for categorizing dead crude oils, it provides sufficient characterization for both downstream refining needs and for upstream concerns, where live-oil properties are needed.

There are two other methods to characterize crude oil besides the SARA method. The first is aliphatic hydrocarbon titration using dead oil; in this method the asphaltene precipitation point is detected by the asphaltene precipitation detection unit (APDU). The second method is the depressurization of a live oil bottomhole sample; this method depends on monitoring the flocculation point due to light transmittance caused by the infrared laser (ASTM, 1980).

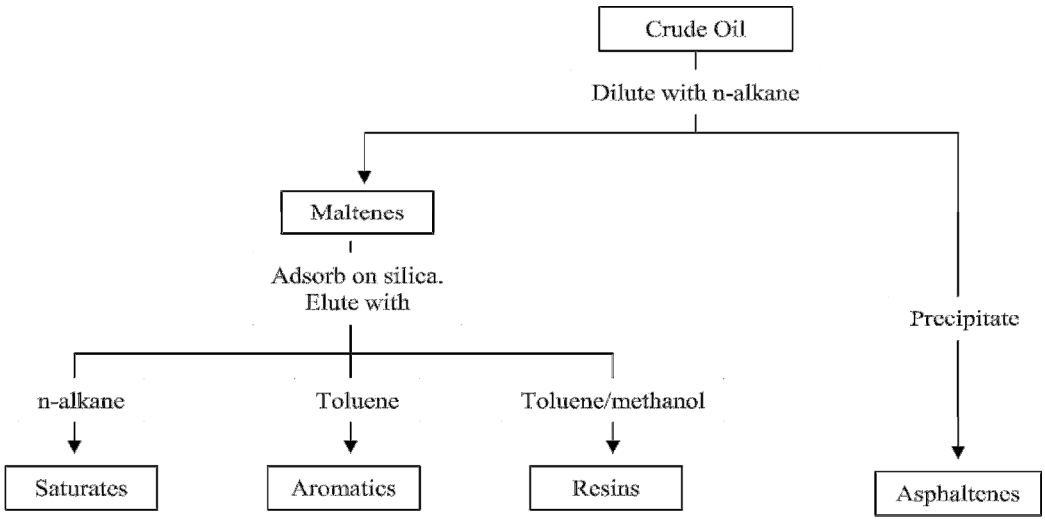

Figure 2.2: SARA Analysis (ASTM, 1980)

2.4 Asphaltene in Oil Reservoir

There are five main factors that govern the level of the asphaltene perception

- Pressure: (*i.e*., natural depletion)
- Temperatures
- Alternation of crude oil composition (*i.e*. CO_2 injection, solvent addition, etc.)
- Properties of asphaltene
- Electrical phenomena (*i.e*., streaming potential generation due to the flow of asphaltenes containing oil in conduits or porous media)

2.4.1 Precipitation, flocculation, and deposition

Before discussing main factors that affect the asphaltene perception, important terminology needs to be defined. Precipitation is the process that triggers the appearance of asphaltene particles. However, when those precipitated particles aggregate, they form bigger particles called 'flocs' and that process is called flocculation. Deposition is the process of exchanging flocs between the solution phase (*i.e*., oil) and the rock surface (ECLIPSE Manual, 2010). **Figure 2.3** shows a clear distinction between the deposition and flocculation process.

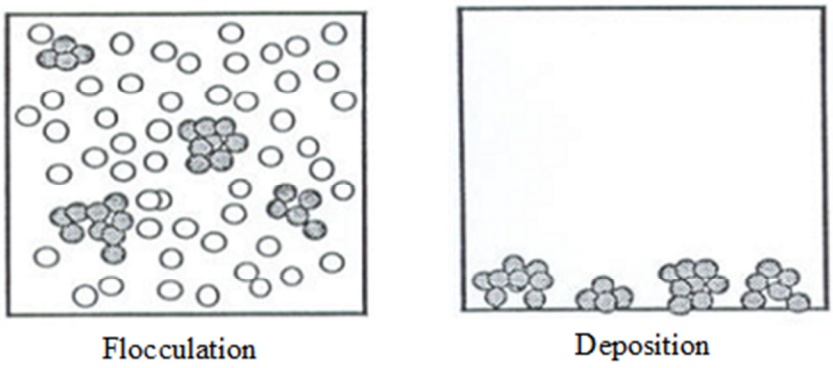

Figure 2.3: Depiction of flocculation and deposition**,** University of Florida

2.4.2 Onset pressure

Another important term is the flocculation onset pressure, which is defined as the pressure at which the oil fraction reaches a threshold limit that initiates the asphaltene flocculation and precipitation. For example, when the CO_2 concentration is high enough, asphaltene dissolved in oil begins to flocculate; the reason for this is attributed to the injected CO_2 that dissolves into smaller adjacent droplets of oil, and then swell, extracting light hydrocarbons from the oil and inducing flocculation (Hamouda *et al*., 2010). Also, the onset of asphaltene flocculation is defined as the least amount of flocculants in which aggregated asphaltene particles appear (Wang *et al*., 2004).

2.4.3 Effect of pressure on asphaltene precipitation

Asphaltene consists of molecules with a wide range of densities. It is suggested that high-density molecules will precipitate after the onset pressure, and then the molecules with intermediate densities precipitate at lower pressures (Afshari *et al.*, 2010). Asphaltene precipitation has implications on production in terms of reservoir natural depletion. Generally, solubility and density parameters trends are proportional to the pressure depletion until the pressure reaches the bubble point (Leontaritis and Mansoori, 1987). Below the bubble point pressure (Pb), the solubility and density of asphaltene precipitation are inversely proportional to the pressure trend. **Figure 2.4** shows an approximate depiction of density and solubility behavior with pressure depletion (assuming constant temperature).

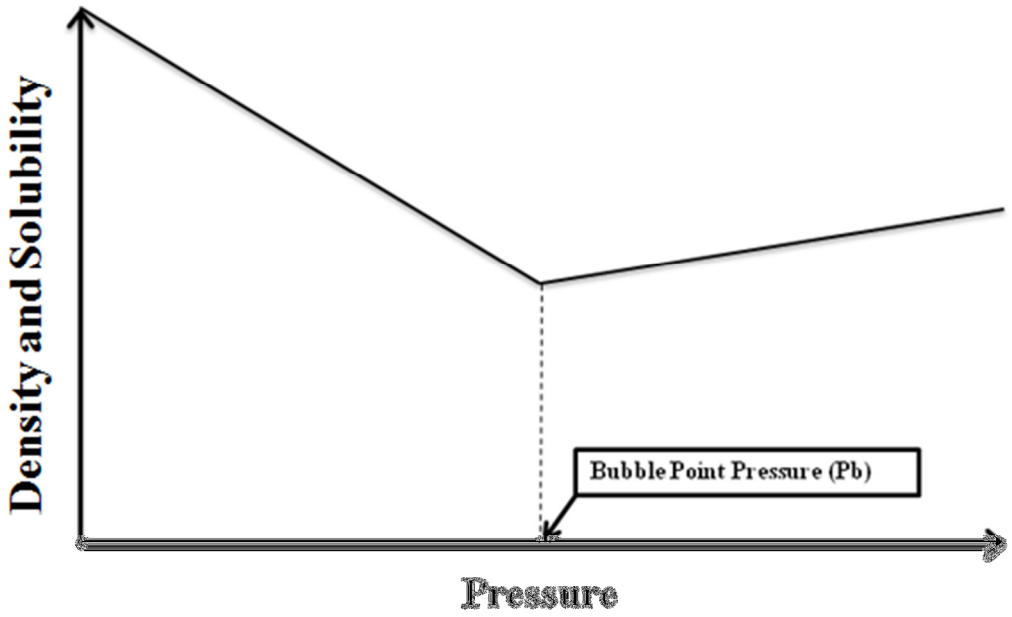

Figure 2.4: Depiction of Density and Solubility Behavior With Pressure Depletion

The density and solubility increase below the bubble point due to the liberation of the lighter hydrocarbons and gases from a crude oil, which in turn increases the asphaltene solubility. Furthermore, the crude will be much denser due to this gas liberation. The amount of asphaltene precipitating will be opposite to the behavior of density and solubility as a function of pressure. Also, an increase in the amount of dissolved gas in live oil is associated with the lower solubility of asphaltene in that oil (Kennicutt *et al*., 1989). **Figure 2.5** shows an approximate depiction of the amount of asphaltene as a function of pressure depletion (assuming constant temperature). The loss of light hydrocarbon components constituting a crude oil reduces the amount of solid deposits that can be held in a solution, which reduces the dissolving power of the crude.

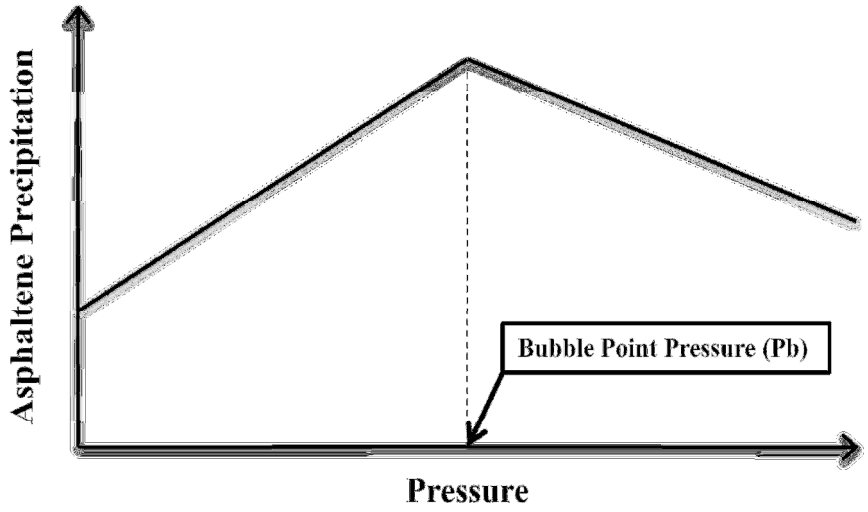

Figure 2.5: Depiction of the Amount of Asphaltene as a Function of Pressure Depletion

From **Figure 2.4** and **Figure 2.5**, we can conclude that the maximum asphaltene precipitation is expected to occur at or close to the bubble point pressure (Pb). Since pressure decreases below the bubble point, the light components separate from oil and move into the gas phase. Therefore, asphaltene solubility increases and some precipitated asphaltene dissolve back into the oil solution. As pressure decreases, above the bubble point, the asphaltene content of the crude oil decreases and the minimum content of asphaltene occurs near the saturation pressure (Pb) as shown in **Figure 2.5**. Actual field experience indicates less asphaltene precipitation problem, when the pressure is below the bubble point, than when the pressure is at the bubble point (Leontaritis and Mansoori, 1987). Many field tests (*i.e*., Hassi-Messaoud field in Algeria and Mata Acema field in Venezuela) show that the heavier crudes (containing a higher amount of asphaltene) have much less precipitation problems compared to the highly under-saturated light crudes (contain small asphaltene content). Formation sand and silt help expedite the formation of deposits when the temperature drops where the dissolving power in the heavier crude is much greater than that the of lighter crude (Kennicutt *et al*., 1989).

2.4.4 Effect of temperature on asphaltene precipitation

During primary oil recovery, the reservoir temperature change is usually negligible; however, the change will be noticeable during secondary and tertiary recovery. According to the literature, there is no clear trend for temperature effect on asphaltene due to the variation of the crude composition. Some researchers (*i.e.,* Leontaritis, 1996) suggested that the asphaltene solubility increases linearly with

temperature until the reservoir temperature, after that, asphaltene solubility will decreases linearly as the temperature increases shown in **Figure 2.6**. Nghiem *et al.* (2000) claimed that a reduction in precipitation could be expected when temperature increases, whereas Burke *et al.* (1990) claimed the opposite. Generally, temperature dependence cannot be easily guessed based on the discrepancy in the temperature dependence results between the researchers. This indicates that more collaborative work is needed to analyze the temperature dependence.

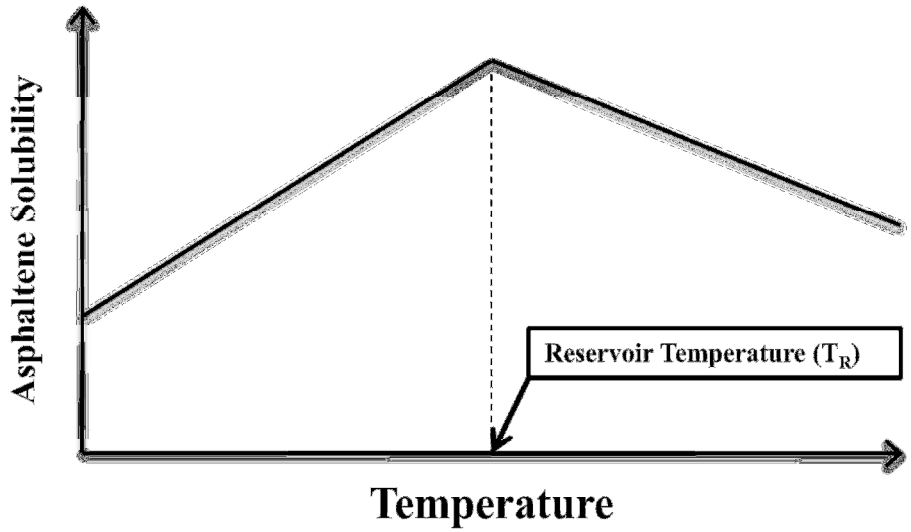

Figure 2.6: Depiction of Asphaltene Solubility as a Function of Temperature (Leontaritis, 1996)

Experimental observations showed that the temperature has the same effect on the recovery of asphaltenic and non-asphaltenic oils; however, the experimental studies showed that higher oil recovery will be anticipated from non-asphaltenic oil compared to asphaltenic oil at the same temperature (Hamouda *et al.*, 2010)

2.4.5 Alternation of crude oil composition

One common problem during gas drives or CO_2 injection is asphaltene instability, which induce precipitation and may cause pore-throat-plugging or wettability reversal (Leontaritis, 1987). Asphaltenes become unstable as the volume fraction of aliphatic components increases. It was experimentally proven that, if a crude oil has a flocculation point, then the region of asphaltene instability would be located between the flocculation point and just below the bubble point (Ellison and Gallagher, 2000). **Figure 2.7** explains this in detail. Also, experiments show that denser asphaltenes have a higher tendency to precipitate initially than less denser asphaltenes (Leontaritis, 1996).

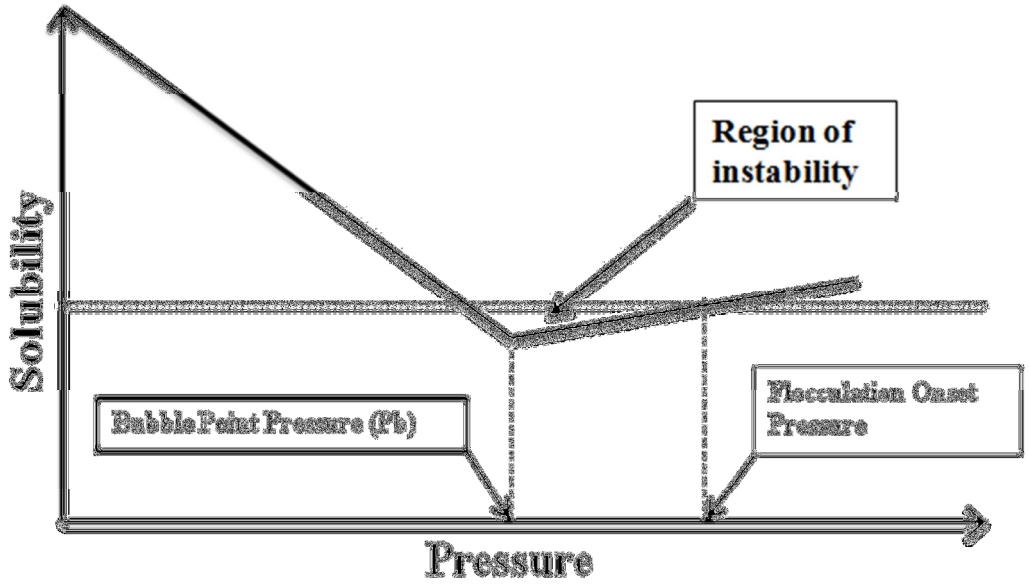

Figure 2.7: Region of Instability Depiction Based on Ellison and Gallagher (2000)

CO_2 injection is one of the main factors that induce asphaltene precipitation and instability. The degree of swelling is dependent on the pressure, temperature, and oil composition. CO_2 can improve oil production by reducing the interfacial tension or

Increasing mobility ($\lambda = k/\mu$), *i.e.*, reducing viscosity. Asphaltene precipitation is initiated by CO_2 when the critical content of CO_2 is exceeded. The critical content point of CO_2 is dependent on a reservoir oil composition, temperature, and pressure and must be evaluated at an early stage of EOR screening (i.e. pilot design) for EOR (IPIMS, 2011).

EOR screening consists mainly of:

- Evaluating available information about the reservoir, oil, rock, water, geology and previous performance.
- Supplementing available information with certain brief laboratory screening tests.
- Selecting those processes that are potentially applicable and eliminating those that definitely are not.

These are the first steps in an enhanced recovery implementation sequence. Subsequent steps would include further evaluation of candidate processes (if more than one satisfies the screening criteria), pilot test design, pilot test implementation, pilot test evaluation, scale-up forecasting, and finally, commercial venture. Laboratory test results, together with the reservoir engineering analysis, form the basis for estimating the enhanced recovery potential of a candidate reservoir.

2.4.6 Electrical phenomena

Asphaltenes exist in crude oil either in the molecular form or in the form of an association of a relatively small number of molecules (Prechshot *et al*., 1943). Several ultracentrifuge experiments were performed to investigate the molecular weight; the

results showed that asphaltene exists in crude oil as particles with a diameter of 30 to 65 ^{o}A (Ray *et al*., 1957). Asphaltene electrical effects were tested by using a crude oil. It was concluded that crude oil containing asphaltene has an electrical effect and the streaming potential caused by the flowing crude oil may cause asphaltene to precipitate (Dykstra and Katz, 1944). Several tests were conducted to examine the reversibility process of asphaltene precipitation and the results showed that it is a reversible process (De Pedroza *et al*., 1996).

2.5 Differences Between Wax an Asphaltene

There has been some confusion between the definition of asphaltene and other terms such as asphalt, resin, and wax in the literature. Therefore, it is important to give a basic definition for each term and highlight the most important distinguishing parameters between them.

2.5.1 Asphalt

Asphalt is a mixture of high molecular weight complex compounds that flocculates out of oil and contains asphaltene particles surrounded by resins, oil, and other liquid entities in the crude oil trapped in the flocculated mass (IPIMS, 2011). Asphalt, is used generally to designate the combination of asphaltene and resins. It is a term used commonly for refinery products, called ″petroleum asphalt″ and ″refinery asphalt″ (Yen and Chilingarian, 1994).

Based on the results from studies of asphalts and related bituminous substances, a classification scheme was developed as presented in **Figure 2.8** (Abraham, 1960), and modified later by Pfeiffer (1950). The study suggested that asphalt can be classified into artificial asphalts and natural asphalts. Artificial asphalts are man-made or synthetic and include basically petroleum-derived asphalts and, to a lesser extent, coal tar, water-gas tars and other substances. Natural asphalts include bituminous materials laid down in natural deposits, such as those in Trinidad and the Bermudez lakes, and also those in natural bitumens (Chilingarian *et all.,* 1978).

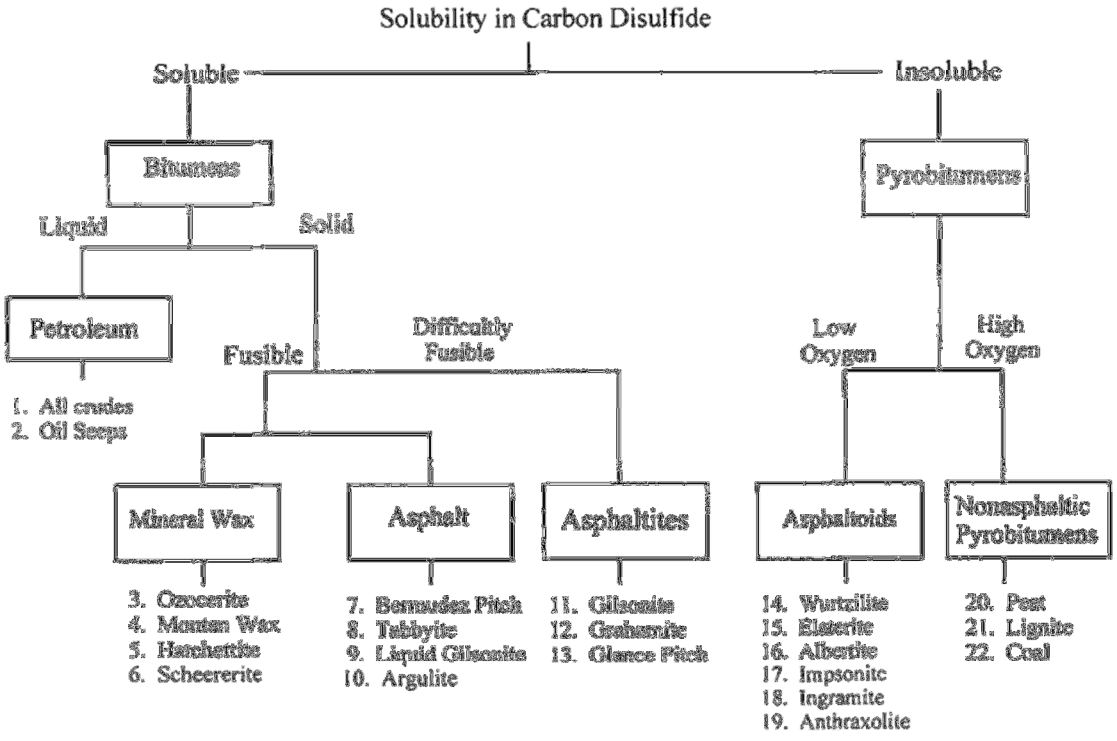

Figure 2.8: Designation and Classification of Natural Asphalt According to Abraham (1960)

Asphalt is classified into three fractions according to Marcusson *et al*., (1931):

- Neutral resins: insoluble in Alkalies and acids and completely miscible with crude oil.
- Asphaltenes: insoluble in light gasoline and petroleum ether.
- Carboids (free carbons): found at high temperatures, completely insoluble in benzene.

Note that both asphaltene and neutral resins are completely soluble in benzene, chloroform, and carbon disulfide.

2.5.2 Resins

On the other hand, resins are polycyclic molecules that exist in the oil in true solution and tend to adsorb easily in common adsorbents (*i.e.* clay and silica gel) and have a molecular weight ranging between 250 to 1000 (Hutton *et al.*, 1994). Other references reported that the molecular weights of resins range from 1100 to 2800 (Speight and Moschopedis, 1981). The resin fractions constitute the main non-hydrocarbon part of residues with high contents of heteroatoms (Yen and Chilingarian, 1994). Under normal conditions, asphaltenes are held in suspension by resins. Changes in the crude composition or pressure and temperature can alter their association with the resins (ASTM, 1980). Resins play an important role in stabilizing and peptizing of asphaltene molecules and help reducing the flocculation and precipitation of the molecules out of the solution. Knowledge of the properties and behavior of the resins could be useful in remedial actions when there is a need for additives or acid treatment.

2.5.3 Wax

Wax, sometimes called ″Paraffin,″ is defined as saturated hydrocarbons with between 18 and 34 carbon atoms in a chain of complex mixtures of high molecular weight alkanes ranging between 360 and 500. Waxes are organic deposits caused by changing wellbore conditions that upset the chemical equilibrium so that various materials in the crude oil precipitate out of the solution. It is of a crystalline structure and can be soft with a high proportion of trapped oil such as vaseline, or can form hard deposits such as candle wax. Paraffins usually exist in waxy crudes and create production problems and formation damage. To eliminate these problems, the deposited paraffin must be removed (Keating and Wattenbarger, 1994). Crude wax or paraffin deposits consist of tiny crystals that tend to agglomerate and form granular wax particles about the size of table salt grains. Deposited paraffin may also contain crude oil, sand, silt, corrosion products, scale, and often water (IPIMS, 2011). ASTM or API methods can be used for conventional wax determination in crude oils. Both methods involve cooling the oil to a specific temperature, precipitating the waxes, collecting, and weighing them. This normally results in compounds containing an average of 22 or more carbon atoms being precipitated.

Often iron sulfide and heavy wax are misidentified as asphaltenes, where asphaltenes are often found mixed with wax or oil. One way to differentiate between them is by a melting test and a weak acid solubility test. Asphaltene solubility can be determined by conducting a series of titration experiments on tank oil (Speight and Moschopedis, 1981). To understand the behavior of waxy crude, we need to know the cloud point,

pour point, wax content, and yield stress of the particular crude. When the temperature drops too low for wax to remain dissolved in the crude, it precipitates out of the solution and deposits itself on pipeline walls, or inside facilities. The temperature at which the wax crystals can first be detected is called the cloud point. The cloud point is also sometimes referred to as the wax appearance temperature (WAT). When the operating temperature in a pipeline system drops below the cloud point, wax crystals will begin to form and deposit. As the temperature drops further, more wax will come out of the solution until the crude in the pipeline effectively gels up. The temperature at which this occurs is the pour point. When the crude in the pipeline gels up, a certain force, yield stress, is required to shear the waxy crude and restart the flow. Crude is generally considered to have a high wax content when there is more than about 10% wax, and a low wax content when there is less than about 4%. Some examples of low wax content crude are shown in **Table 2.2**.

Table 2.2: Low Wax Content Crude Oils According to IPIMS (2011)

LOW WAX CONTENT CRUDE OILS			
NAME	**DENSITY kg/m^3**	**WAX CONTENT (SHELL) % WT.**	**POUR POINT (ASTM D97) ^{o}C**
Arabian Light	854	4	-36
Kuwait	870	4	-21
Basrah	855	4	-12
Forties	839	4	0
Labuan	863	4	9

Although the wax content of all these crude is 4%, there are considerable differences in the pour point. As shown in **Table 2.2**, we notice that the Malaysian Labuan crude would gel up at 90 ^{o}C, whereas the Saudi Arabian Light crude would gel only if the

temperature drops below -36 ^{o}C. **Table 2.3** summarizes the behavior of waxy crude that have relatively high pour points.

Table 2.3: High Wax Content Crude Oils According to IPIMS, 2011

HIGH WAX CONTENT CRUDE OILS			
NAME	**DENSITY kg/m^3**	**WAX CONTENT % WT.**	**POUR POINT (ASTM D97) ^{o}C**
Cabinda	868	10	21
Gamba	868	12	33
Shengli	908	12	27
Sarir	847	16	24
Beatrice	832	16	27
Bombay High	832	16	33
Taching	864	20	33

Wax formation in crude oil flowing in pipelines (**Figure 2.9**) can be predicted by sampling and analyzing the crude based on the following four properties:

- Cloud point: measured using the cold finger technique or cross polar microscopy
- Pour point: measured using differential scanning calorimetry (DSC)
- Wax content: measured using solid phase analysis
- Carbon distribution: measured using high temperature gas chromatography (HTGC)

It is important to use a representative sample of the crude for testing and to follow the correct experimental procedures in order to achieve the most accurate results. These results may be used as the base input parameters for a simulation model. Waxy crude with high cloud points and pour points will need a special design to take into account the operational challenges.

Figure 2.9: Severity of Wax Deposition (http://omrpublic.iea.org)

Designers and operators of the pipeline need to thoroughly evaluate the above factors when waxy crude is found in their system. When deciding how to manage the production and transportation of waxy crude, it is important to consider both capital and operating cost over the whole life cycle of the field for different options.

A development plan for managing a waxy crude field will be different and probably more costly than a non-waxy crude field. Hence, early prediction in terms of compositional simulators, especially for wellbore vicinity is very important. There are several models being developed that take into account wax deposition in the wellbore. Waxy crude production can be handled using the following options (IPIMS, 2011):

- Using wax inhibitors, growth modifier, or dispersants
- Using a pour point reducer
- Using dilution, in order to minimize wax content

- Using sophisticated pipeline insulation techniques
- Using heating systems or steam tracing for the pipeline

2.6 Asphaltene Properties

Production and processing operations of crude oil require a thorough understanding of phase behavior. Pressure-volume-temperature (PVT) properties play a crucial role throughout the life of the reservoir. Reservoir fluid properties provide the main input for any simulator used to predict asphaltene precipitation or describing the fluid properties as a function of pressure, temperature, and composition. Consequently, accurate PVT properties are required to get appropriate and representative simulation results.

As mentioned earlier in Section 2.4, the main factors affecting asphaltene precipitation are pressure, temperature, and composition. However, a good understanding of properties' behavior is needed. These properties are density, solubility, viscosity and molecular weight, which can be directly affected by any changes in pressure, temperature, or composition. For that purpose those four factors will be highlighted in detail in the following sections.

2.6.1 Density

Density is a physical property strongly related to the molecular topological characteristics and also to the molecular size of the molecules (Satou *et al*., 2000). Density can be easily determined in a lab and it is often used to calculate other thermo-physical properties. It is suggested that at a constant temperature, the density parameters trend is proportional to the pressure depletion until the pressure reaches the bubble point (Leontaritis and Mansoori, 1987). Below the bubble point pressure (Pb), the density is inversely proportional to the pressure trend as shown in **Figure 2.10**.

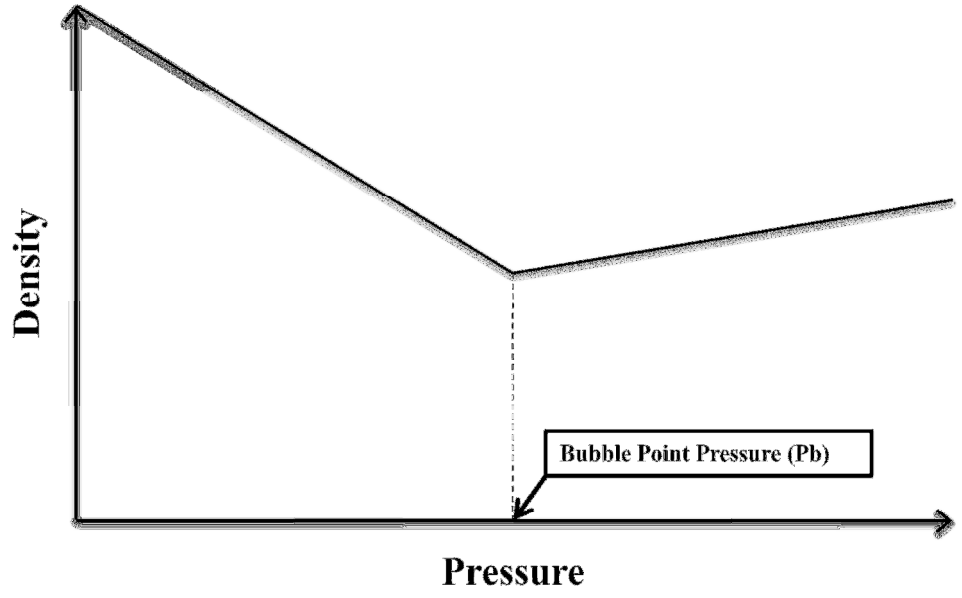

Figure 2.10: Depiction of Density Behavior With Pressure Depletion (at Constant Temperature)

Asphaltene density can be indirectly determined from measurements of a known concentration of asphaltene in toluene using the Anton Paar device (Yarranton and Masliyah, 1996). During the past few years, molecular dynamics and molecular mechanics simulations have been successfully used to describe and determine

thermodynamic properties such as density (Van Gunsteren *et al.*, 1990). Recently, density values for average structures of asphaltenes from the Berri Middle-Eastern field have been calculated using molecular dynamic simulations (Diallo *et al*., 2000), it has been found that the densities of different solid products of crude oil correlate very well with the H/C ratio and also with solubility. Rogel and Carbognani (2002) carried out a simulation study that utilizes ″molecular mechanic and molecular dynamic simulations″ to determine the density of average structures of various representative asphaltenes samples. The effect of structural aspects such as H/C ratio on the calculated densities was investigated as well. The study compared the calculated densities using molecular simulations with experimental values. The initial density for the average structure was estimated from a correlation between the density and H/C ratio based on experimental data that include asphaltenes from virgin and processed crude oils. This correlation is the following:

$$\rho = 1.3447\ H/C - 0.5396\ . \qquad (\mathbf{2.7.1})$$

The results of the study showed that the density increases as the H/C ratio decreases and that the introduction of heavier atoms in the molecule may cause an increase in the molecular interactions due to the presence of heteroatoms. The authors highlighted that the calculation of asphaltene density using average structures by molecular dynamic simulations was subject to large errors; however, it generated values that are qualitatively correct and in the right range.

Yarranton and Masliyah (1996) conducted several experimental works that include density measurements. Density was measured using the Anton Paar device. It was measured for solutions of asphaltene in toluene at concentrations of 0 to 1.14 wt.%. The regular solution behavior was assumed due to the low concentration obtained. The asphaltene density then can be determined indirectly from **Equation** (**2.7.2**) and **Equation** (**2.7.3**), utilizing a plot of the inverse mixture density versus asphaltene mass fraction as shown in **Figure 2.11**.

$$\frac{1}{\rho_M} = \frac{1}{\rho_T} + \left(\frac{1}{\rho_A} - \frac{1}{\rho_T} \right) x_A \quad , \tag{2.7.2}$$

$$\rho_A = \frac{1}{S + I} \quad , \tag{2.7.3}$$

where

ρ_M is the mixture density (kg/m^3)

ρ_T is the toluene density (kg/m^3)

ρ_A is the average asphaltene density (kg/m^3)

x_A is the asphaltene mass fraction

S is the slope of the mixture density plot

I is the intercept of the mixture density plot

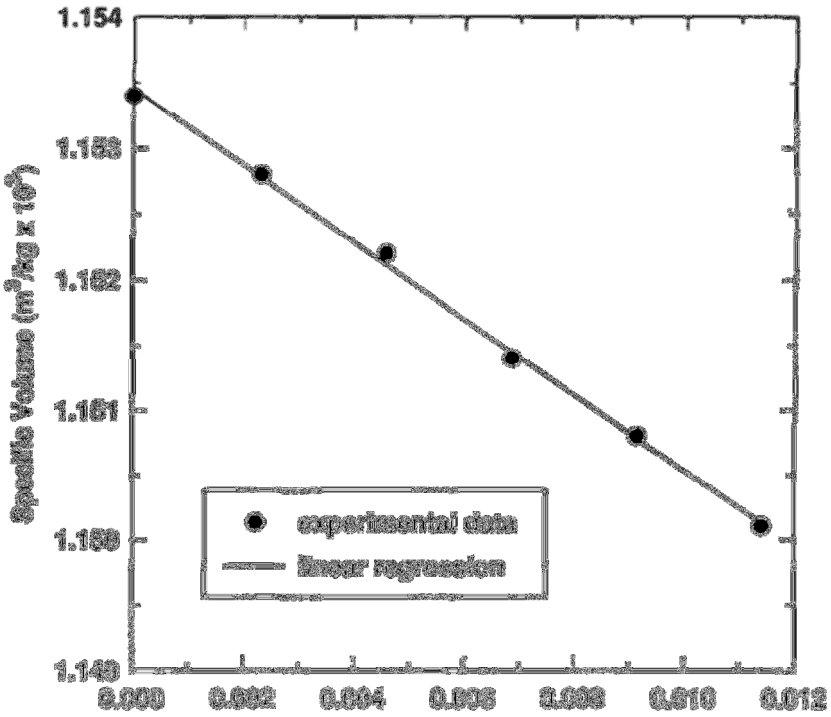

Figure 2.11: Dependence of Asphaltene-Toluene Mixture Density on Asphaltene Concentration According to Yarranton and Masliyah (1996)

The study concluded that the scattered results in density determination illustrate the difficulty in obtaining distributions and explain the small amount of data on asphaltene densities in the literature. The study suggested more testing for the correlation to verify the density determination robustness on asphaltenes density from other sources and with different solvents.

2.6.2 Viscosity

Viscosity variations are known to match those of the volume of a colloidal aggregate occupied per unit mass of asphaltene (Johansson *et al*., 2009). When precipitation occurs, asphaltene fines may alter the viscosity of the transporting phase which is oil phase. The precipitation tends to increase the oil viscosity and the deposition of heavier components tends to make the oil lighter and therefore reduces its viscosity. The viscosity alteration can be modeled in two different ways (ECLIPSE, 2009):

- Generalized Einstein model

$$\frac{\mu}{\mu_0} = 1 + aC_P \ , \qquad (\mathbf{2.7.4})$$

where

a = 2.5 (default value)

C_p is the volume concentration of precipitate

μ_0 is the oil viscosity at $C_p=0$

- Krieger and Dougherty model

$$\frac{\mu}{\mu_0} = (1 - C_P \frac{C_P}{C_{P0}})^{-\eta C_{P0}} \ , \qquad (\mathbf{2.7.5})$$

where

η is the intrinsic viscosity, $\eta = 2.5$ for spherical colloids

Cp_0 is the volumetric concentration for maximum packing, equal to 0.65 for spheres packing.

2.6.3 Solubility

Several attempts were made to model asphaltene solubility using experimental measurements of density which is then correlated with molar mass. Asphaltene solubility in crude oil has been the subject of several theoretical investigations. Hirschberg *et al*. (1984) combined Hildebrand regular solution theory with a Flory-Huggins theory to express asphaltene solubility in crude oil as a function of molar volume and the solubility parameter. Since asphaltenes are mixtures of molecules, the solubility can be determined using flash calculation. With the large molecules size of asphaltenes, it is necessary to use the Flory-Huggins theory. The solubility parameter is defined as follows:

$$\delta_i^l = \left(\frac{\Delta U^{\text{vap}}}{v_i^l}\right)^{1/2} \quad , \qquad \textbf{(2.7.6)}$$

where

ΔU^{vap} is the internal energy (J/mol) of vaporization

v_i^l is the liquid phase molar volume (m^3/mol)

δ_i^l is the solubility parameter ($MPa^{1/2}$)

The solubility parameter can be correlated to molar mass using **Equation** (**2.7.6**) by treating asphaltene as a homogenous composition. The effect of temperature on the solubility parameter of asphaltene is shown in **Figure 2.12**. The solid line represents a linear regression line through the data points. The figure clearly indicates that the solubility parameter of asphaltene decreases linearly with temperature. This trend can be explained by the fact that as the temperature of a crude oil decreases, the crude solubility

decreases as well and can no longer keep the particles in suspension. As a result, the particles will settle and form deposits. A linear decrease of the asphaltene solubility parameter with temperature has also been reported by Hirschberg *et al*. (1984).

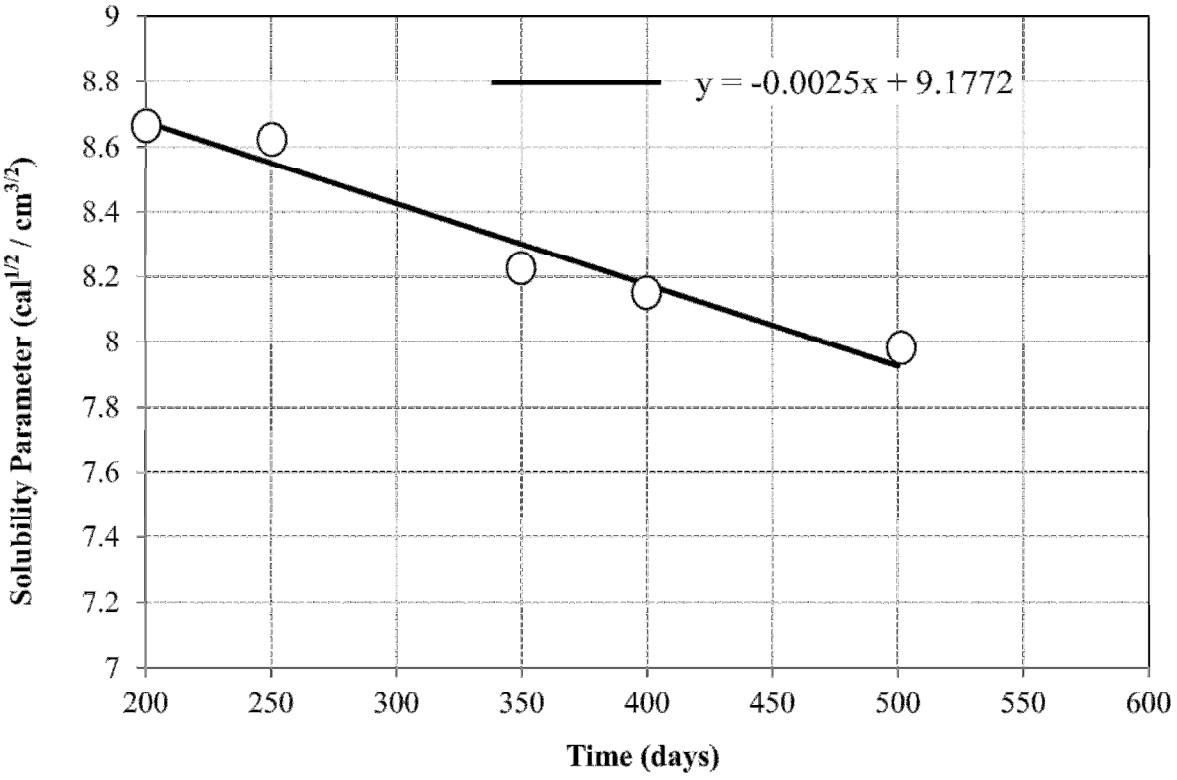

Figure 2.12: Solubility Parameter of Asphaltene as a Function of Temperature for P = 100 bar as Indicated by Yen and Chilingarian (1994)

The effect of pressure on the solubility parameter of asphaltene at T = 300 K is shown in **Figure 2.13**. The solid line represents a linear regression line through the data points. It indicates that the solubility parameter of asphaltene is not affected very much with the change in pressure. However, as discussed earlier in Section 2.4, Leontaritis and Mansoori suggested that at constant temperature, the solubility parameter's general trend is proportional to the pressure depletion until the pressure reaches the bubble point.

Below the bubble point pressure, the solubility is inversely proportional to the pressure trend as depicted in **Figure 2.14**. Generally, pressure holds dissolved gases and light hydrocarbon components in solution and helps maintain a constant temperature. As pressure drops, the temperature drops, because of gas expansion. As a result, the heavier components will settle and form deposits.

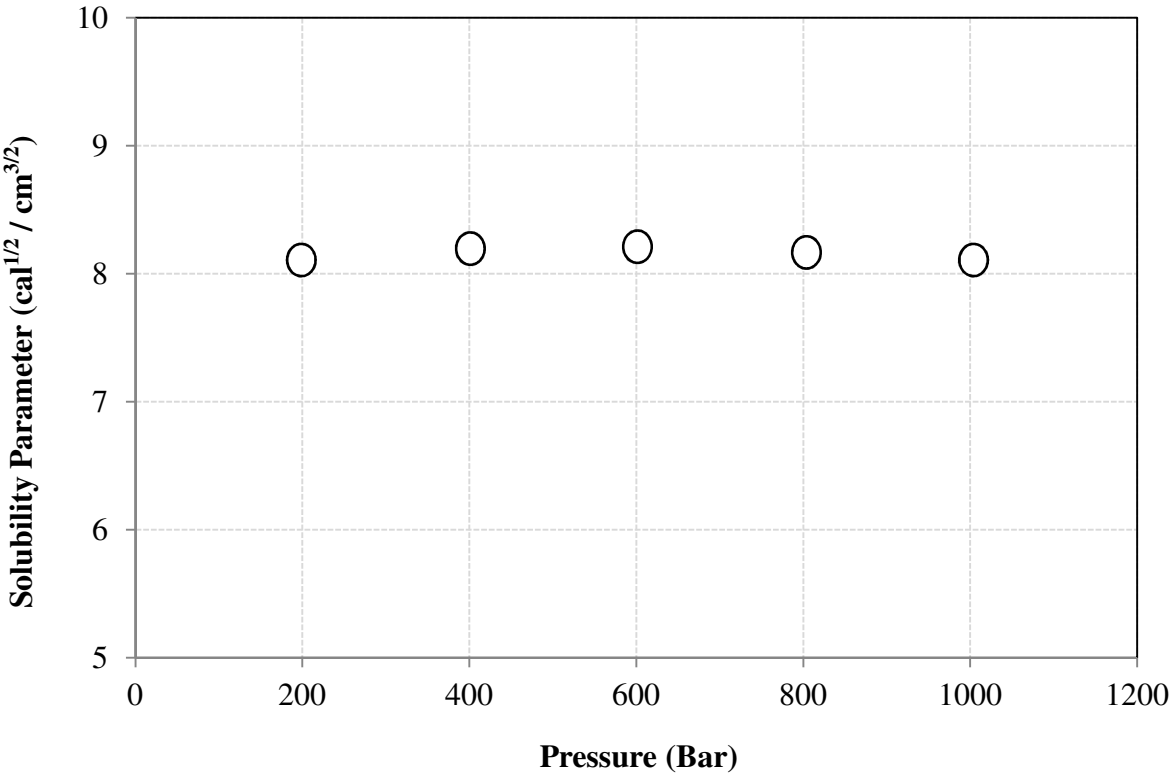

Figure 2.13: Solubility Parameter of Asphaltene as a Function of Temperature for T = 300 K as Indicated by T.F Yen and G.V. Chilingarian

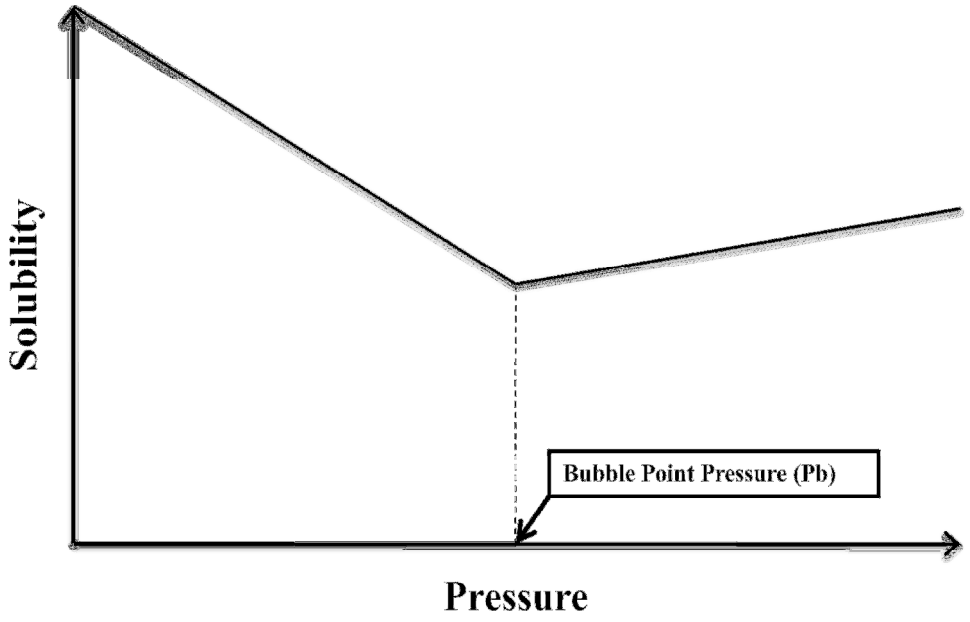

Figure 2.14: Depiction of Solubility Behavior With Pressure Depletion (at Constant Temperature)

2.6.4 Molecular weight

Asphaltenes' molecular weight is difficult to measure since it depends on three factors (Wang, 1998):

- Nature and amount of solvent (can be controlled by using specific types of solvents that prevent aggregation)
- Temperature
- Contact time

Most of the available asphaltene modeling techniques were developed before the recent advancements in measuring the asphaltene molecular weight. Researchers (*i.e.*, Sanchez and Mansoori, 1998) believe that asphaltenes exhibit a wide range of molecular weight. There is still some debate about the size/structure of individual asphaltene molecules.

Several techniques have been recently developed to study heavy oil fractions such as asphaltenes, wax, and resins. However, mass spectrometry and molecular diffusion provide distinctive and accurate measurements of asphaltene molecular weight and size.

- *Mass spectrometry*

Mass spectrometry depends on measuring the ratio of ion charges (resulting from an electromagnetic field) to mass. Mass spectrometry can identify molecules based on the knowledge of their mass, provided that the molecule can be ionized (*i.e.*, charged and vaporized). One of the main resources for asphaltene studies using mass spectrometry is the National High Magnetic Field Laboratory at Florida State University. **Table 2.4** shows a summary of mass spectrometry measurements with a short description for each technique.

- *Molecular diffusion*

Molecular diffusion basically depends on monitoring the diffusion of individual molecules using special measuring techniques (*i.e*., fluorescence techniques). The slower the diffusion, the larger the molecule size and vice versa. This type of measurement is very helpful, because the estimated molecule size is used to infer the molecule weight by a comparison with model compounds (Schlumberger, 2007). **Table 2.5** shows a summary of mass spectrometry measurements with a short description for each technique.

Table 2.4: Measurement Methods Using Mass Spectrometry in Terms of Molecular Weight (Courtesy of Schlumberger, 2007)

Method	Brief Description	Molecular weight	Reference
Electro-Spray Ionization (Nobel Prize-Winning ionization Method)	This method evaporates the solvents, which make the large molecules to go into the vapor phase	Between 400 and 800 g/mol	Rodgers and Marshall, 2004
Atmospheric Pressure Photo Ionization	This method uses the light to ionizes the nebulized gas samples in order to get the mass/charge ratio of the asphaltenes.	750 g/mol	Merdrignac et al., 2004
Laser Desorption Ionization	This method exposes a solid asphaltene sample to a laser pulse which creates a gas cloud (for improved accuracy: low laser power and low gas densities are required)	Between 800 and 1,000 g/mol	Hortal et al., 2006
Field Ionization	This method exposes vaporized asphaltenes to a high-energy electric field	800 (g/mol)	Boduszynski, 1981
Field Desorption Ionization	This method uses deposited asphaltene samples on "a needle-like" surface which will desorbed and ionized when subjected to a high electric field and sufficient heat in order to get the mass/charge ratio of the asphaltenes	1,000 g/mol	Qian et al., 2007

Table 2.5: Measurement Methods Using Molecular Diffusion in Terms of Molecular Size (Courtesy of Schlumberger, 2007)

Method	Brief Description	Molecular Size	Reference
Nuclear Magnetic Diffusion	This method exposes asphaltene molecules to an NMR field to measure their diffusivity	2.6 nm diameter	Freed et al, 2007
Fluorescence Correlation Spectroscopy	This method measures the diffusion coefficients of fluorescing molecules, which allow measuring a length corresponding to a sphere radius	2.4 nm, which is equivalent to 750 g/mol	Andrews et al., 2006
Taylor Dispersion Diffusion	This method measures the diffusion coefficient of molecules in laminar flow which allow measuring the molecular size	1.4 nm diameter	Wargadalam et al., 2002
Time-Resolved Fluorescence Depolarization	This method depends on measuring the diffusion constants of asphaltene molecules, which is achieved by detecting the rate of decay	2 nm diameter, which is equivalent to 750 g/mol	Groenzin and Mullins, 2000

There are some techniques such as gel-permeation chromatography and vapor-pressure osmometry that give inconsistent measurements for heavy molecular weight fraction (*i.e.,* asphaltene, resins, and wax); however, these techniques provide accurate measurements when used in characterizing lighter hydrocarbon fractions. These advanced measurements facilitate an understanding of petroleum heavy constituents. A new research field called ″petroleomics″ has started receiving more attention; it is based on integrating the different knowledge of chemical composition of petroleum (*i.e.,* molecular weight, density, structure, etc.) to develop correlation studies and improve the prediction of asphaltene phase behavior. Future research should focus on understanding the wettability effects, and the analysis of downhole fluids to identify potential production problems related to asphaltenes.

2.7 Production Strategies for the Prevention of Asphaltene Problems

2.7.1 Introduction

Taking preventive measures is always a wise solution rather than attempting to resolve issues as they occur. Asphaltene can cause reservoir impairment, plug wells and flowlines through deposition, and also cause separation difficulties at the separation facilities. There is no specific resource or research that discusses strategies of preventing or delaying asphaltene problems such as precipitation and deposition, which can cause a decline in productivity and increase maintenance costs. However, some research (*i.e.,* Allenson *et al*., 1997) suggests several remedial actions to help prevent or delay asphaltene problems. Actions need to be taken for the mitigation of asphaltene deposition to eliminate massive additional costs such as deposit removal treatments, loss of productivity due to shutdown and even loss of some wells **(Table 2.6)**. It is more likely to have asphaltene deposition during the exploitation of deep water wells.

Table 2.6: Typical Additional Cost Due to Asphaltene Deposition Problems (Vargas *et al*., 2009)

OPERATION	COST
Deposit Removal	$300,000 - $3,500,000 per well
Side Track	$50,000,000 per well
Downtime	$700,000 per day (for a production of 7,000 BPD)

Asphaltene precipitates are produced by different mechanisms; however, as discussed earlier in Section 2.4.3 and Section 2.4.4, they are strongly influenced by pressure and temperature. Flow assurance engineers usually assess the precipitation behavior by using pressure and temperature (P-T) diagram. The reason why the P-T phase boundaries are

plotted together is to investigate the pressure and/or temperature that help show the possibility of having asphaltene precipitation. **Figure 2.15** shows the P-T diagram for Gulf of Mexico black oil with indication of potential areas of asphaltene, wax, and hydrates.

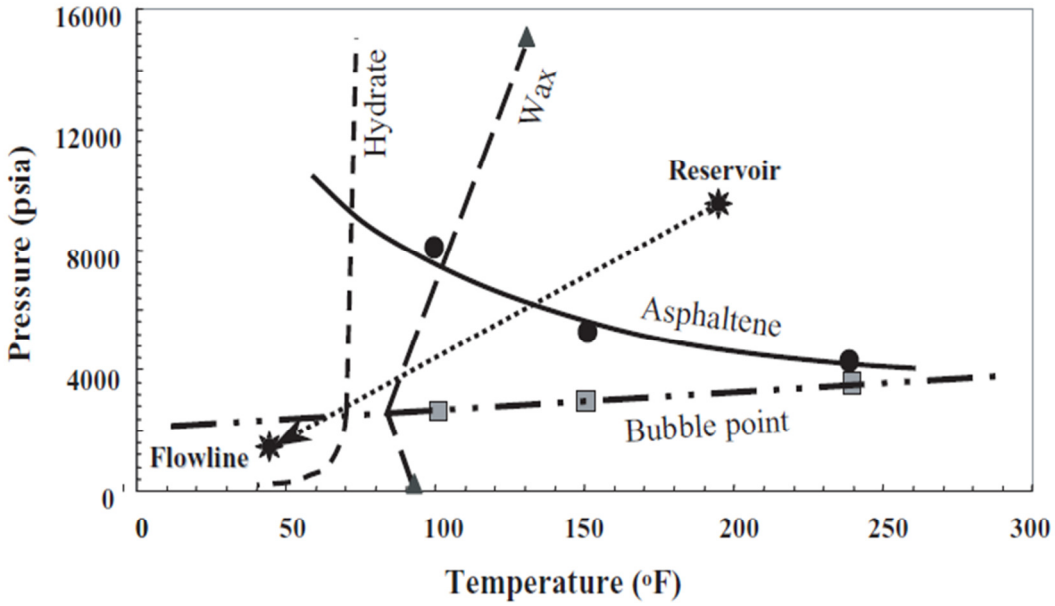

Figure 2.15: Gulf of Mexico Black Oil Phase Diagram According to (Ahmed Hammami and John Ratulowski, 2000)

It is clear why many companies search for reliable predictive scenarios or mechanisms that help them to achieve an efficient and less costly operation process. This section will provide insight and knowledge of proper control and remediation strategies that must be incorporated into the production and reservoir systems from the beginning. The section will also highlight the risks associated with asphaltene problems and suggest actions to avoid them.

2.7.2 Effect of asphaltene on productivity

A numerical simulation study of a homogenous sandstone formation conducted in China in 2010 to study the impact of asphaltene deposition on water cut. The study showed that the water-cut profile without asphaltene deposition will be less than that with asphaltene deposition (Ju *et al*., 2006). The reason for this difference in water cut can be attributed to the wettability change caused by asphaltene deposition onto the pore walls of the sandstone formation. The wettability of the pore walls of sandstone oil formation was originally water-wetting. However, asphaltene adsorption onto pore surfaces of the sandstone formation leads to wettability change from water-wet to oil-wet, which leads to a higher flow proportion of water to oil at the same water saturation. Therefore, less oil recovery will be expected for asphaltene deposition in oil formation during the production history in theory (Binshan *et al.*, 2010). When a well produces water in appreciable amounts, steel tubing will be water-wet, thus, reducing the deposition tendency. Since asphaltene deposition on the pore walls of the sandstone formation can lead to a wettability change, the adsorption of asphaltene may cause a relative permeability shift from a water-wetting system to an oil-wet system (Moore *et al*., 1965). Also, asphaltene deposition may cause pore throat plugging, which decrease the pore spaces, permeability, and enhance formation damage. One way to control or delay the asphaltene problems related to water cut is to implement an effective water management strategy (*i.e.* cyclic production, operating constraints, etc.). This strategy should lead to the water cut reduction as much as possible, which in turn, will help achieve satisfactory flow assurance.

2.7.3 Operational challenges

Heavy crude with high cloud points and pour points will need a special design that considers the operational challenges. Some operational challenges associated with asphaltene deposition include the following:

- Solid deposition on flow lines and pipeline walls reduces the internal diameter (**Figure 2.9**), causing pressure and production loss. Also, permeability reduction and formation damage when it occurs around the wellbore and its vicinity.

- Changes in the reservoir fluid composition and fluid rheology due to phase separation as asphaltene precipitates.

- Removal of wax deposits, which may require production shutdowns and cause loss of revenue or extra costs.

- Design flow lines and pipelines using sophisticated insulation materials to ensure that the crude temperature remains above the wax deposition temperature.

- The high cost of adding chemicals to prevent wax formation and deposition. For instance, chemical injection is necessary before a required shutdown to prevent the crude from cooling below the pour point and gelling up in the pipeline. Xylene is known to be the best paraffin solvent in the field for this preventive measure.

2.7.4 Production strategies

Actual field experiences indicate less asphaltene precipitation problems when the pressure is below the bubble point than when the pressure is at the bubble point. Many field tests (*i.e.,* Hassi-Messaoud field in Algeria and Mata Acema field in Venezuela) show that the heavier crudes have much fewer precipitation problems than highly under-saturated light crudes (Leontaritis and Mansoori, 1987). The reason of this observation is attributed to the fact that the dissolving power in the heavier crude, containing a larger amount of asphaltene, is much greater than the lighter crude, containing small asphaltene content. Based on this fact, it is recommended to maintain an appropriate production strategy relative to the type of crude. There are three important strategies used to control solid particles in crude oil (IPIMS, 2011):

- Thermodynamic control: This involves keeping the system pressure and temperature in a region where the solids are unstable.
- Kinetic control: This involves controlling the conditions of solid formation such that asphaltene does not deposit.
- Mechanical control: This involves allowing solids to deposit, then periodically removing them.

In under-saturated reservoirs, a good strategy to reduce the risk of asphaltene well-plugging is to keep the pressure at the bubble point by producing from the upper part of the field. In retrograde reservoirs, asphaltene drop-out around the wellbore might occur where asphaltene stability is very sensitive to the dissolution of condensate and can be reduced by specifying a constraint, such as a lower producing gas oil ratio (GOR)

(Afshari, *et al.*, 2010). Note that strong under-saturation may occur in fields with a natural gas cap if the hydrocarbon column is of a large vertical extent. In such a case, wells at the lower horizon are expected to show more asphalt problems than wells that are higher in the structure. Thus, it is advisable to place the wells in such cases as high as possible.

2.7.5 Intervention techniques

A very important aspect of preventing asphaltene precipitation and deposition problems is by maintaining an appropriate wellbore condition and an advanced monitoring system that can keep track of those conditions and fix any anomaly in a timely manner (IPIMS, 2011). One of the main suggested routine actions used by production and flow assurance engineers is stimulating the wells periodically to improve the productivity index (PI) with a treatment program that should include:

- Acid for stimulation
- Xylene and mutual solvent for dissolving and cleaning the asphaltenes

Asphaltene can deposit anywhere in the production system, but the near-wellbore region is the most damaged zone as shown in **Figure 2.16**. Deposited asphaltene particles may block many pores that are difficult to access in case of remediation. Conventional asphaltene flocculation-inhibitor treatments involve either periodic intervention with solvent or continuous chemical injection into the wellbore. These methods are effective in preventing precipitation and deposition of asphaltenes in flowlines, but they do not

protect the producing formation, because the chemical interaction with the oil after it has left the formation leaves a potentially large amount of asphaltene behind. An improved method developed by Nalco Energy Services adds chemicals to the crude oil while it is still in the formation (Allenson *et al*., 1997). The method includes squeezing an asphaltene-deposition inhibitor into the formation to stabilize the asphaltene before flocculation occurs. Some of the effective and necessary steps, suggested by State Oil Company of Azerbaijan Republic (SOCAR) Journal proceedings (2010), in preventing and reducing the severity of the deposition are the following:

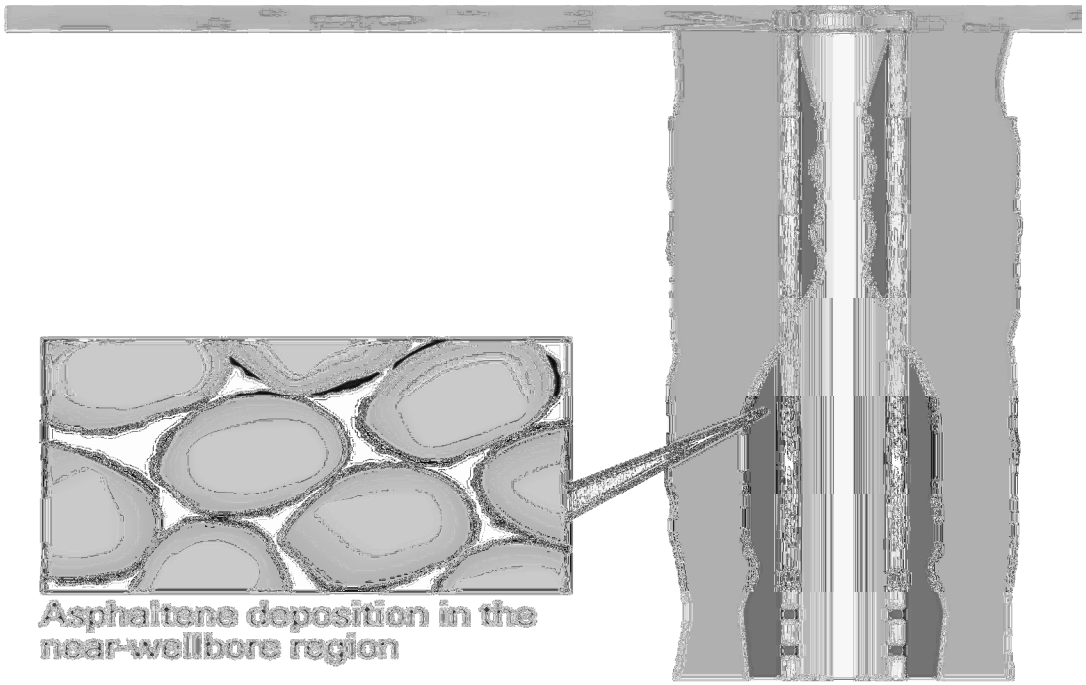

Figure 2.16: Asphaltene Deposition in the Wellbore System (Courtesy of Schlumberger, 2007)

- Predictive modeling and analysis

The use of laboratory or field data is necessary to quantify and characterize the crude oil or asphaltene will help shed light on the reason asphaltene deposition. With the proper incorporation of these data in a realistic model that takes into account all the factors affecting asphaltene precipitation and deposition, the problem will be anticipated and predicted before it occurs.

- Dual completion

It is reported that the use of standard well completion techniques will result in costly workovers for deposit removal resulting from asphaltene and other heavy organics (Garcia-Hernandez *et al*., 1989). Dual completion is suggested instead to control the deposit formation **(Figure 2.17)**. The main purpose of dual completion is to use the inner tubing strings for solvent injection or circulation, allowing the lowering of production testing devices. Also, when the main string is shut-in for maintenance or cleaning deposits, the inner tubing string is used for production instead.

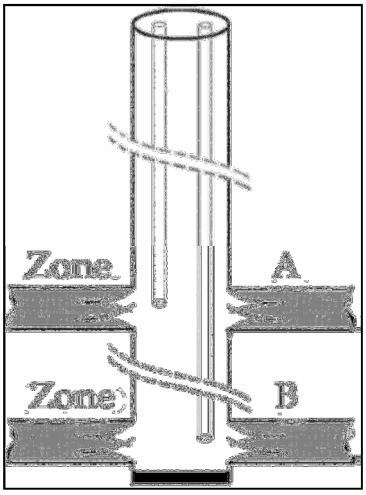

Figure 2.17: A Well With a Dual Completion According to SOCAR (2000)

- Compatibility test

It is suggested that all well stimulation, injection, and EOR fluids should be tested for static and dynamic compatibility with the reservoir fluids prior to operations. This should especially be performed when asphaltenic crudes are present (Garcia-Hernandez *et al.*, 1989). It is possible to perform certain experimental measurements to obtain a simple phase envelop representation, through which we can define the composition of heavy crudes at certain temperature and pressures.

- Composition gradient

The composition gradients of heavy crude in oil reservoirs with deeper zones usually have higher fractions of the heavy crude. In the case of heavy crude or asphaltene, it is advisable to produce first the top zones of the reservoir, which generally have a smaller tendency to heavy particle deposition.

- Mechanical removal techniques

In some cases, mechanical removal techniques, especially wirelining may represent an effective means in handling heavy crude problems. This can be verified by conducting a study to indicate whether or not a mechanical removal method of cleaning is preferred over cleaning by using solvents.

- Solvent treatment

Solvent dilutes the crude oil and reduces the tendency of asphaltene precipitation. Xylene is generally the most effective solvent to use in well stimulations, workovers, and cleaning. In some cases xylene injection through the non-producing string (inner tubing) may help minimize the deposition problems.

- Hot Oil treatment

Circulation with hot oil maybe used to prevent or reduce the asphaltene deposition problem. A combination of solvent treatment with hot oil circulation has been tested in the past in some oil wells with mixed results (Tuttle, 1983).

2.8 Asphaltene Models

2.8.1 Introduction

To model asphaltenes, we need to know more about their phase behavior, size, and molecular weight distributions beside the previous knowledge we discussed earlier about pressure, temperature, etc. The model has to incorporate the interaction of asphaltene and oil in terms of solubility in oil and the suspension characteristics attributed to resin. Several asphaltene precipitation and deposition models have been developed to incorporate reliable experimental data into simulators. These models improved the understanding of asphaltene behavior at varying conditions throughout production from the formation to the wellbore.

2.8.2 Asphaltene modeling

Precipitation is the process that triggers the appearance of the asphaltene particles. However, when those precipitated particles aggregate together they form bigger particles called ″flocs″ in the flocculation process (CMG/GEM, 2009). Several models (Hirschberg *et al*., 1982; Leontaritis and Mansoori, 1987; Chung, 1992) describing asphaltene precipitation and flocculation have been developed during the past three decades. These models generally incorporate experimental results on asphaltene precipitation and flocculation. Yet, there are still challenges related to the accurate simulation of asphaltene precipitation, flocculation, and deposition. Generally, asphaltene models can be divided into three main groups as shown in **Figure 2.18**:

- The real solution models
- The colloidal models
- The association equation-of-state (EOS) models

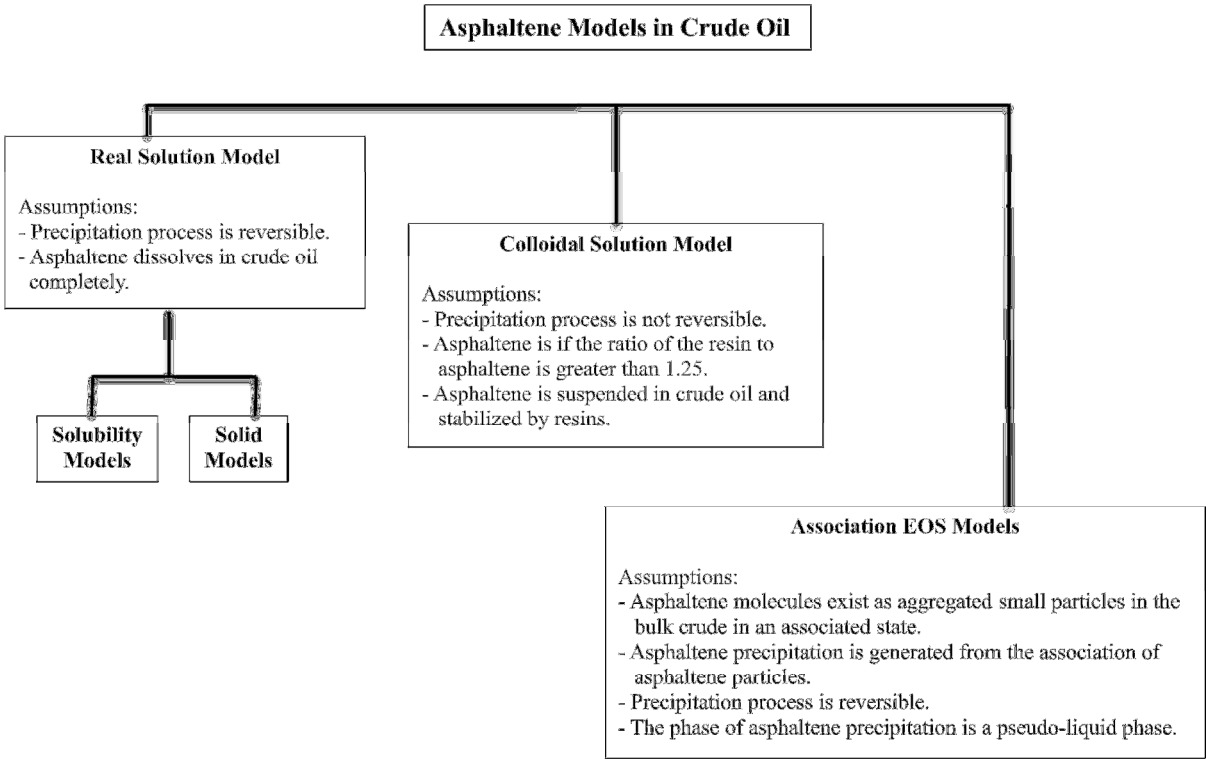

Figure 2.18: Asphaltene Models in Crude Oil

2.8.3 Real solution models (Nghiem *et al.*, 2000)

This model incorporates two main assumptions:

- Asphaltene dissolves in crude oil completely

- The process of asphaltene precipitation and dissolution is reversible

The real solution model can be subdivided into two main models:

- Solubility models

- Solid models

- Solubility models

Solubility models are the most widely used models to predict asphaltene precipitation; they are based on the Flory-Huggins theory (Flory, 1942). The theory was developed for mixtures of polymers with very large molecules and solvents with much smaller molecules (Mousavi-Dehghani *et al*., 2008). The first of such a model was established by Hirschberg in 1984; it employs a thermodynamic approach to describe asphaltene stability in terms of reversible solution equilibrium based on the Soave equation-of-state (Soave, 1972). In the Hirschberg model, the vapor-liquid equilibrium (VLE) was first calculated to determine the liquid phase properties. Then, the liquid-liquid equilibrium (LLE) calculation was performed using the Flory-Huggins theory. The asphaltene was treated as a pseudo-liquid, assuming the precipitated asphaltene phase (LLE) does not affect the previously calculated VLE. Some researchers suggested implementing a three-phase equilibrium calculation utilizing the effect of asphaltene precipitation on the gas phase (Kawanaka and Mansoori, 1991). After that, a new model was developed by Cimino and his colleagues (1995) on the basis of extending the previously established model by Hirschberg to include polymer solution thermodynamics. This recent improvement in the model can lead to an appropriate representation of asphaltene phase behavior if calibrated by experimental results, but may not accurately estimate asphaltene precipitation in fluids with compositions different from those of the calibrated crude oil (Schlumberger, 2007). According to this model, the solubility of asphaltene in oil is given by

$$\phi_a^L = \exp[-1 + \frac{v_a}{v_L} - \frac{v_a}{RT}(\delta_a - \delta_L)^2] \ . \qquad \textbf{(2.9.1)}$$

Equation 2.9.1 is derived from the original Flory-Huggins polymer solution theory in which the partial molar Gibb's free energy or chemical potential of component 1 is

$$\Delta\bar{G}_1 = \Delta \quad \mu_1 = \Delta\bar{H}_1 - T\Delta\bar{S}_1 \ , \qquad (\mathbf{2.9.2})$$

where $\Delta\bar{H}_1$ is the partial molar enthalpy, which represents the residual term, and $\Delta\bar{S}_1$ is the partial molar entropy, which represents the combinatorial term. At the original Flory-Huggins polymer solution theory, the ″residual and combinatorial″ terms are defined as follows:

$$\Delta\bar{H}_1 = \nu_1(\phi_2)^2 \ (\delta_1 - \delta_2 \ )^2 , \qquad (\mathbf{2.9.3})$$

$$\Delta\bar{S}_1 = -R[\ln\phi_1 + (1 - \frac{v_1}{v_2})\phi_2] \ , \qquad (\mathbf{2.9.4})$$

where subscript 1 represents the polymer (asphaltene) and subscript 2 denotes asphaltene-free solvent (oil and/or precipitant and/or solvent). The residual term (enthalpy change of mixing) in the Flory-Huggins theory can be modified by introducing the pair interaction parameter (I_{12}). In other words, **Equation 2.9.3** changes to

$$\Delta\bar{H}_1 = \nu_1(\phi_2)^2 \ [(\delta_1 - \delta_2 \ )^2 + 2I_{12}\delta_1\delta_2] \ . \qquad (\mathbf{2.9.5})$$

- Solid models

Solid models treat the precipitating asphaltene as a single, solid-phase (liquid-solid equilibrium) component residing in different fluid phases and modeled using a cubic EOS. Solid models may need several empirical parameters and tuning to match the experimental data (Thomas *et al*., 1993). Nghiem's *et al*. (1987) solid model considers asphaltene as a single dense phase and assumes that the heaviest components of the crude oil can be divided into precipitating and non-precipitating components. The precipitating components are assumed to be asphaltenes. This model is easy to implement, but requires experimental data to determine the main input parameters to implement in the simulator. The general equation that relates the solid fugacity to liquid fugacity of a pure component is (Nghiem *et al*., 2000)

$$\ln f_s = \ln f_s^* + V_s \frac{(P_1 - P_o)}{RT_o} \quad , \qquad \textbf{(2.9.6)}$$

where

f_s is referred to as the solid fugacity
f_s^* is referred to as the reference fugacity
P_o and T_o are reference conditions for pressure and temperature
V_s is the molar volume of the solid

Chung's (1992) solid model, assumes that asphaltenes are treated as a lumped pseudo-component, and all other components are considered solvents. The method is simple, and allows direct calculation of asphaltene solubility, but does not include pressure effects, which is a very important factor of asphaltene stability.

2.8.4 Colloidal solution model (Leontaritis and Mansoori, 1987)

Colloidal models have their basis from thermodynamics and colloidal science. The model assumes that asphaltenes exist in the crude oil as solid particles in colloidal suspension, stabilized or peptized by resins adsorbed on their surfaces. Based on this, colloidal models are able to predict the onset of asphaltene flocculation. In this model, the VLE is calculated using an EOS, taking into account the liquid phase composition from which asphaltene may flocculate. More evidence shows the invalidity of this model as it neglects the very important and widely accepted reversibility process.

This model incorporates the following assumptions:

-Asphaltene is stable in crude oil if the ratio of the resin to asphaltene content is greater than a certain value such as 1.25

-The process of asphaltene precipitation and dissolution is not reversible

-Asphaltene is suspended in crude oil and stabilized by resins

2.8.5 Association EOS models:

The asphaltene precipitation model developed by the Schlumberger Company is an association EOS model. This model incorporates the following assumptions (JL and Zhang, 2004):

- Asphaltene molecules exist mainly as small molecules in the bulk crude oil and aggregate in an associated state in the precipitation phase
- Asphaltene precipitation is generated from the association of asphaltene particles
- The process of asphaltene precipitation is thermodynamically reversible

- Asphaltene precipitation is a pseudo-liquid phase

This model combines terms describing the physiochemical effects of the association of asphaltene molecules. It requires the knowledge of size, composition, molecular weight, and interaction coefficients of each component. Vafaie *et al.* (2003, 2006) applied the association theory to the prediction of asphaltene deposition.

2.8.6 Summary of precipitation models

In summary, there are three main models for modeling asphaltenes. The first one is the real solutions models which assume that asphaltenes existing in crude oil are real solutions, and that the precipitation of asphaltenes is a reversible process. The real solution models, including solubility models and solid models, are the most common models used to describe the precipitation process. The second most common are the colloidal models which assume that asphaltenes are suspended in the crude oil and stabilized by resins, and the precipitation process is irreversible. Therefore, the colloidal models can be applied to describe the flocculation of asphaltenes in crude oil (Mansoori, 1997). The colloidal models were criticized for ignoring the experimentally proven reversibility process. The third one is the association EOS models which assume that asphaltene molecules exist as aggregated small particles in the bulk crude in an associated state. The association EOS models can be used to model asphaltene deposition.

Most of the above asphaltene precipitation models are lacking the reliable experimental data which are necessary for matching purposes. In many published research studies related to asphaltenes modeling, it is claimed that the three models could give an accurate prediction from a theoretical point of view. However, most of the asphaltene precipitation models are subjected to development due to the fact that most of them were developed before the new field advancements of asphaltene molecular weight and structure. Until new advancements in the models that allow the incorporation of the most recent experimental findings, the three abovementioned models will be applicable respectively in corresponding calculations.

2.8.7 Deposition modeling

Deposition is the process of exchanging flocs between the solution phase (oil) and the rock surface. There are three scenarios of the deposition process (ECLIPSE Manual, 2009):

- The flocs can adsorb on the rock surface
- The flocs can be trapped within the porous media because of their size (plugging)
- The flocs can be entrained and returned to the oil phase because of high, local velocity (shear)

Few deposition models have been developed in the past few decades, the main three models according to Wang (2000) are the following:

- Leontaritis' (1998) model

This model was the first to predict asphaltene deposition in the new wellbore region with the following assumption:

- Production rate is constant
- Transient flow period is neglected
- Asphaltene deposition occur around the wellbore vicinity
- Formation damage area is constant

The colloidal model was used to simulate the asphalt phase behavior. The results of this model were unsatisfactory, where the asphaltene dissolved in the oil during the primary oil recovery stage and did not adhere to the colloidal model assumptions.

- Nghiem et al.'s (1998) model

Nghiem *et al*. used the same concept of solid models, LSE, assuming that the asphaltene deposition is a pure adsorption process. The permeability resistance factor was used to model permeability reduction. The model was criticized for ignoring deposition in the pore space which was considered to be an important factor.

- Wang and Civian's (2000) model

This model can simulate the formation damage caused by asphaltene deposition in horizontal and vertical wells reservoirs during primary oil recovery. The surface deposition, pore throat plugging, and entrainment were presented in the deposition model, and porosity and permeability reduction were incorporated in the simulator. The results suggest that asphaltene can deposit everywhere rather than the near-wellbore area. This model does not have a solid theoretical base, it only a curve-fits to data.

The deposition model is shown in the following relationship:

$$\frac{\partial E_A}{\partial t} = \alpha C_A \phi - \beta E_A \left(v_L - v_{cr,L} \right) + \gamma \mu_L C_A \ , \qquad (\mathbf{2.9.7})$$

It is assumed that the critical interstitial velocities of liquid to move asphaltene deposits are the same. In **Equation 2.9.7,** the first term represents the surface deposition, the second term represents the entrainment, and the last term represents the pore throat plugging

where

α is the surface deposition rate coefficient (1/sec)
C_A is the volume fraction of the suspended asphaltene precipitates in the liquid phase
$\varnothing$ is the porosity of the porous media
β is the entrainment rate coefficient (1/cm)
E_A is the ratio of the deposited asphaltene volume fraction to the bulk volume of the porous media
v_L is the interstitial velocity (cm/sec)
$v_{cr,L}$ is the critical interstitial velocity (cm/sec)
γ is the pore throat plugging coefficient (1/cm)
μ_L is the flux of the liquid phase

2.8.8 Comparison of Asphaltene Precipitation Models in UTCOMP, CMG/GEM, and ECLIPSE

- Relative permeability reduction modeling in UTCOMP

Nghiem *et al*. (1994) proposed a relative permeability model reduction model that can be used to compute the change in relative permeability resulting from asphaltene precipitation, is given by:

$$k_r = \frac{k_{ro}}{1+\alpha R_{f0}} \qquad \text{(for water and oil phases)} \qquad \textbf{(2.9.8)}$$

$$k_r = \frac{k_{ro}}{1+0.5\alpha R_{f0}} \qquad \text{(for gas phase),} \qquad \textbf{(2.9.9)}$$

where:

k_{ro} is the original relative permeability without considering asphaltene precipitation

R_{f0} is the resistance factor

α is an adjustable parameter

This is a simple approach, but it is difficult to determine the value of α. The default value of α used in UTCOMP is 1. However, the user may specify any value.

- Porosity reduction model in UTCOMP

UTCOMP assumes that the precipitated asphaltene can be treated as part of reservoir rock. The porosity model with the presence of asphaltene is given by

$$\varphi = \varphi^*\left(1-\frac{V_a}{\varphi^* V_b}\right) , \qquad \textbf{(2.9.10)}$$

where

φ^* is the original porosity without asphaltene precipitation

V_a is the volume of precipitated asphaltene

V_b is the bulk volume of the grid block

- Rock permeability model in UTCOMP

UTCOMP treats asphaltene as part of the rock matrix and considers only the change in permeability related to porosity; this permeability can be given by a power-law model as

$$k = a\varphi^b \ , \qquad \textbf{(2.9.11)}$$

where a and b are constants. Thus, the change in permeability can be computed by

$$\frac{\Delta k}{k} = 1 - (1 - \frac{\Delta \varphi}{\varphi})^b \ , \qquad \textbf{(2.9.12)}$$

where $\Delta\varphi$ $(\varphi^* - \varphi)$ is the porosity change due to precipitated asphaltene.

- Relative permeability reduction modeling in CMG/GEM

CMG/GEM uses a simple model for the partial plugging phenomena based on the following resistance factor:

$$\text{rfact} = 1 + (\text{rf max} - 1)\frac{W_i}{W_{i,\,max}} \ , \qquad \textbf{(2.9.13)}$$

where

rfact is the permeability reduction factor

rfmax is the maximum permeability reduction factor

The maximum permeability reduction factor (rfmax) and the maximum mass of adsorbed solid per unit mass of rock ($W_{i,\,max}$) are obtained from experimental data.

- Asphaltene adsorption model in CMG/GEM

Multi-component solid adsorption is modeled in CMG/GEM using the Langmuir isotherm model

$$W_i = \frac{W_{i,\,max} C_i\ c_{io}}{1 + C_i\ c_{io}}\ , \qquad (\mathbf{2.9.14})$$

where

W_i is the mass of adsorbed solid per unit mass of rock

$W_{i,\,max}$ is the maximum mass of adsorbed solid per unit mass of rock

c_{io} is the concentration of solid in the oil phase

C_i is the parameter for the Langmuir isotherm model

- Viscosity alterations modeling in ECLIPSE/E300

When precipitation occurs, asphaltene precipitates may alter the viscosity of the transporting phase, which is oil phase in our case study. The precipitation tends to increase the oil viscosity and the deposition of heavier components tends to make the oil lighter, therefore reducing its viscosity. The viscosity alteration can be modeled in two different ways:

- Generalized Einstein model

$$\frac{\mu}{\mu_0} = 1 + aC_P \ , \qquad \textbf{(2.9.15)}$$

where

a = 2.5 (default value)

C_p is the volume concentration of precipitate

μ_0 is the oil viscosity at $C_p=0$

- Krieger and Dougherty model

$$\frac{\mu}{\mu_0} = (1 - C_P \frac{C_P}{C_{P0}})^{-\eta C_{P0}} \ , \qquad \textbf{(2.9.16)}$$

where

η is the intrinsic viscosity; $\eta = 2.5$ for spherical colloids

Cp_0 is the volumetric concentration for maximum packing, equal to 0.65 for sphere packing

- Asphaltene damage modeling in ECLIPSE

Porosity reduction modeling:

Asphaltene deposition will cause a reduction of the porosity, which can be written as

$$\varphi = \varphi_0 - \int_0^t \frac{\partial \varepsilon}{\partial \varphi_0} dt \ , \qquad \textbf{(2.9.17)}$$

where

φ_0 is the initial porosity (without asphaltene precipitation)

ε is the volume fraction of asphaltene deposit

- Permeability reduction modeling in ECLIPSE

If there is a correlation between porosity and permeability, the parameterized power-law relationship can be used to measure the permeability reduction using the following formula:

$$\frac{K}{K_0} = (1 - \frac{\varepsilon}{\varphi_0})^{\delta} \ , \qquad \textbf{(2.9.18)}$$

where

δ is a user input based on core experiment data

K_0 is the initial permeability (md)

Chapter 3: ASPHALTENE PHASE BEHAVIOR MODELING

3.1 Introduction

Laboratory experiments provide valuable information for the technical and economic aspects of an EOR process; however, it is impractical to perform experimental work for large-scale field reservoirs. In such cases, the use of numerical simulation tools for prediction purposes is an asset. Compositional simulators are the most appropriate simulators to model phase behavior; however, it requires large amount of data to define the fluid composition and the related parameters used in calculating the phase behavior and fluid properties (Ali, 2007). This section include five case studies, the predictions of these case studies are validated with experimental data obtained from five different Middle-Eastern reservoirs which helps increase confidence in using the prediction results. For example, experimental data for saturation pressures for various CO_2 concentrations are provided and can be used to achieve more realistic simulation results of phase behavior, which in turn lead to more accurate recovery estimates.

3.2 Phase Behavior

Asphaltene precipitation has a significant impact on oil production during primary recovery (*i.e.,* pressure depletion), secondary recovery (*i.e.,* water flooding) and tertiary recovery (*i.e.,* Co_2 injection). It reduces the oil relative permeability (*i.e.,* rocks becomes more oil-wet), and increases the chances of formation damage and plugging effects. Therefore, it is important to simulate the precipitation behavior of asphaltene during the oil production process in order to design an optimum production strategy that

prevents or reduces asphaltene precipitation problems and sustains a reliable flow assurance system.

3.2.1 Background

Different samples from five Middle-Eastern wells (B-1, B-2, B-3, A-1, and A-2) will be used in our case study. At the beginning we focus on phase behavior calculation in detail for a reservoir oil sample taken from well B-1, and then we will summarize the same calculation for the other four wells in **Appendix A**. The well B-1 case study describes a procedure for modeling the precipitation of asphaltene from an oil reservoir due to pressure depletion using a phase behavior property program called WinProp. WinProp uses an enhanced solid thermodynamic model (Nghiem *et al*., 1996) to describe the precipitation behavior of asphaltene and petroleum reservoir fluid. This newly enhanced model treats the precipitates as a multi-component solid rather than a single-component pure solid phase. The model can incorporate a maximum of three fluid phases in equilibrium with the solid. This section is intended to provide a detailed description of phase behavior calculation for asphaltene precipitation for a reservoir oil sample taken from well B-1 using WinProp. The Peng- Robinson EOS (PR EOS) (1976) is one of the most used EOS models to predict the state of oil and gas phases. The form of the PR EOS in terms of explicit pressure is

$$P = \frac{RT}{v-b} - \frac{\alpha a}{v^2 + 2bv - b^2}\ , \qquad (\mathbf{3.2.1})$$

where v is the molar volume and α is the acentric factor.

$$\alpha = \left[1 + \left(0.37464 + 1.54226\omega - 0.26992\omega^2\right)\left(1 - \sqrt{T_r}\right)\right]^2 \quad \textbf{(3.2.2)}$$

The PR EOS conserved the dependency of the temperature. Coefficients "a" and "b" are made functions of the critical properties and can be computed from

$$a = 0.45724\frac{R^2 T_c^{\,2}}{P_c} \quad \textbf{(3.2.3)}$$

$$b = 0.07780\frac{RT_c^{\,2}}{P_c} \ . \quad \textbf{(3.2.4)}$$

The PR EOS in Z becomes

$$Z^3 - (1-B)Z^2 + \left(A - 2B - 3B^2\right)Z - \left(AB - B^2 - B^3\right) = 0 \ , \quad \textbf{(3.2.5)}$$

where

$$A = \frac{\alpha a P}{R^2 T^2} \quad \textbf{(3.2.6)}$$

$$b = \frac{bP}{RT} \ . \quad \textbf{(3.2.7)}$$

The PR EOS mixing rules are

$$a_m = \sum\sum y_i y_j a_{ij} \quad \textbf{(3.2.8)}$$

$$a_{ij} = \sqrt{a_i a_j}\left(1 - k_{ij}\right) \quad \textbf{(3.2.9)}$$

$$b_m = \sum_i y_i b_i \ . \quad \textbf{(3.2.10)}$$

Binary interaction coefficients (k_{ij}) play an important role in terms of fitting the simulated parameters to the experimental data and obtain the proper trends in solubility (Adewumi, 2011).

WinProp models the precipitated asphaltene as a pure dense (liquid or solid) phase. The model assumes that the heaviest asphaltene fraction in oil can be divided into two parts: a precipitating and a non-precipitating component (Nghiem *et al.*, 1987). The precipitated component is assumed to be asphaltene. The PR EOS was used as well with interaction parameters, which was then used to fit the precipitation curve.

Fugacity is the most important term in calculating the precipitating components of asphaltene. Fugacity of asphaltene in the solid phase cannot be calculated properly from EOS since it depends on its molar fraction (Gupta, 1986). Writing the equation describing the fugacity of the solid component in the solid phase for isothermal conditions gives

$$\ln f_s = \ln f_s^* + V_s \frac{(P_1 - P_o)}{RT_o} \quad , \qquad \textbf{(3.2.11)}$$

where

f_s^* is referred to as the reference (asphaltene) fugacity

P_o and T_o are reference conditions (asphaltene onset) for pressure and temperature

V_s is the molar volume of the solid (asphaltene)

P_o is critical to the simulation of asphaltene precipitation; it should be obtained from experimental data. In a multi-phase flow where asphaltene, liquid, and vapor coexist, the following conditions must be satisfied:

- Vapor and liquid fugacities are equal

$$\ln f_{iv} = \ln f_{il} \qquad for\, i = 1, 2, 3, \ldots, n_c - 1 \qquad \textbf{(3.2.12)}$$

- The mixture fugacities of asphaltene, vapor, and liquid are equal

$$\ln f_{n_c v} = \ln f_{n_c l} = \ln f_s \qquad \textbf{(3.2.13)}$$

- The solid phase exists if the mixture fugacity of liquid is greater than or equal to the asphaltene fugacity

$$\ln f_{n_c l} \geq \ln f_s \ . \qquad \textbf{(3.2.14)}$$

A three-phase flash algorithm was used to solve **Equations (3.2.12)** and **(3.2.13)**. The n_c^{th} fraction is assumed to be the asphaltene component in the liquid phase. The advantage of this model is its efficient implementation. However, it needs experimental data to determine the onset conditions for pressure and temperature.

The main steps required to develop a precipitation model are the following:

- Fluid characterization
- Distribution models
- Regression
- Asphaltene model selection
- Prediction of asphaltene precipitation

We will describe each step in detail. To begin this case study, the data sets obtained from the five Middle-Eastern wells were analyzed and prepared by defining the compositions of their components up to C_{11}, and pseudo-components describing the C_{12+} fraction. Each data set is then named and saved in the WinProp templates directory; we then begin using those data. The first case utilizes the reservoir oil sample taken from well B-1.

Composition and saturation data for well B-1 are shown in **Table 3.1** and **Table 3.2,** respectively. All the data obtained from the rest of the four wells are analyzed using the same approach.

Table 3.1: Molecular Weight and Composition Data for Well B-1

Component	Reservoir Fluid	MW	Std. Density
	mole %	lb/lb_{mol}	lb/ft^3
N_2	0.16	28.01	
CO_2	2.00	44.01	
H_2S	0.00	34.08	
C_1	33.36	16.04	
C_2	7.71	30.07	
C_3	7.39	44.10	
i-C_4	1.98	58.12	
n-C_4	4.81	58.12	
i-C_5	2.20	72.15	38.50
n-C_5	2.84	72.15	38.80
n-C_6	3.70	85.58	41.50
C_7	3.80	94.90	44.60
C_8	3.71	109.09	45.60
C_9	3.23	122.4	46.50
C_{10}	2.92	135.24	48.30
C_{11}	2.21	151.42	48.30
C_{12+}	17.97	313.02	54.50

Table 3.2: Saturation Pressure and Temperature Data for Well B-1

No.	Pressure	Temperature
	psia	F^o
1	2112	250
2	1739	165
3	1462	130

3.2.2 Fluid characterization

Reservoir fluid analysis reports usually include the composition of all light, intermediate and heavy components. Gas chromatography is one of the methods used to analyze the reservoir fluid. The important step in modeling asphaltene phase behavior is the split of the heaviest component in the oil into a non-precipitating component (*i.e.*, C_{36+}) and a precipitating component (*i.e.*, asphaltene). These two components have identical critical properties and acentric factors, but different interaction coefficients with the light components. The precipitating component (asphaltene) has larger interaction coefficients with the light components, which lead to more precipitation as the amount of light component in the solution increases.

The process includes splitting (breaking down) fractions such as C_{7+} or C_{12+} into a Single Carbon Number (SCN) fraction up to C_{36+} (sometimes lower than C_{36+} and sometimes higher), WinProp suggests that it should have a molecular weight close to asphaltene (>500 lb/lb_{mol}). Using the 'Plus Fraction Splitting' tab (**Figure 3.1**) in WinProp, the C_{12+} fraction can be splitted into a number of pseudo-components.

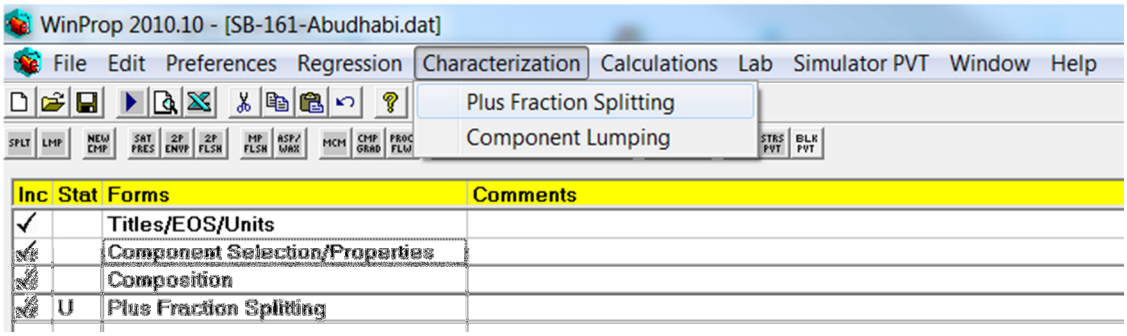

Figure 3.1: Plus Fraction Splitting Tab as It Appears in WinProp

Now, after entering in the initial components and their composition, the input file can be run in order to get the pseudo-components. The properties for each SCN are estimated by empirical correlations and then regrouped into a smaller number of pseudo-components (C_{12}-C_{17}, C_{18}-C_{22}, C_{23}-C_{33}, C_{34}-C_{35}, C_{36+} and Asphaltene) via the Lee-Kesler (1975) mixing rule. The pseudo-components of well B-1 are shown in **Figure 3.2**.

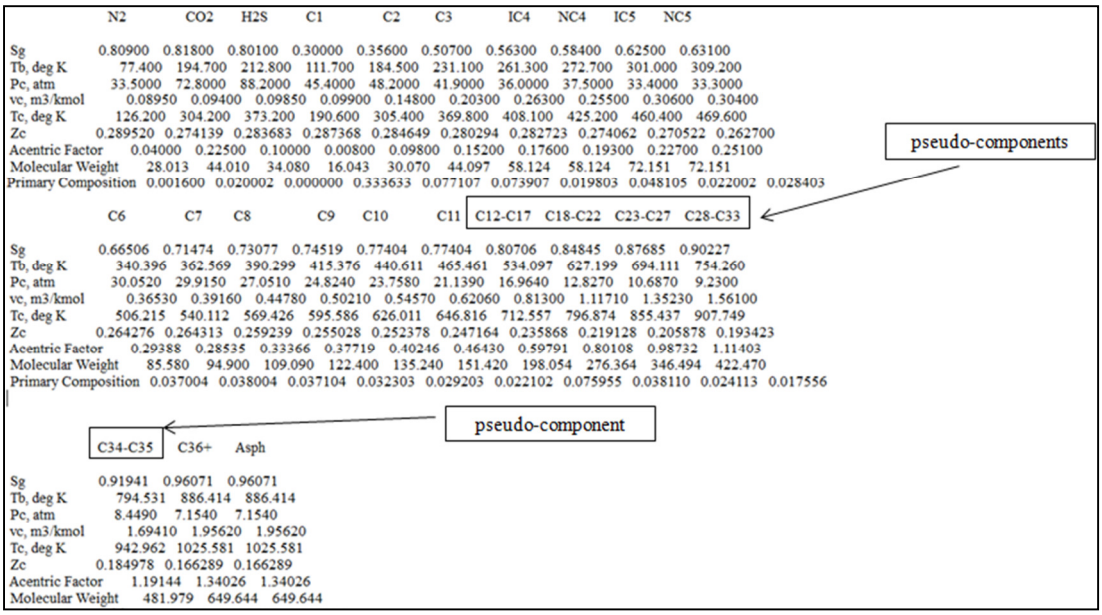

Figure 3.2: The Pseudo-Components of Well B-1 as They Appear in the Output File

The next step is to update and modify the component selection section to reflect the results of the splitting calculation step, we add the pseudo-components one by one followed by C_{36+} and asphaltene using the ″insert own component tab″ as shown in **Figure 3.4**, where only the molecular weight and specific gravity are reported as shown in **(Figure 3.3)**.

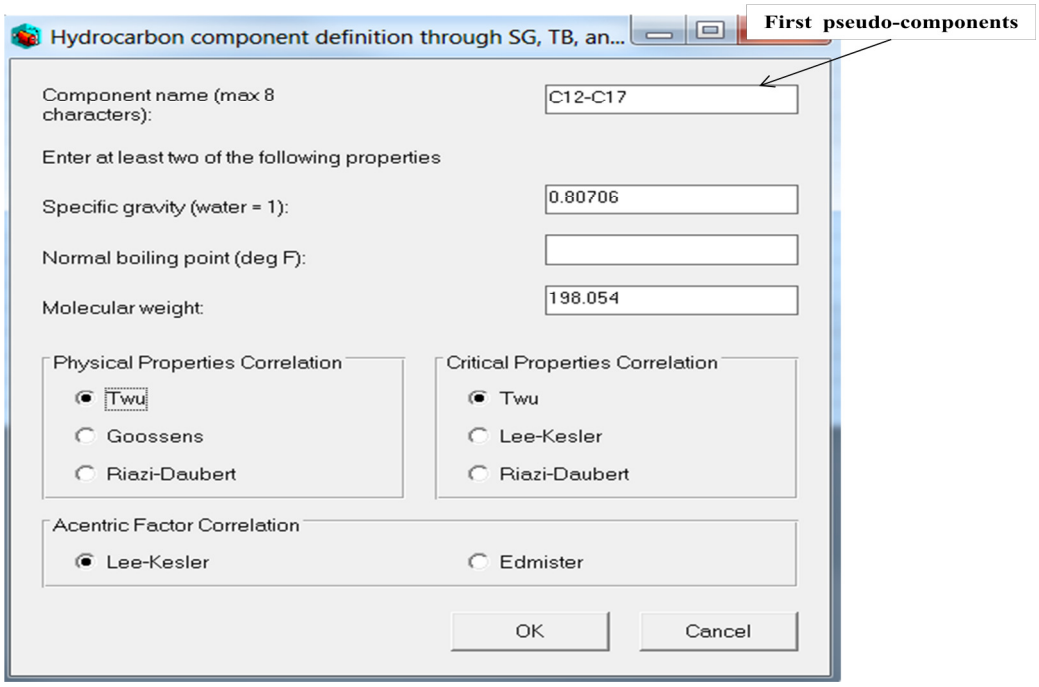

Figure 3.3: The Window Through Which We Insert the Pseudo-Components, C_{36+} and Asphaltene

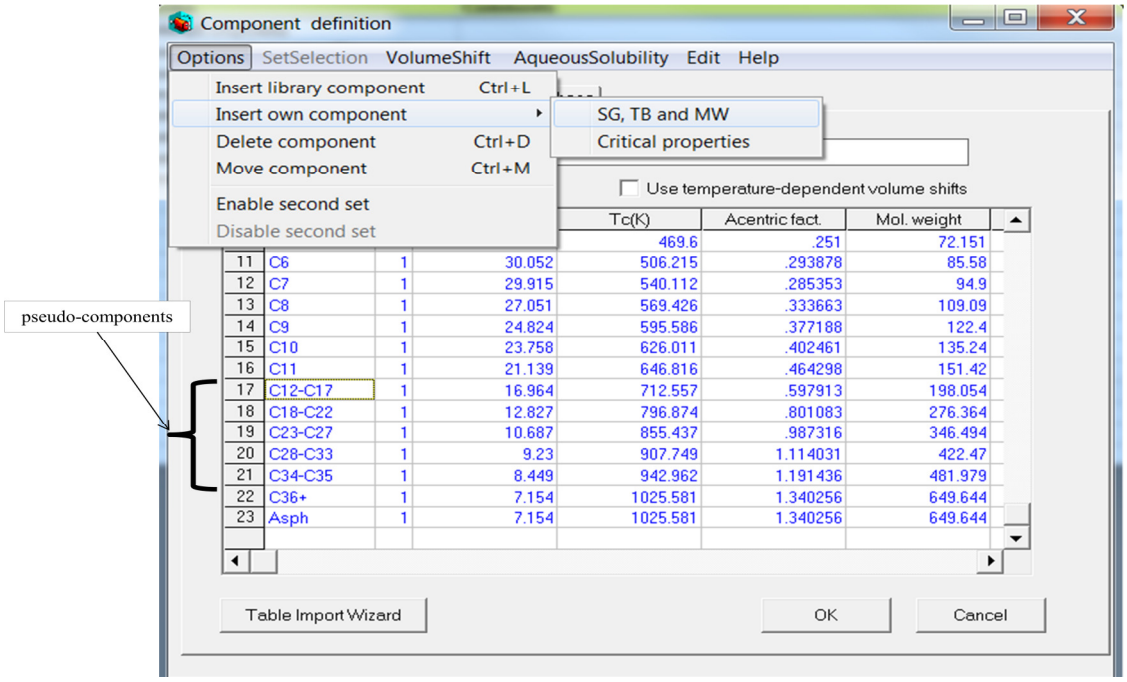

Figure 3.4: The Component Selection Window After Adding the Pseudo-Components, C_{36+} and Asphaltene

Note that after the splitting phase was initiated to obtain the pseudo-components, the resulting output file reports the mole fraction of all components except the mole fraction of C_{36+} and asphaltene reported as one value. Therefore, the next step is to calculate the mole fraction of C_{36+} and asphaltene component. The mole fraction of the asphaltene component can be determined from the following relation:

$$\text{Mole\% of Asphaltene} = \text{Weight \% of Asphaltene} \times \frac{\overline{MW}_{oil}}{MW_{Asphaltene}} \qquad \textbf{(3.2.15)}$$

$$\overline{MW}_{oil} = \sum X_i \times MW_i \ . \qquad \textbf{(3.2.16)}$$

We can calculate the average molecular weight using the data from the output file **(Figure 3.2)** of well B-1; the average molecular weight of the oil is 99.31 and the asphaltene content of the stock tank oil is given as 0.21 wt% **(Table 3.3)**. From the component table, the molecular weight of the asphaltene component is 649.6, so the mole fraction of asphaltene component is the following relation:

$$\text{Mole\% of Asphaltene} = 0.21 \times \frac{99.31}{649.644} = 0.0316\%$$

$$\text{So, the Mole\% of C36+} = 0.019971 - 0.000316 = 1.9655\ \%$$

Table 3.3: C_{36+} and Asphaltene Before and After Splitting

Before Splitting	
Asphaltene	0.019971
C36+	

$\overline{MW}_{oil}$	99.31
$Mw_{Asphaltene}$	649.644
Weight % of Asphaltene	0.21

After Splitting	
Asphaltene	0.019654968
C36+	0.000316032

This results in a mole fraction of 0.0316 % of the precipitating component and 1.97 as the mole fraction for C_{36+}. Now, we can go back to the composition section in the WinProp and add the missing composition of C_{36+} and asphaltene as shown in **Figure 3.5**.

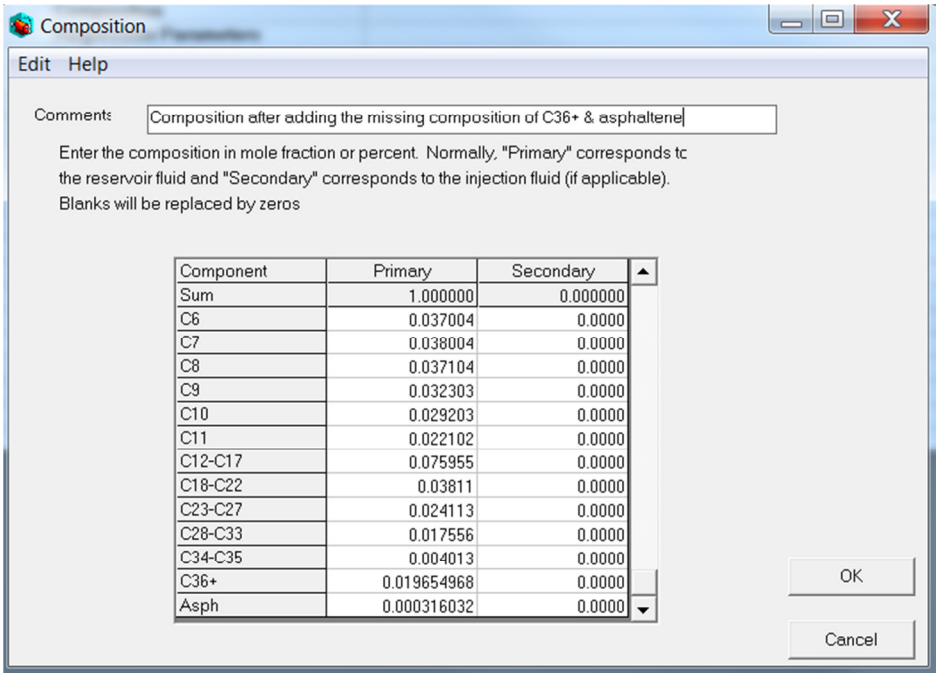

Component	Primary	Secondary
Sum	1.000000	0.000000
C6	0.037004	0.0000
C7	0.038004	0.0000
C8	0.037104	0.0000
C9	0.032303	0.0000
C10	0.029203	0.0000
C11	0.022102	0.0000
C12-C17	0.075955	0.0000
C18-C22	0.03811	0.0000
C23-C27	0.024113	0.0000
C28-C33	0.017556	0.0000
C34-C35	0.004013	0.0000
C36+	0.019654968	0.0000
Asph	0.000316032	0.0000

Figure 3.5: The Composition Selection Window Including the Pseudo-Components, C_{36+} and Asphaltene

It is well known that cubic EOS generally cannot accurately predict laboratory data of oil/gas mixtures without the tuning of the EOS parameters (Coats *et al.*, 1986). The advantage of characterizing the plus fraction is that it reduces the need for extensive tuning of the EOS, where problems start occurring with the C_{7+} and C_{12+} (Naji, 2010). Therefore, it is considered to be the most important step. It is convenient to split the plus fraction into SCN fractions using one of the distribution models described in the following section.

3.2.3 Distribution models

There are several types of oils (light oil, black oil, heavy oil, gas condensate, etc.); hence, there is a need for specific models that describe the molar distribution as a function of molecular weight for each type. There are many distribution models available for splitting the plus fraction. However, the following three choices are available in WinProp (2010):

- Exponential (for gas condensates and light fluids)
- Two-Stage exponential (suitable for simulating black oil)
- Gamma (suitable for all type of fluids)

In our case studies, the two-stage exponential function is used to describe the molar distribution as a function of molecular weight. The 'plus fraction' are lumped into five pseudo-components and then their critical properties are calculated. WinProp provides the following three correlations to calculate the critical properties of the pseudo-components (WinProp, 2010):

- Kesler and Lee (1975)
- Riazi and Daubert (1980)
- Twu (1984)

In our case, the Twu (1984) mixing rules correlation is used as shown in **Figure 3.6.**

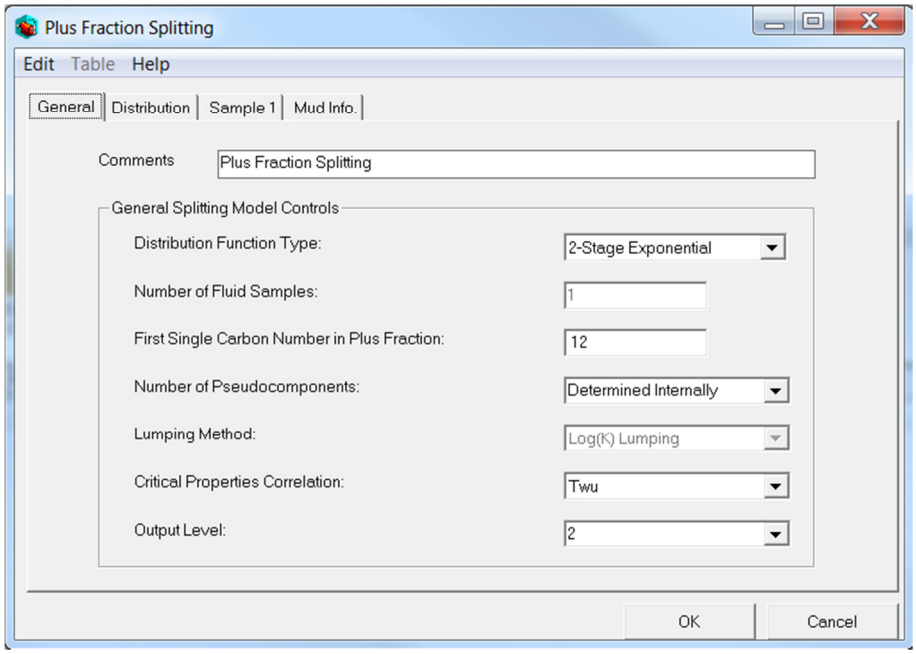

Figure 3.6: The Details of the "Plus Fraction Splitting" General Tab as It Appear in WinProp

The default values used for SCN fraction molecular weight, distribution function cut-off (used to determine the number of pseudo-components for lumping) and SCN molecular weight endpoints (minimum) are 14.026, 0.95, and 0.75, respectively, as shown in **Figure 3.7**.

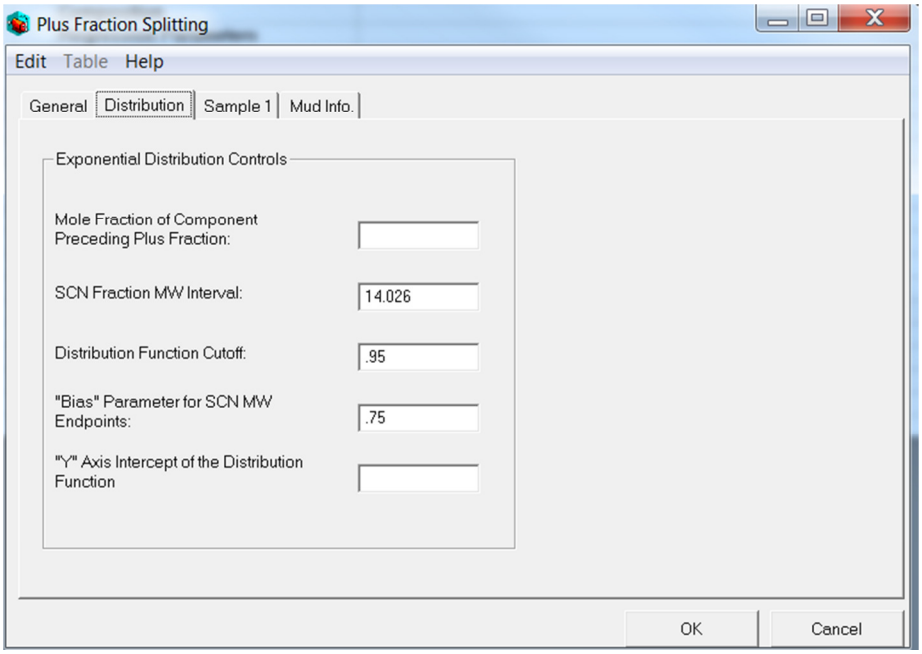

Figure 3.7: The Details of the ″Plus Fraction Splitting″ Distribution Tab as It Appear in WinProp

The specific gravity and normal boiling point for the SCN fractions are calculated using the Harin-Sage correlation (Harin *et al.*, 1969) and assume the constant Watson's characterization factor (Watson *et al.*, 1986). The following options are available for calculating the pseudo-components in WinProp (WinProp, 2011):

- No lumping: (default SCNs will be used)
- Determined internally: (WinProp will estimate the number of pseudo-components)
- Input value: (The desired number of pseudo-components will be specified)

3.2.4 Regression

After performing the splitting calculation, the EOS model can be tuned to any available PVT data using regression. The objective of the regression is simply to obtain a closer value to the experimental data. WinProp uses the regression procedure of Agarwal *et al.* (1987). We begin this step by choosing the regression parameters followed by entering the hydrocarbon interaction coefficient exponent to get a closer value to pressure saturation data presented in **Table 3.2**. Then, under the regression control tab, the convergence tolerance **(Figure 3.8)** is set to be 1×10^{-5} or lower to achieve an acceptable match with the experimental data.

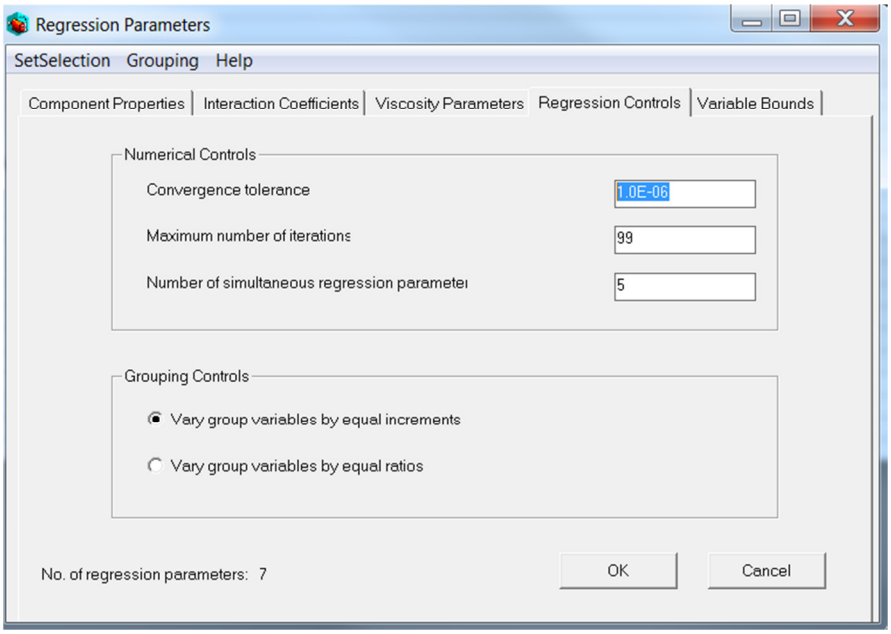

Figure 3.8: Details of the ″Regression Parameter″ Control Tab as It Appears in WinProp

After that, we open a new data entry for the saturation pressure from the calculation tab in the main window and populate it with data we have such as the temperature (250^{o} F),

the experimental saturation pressure (2112 psi) and an estimated saturation pressure (2000 psi) as shown in **Figure 3.9**. Note that in the measurements table in **Figure 3.9**, we input the saturation pressure only; however, if the other parameters are available, the saturation pressure estimation will be improved.

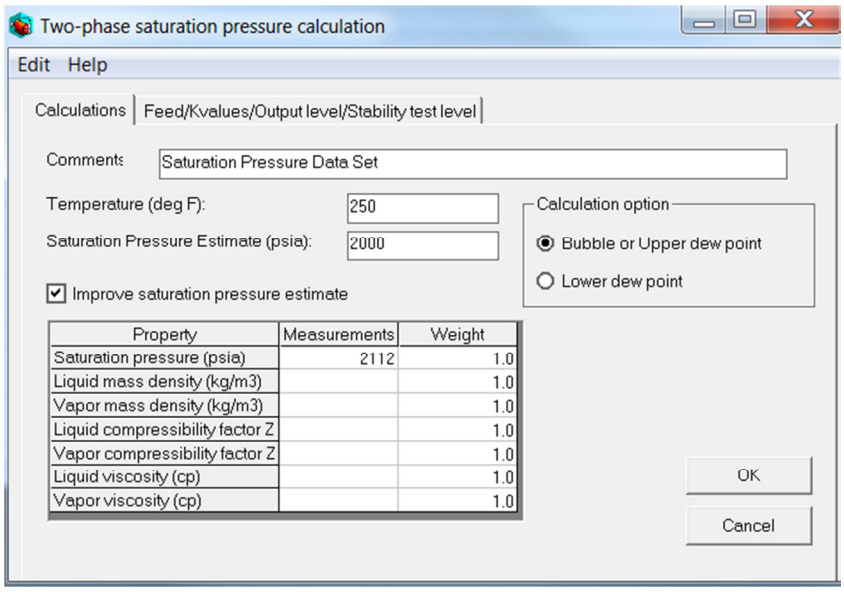

Figure 3.9: Details of the ″Saturation Pressure″ Calculation Tab as It Appears in WinProp

Finally, our data set is ready for modeling **(Figure 3.10)**. Upon running WinProp, the regression summary table at the end of the output file shows that an exact match to the saturation pressure is achieved as shown in **Figure 3.11**. The good match is a result of using several trials by manipulating the matching parameter (*i.e.,* volume shift and molecular weight), especially for the pseudo-component, to obtain the closest simulation results to the experimental data.

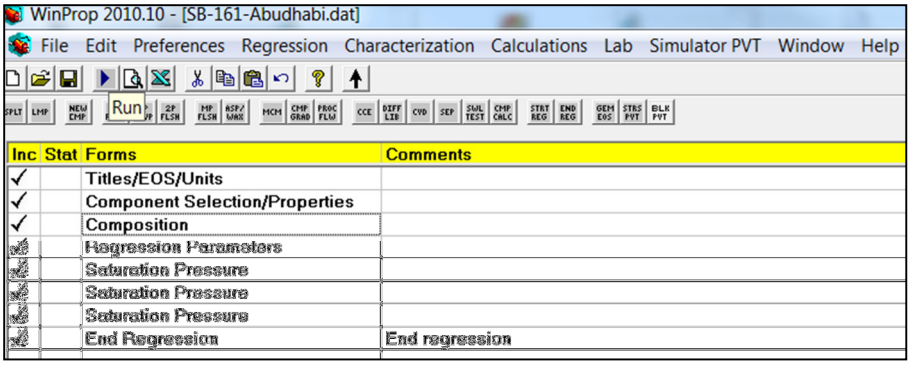

Figure 3.10: The WinProp Main Window After Entering All the Necessary Regression Data

We noticed the improved error reduction before and after regression in the regression summary in **Figure 3.11**. For example, the saturation pressure is 2112 psi **(Table 3.1)**. Before regression it was 2456.4 psi, and after regression it is 2107.7 psi for the first experimental data set. The same improvement in error reduction applies for the other set of saturation pressures (1739 psi and 1462 psi).

```
************************************************
Summary of Regression Results

   Calculation Data   Pressure  Experimental  Before     After      ERROR      ERROR     Weight
    option    type  (MF-SWELL)      data     regression regression reduction  after     factor
   ---------- ----  ---------- ------------ ---------- ---------- ---------- ---------- ----------
    5 PRESSAT
          PSAT      2.1120E+03  2.4564E+03  2.1077E+03  1.6101E-01  2.0396E-03 1.0000E+00
    5 PRESSAT
          PSAT      1.7390E+03  2.0985E+03  1.6934E+03  1.8051E-01  2.6201E-02 1.0000E+00
    5 PRESSAT
          PSAT      1.4620E+03  1.9168E+03  1.4954E+03  2.8828E-01  2.2812E-02 1.0000E+00

   ERROR Reduction = ERROR before regression - ERROR after regression
   ERROR = (experimental - calculated) / experimental

************************************************
```

Figure 3.11: Differences Between Experimental and Simulated Data as Shown in the Output File

The accuracy of the EOS depends solely on the accuracy of the data used in the regression. In order to avoid any problems related to the EOS, we need to make sure that the tuned parameters are within acceptable limits (WinProp, 2010).

- Selection of regression parameters

The selection of regression parameters is one of the most important steps that determine the degree of matching between the experimental and predicted data. Several parameters can be selected as the best regression parameters. However, WinProp uses a regression technique that selects the most important regression parameters, which reduces the number of trials needed and helps eliminate the problem associated with choosing the most important regression parameters (Burke *et al*., 1990). To match the experimental data, we will need to modify and manipulate the volume shift parameters of the heavy fraction pseudo-components. The volume shift of the asphaltene component will not be adjusted during regression, because it affects the amount of precipitate, as well as the liquid density (WinProp, 2010). The model is now ready for asphaltene precipitation prediction.

3.2.5 Asphaltene model selection

WinProp uses the solid precipitation model, which assumes that the asphaltene precipitation process is reversible. This assumption has been experimentally proved, where precipitated asphaltene will go back into the solution at lower pressures. Usually, the maximum amount of precipitation occurs close to the bubble point pressure (Pb) of the fluid as discussed in Section 2.4.2. Basically, gas is liberated from the oil, changing the solubility of the crude oil and inducing the re-dissolution of the precipitated asphaltene during the pressure depletion process.

The parameters that control this behavior in the solid model are the solid molar volume (V_s) and the interaction parameter (k_{ij}). Increasing the solid molar volume increases the maximum amount of precipitation at the saturation pressure, which is desired. Furthermore, increasing the interaction parameters between the heavy components (*i.e.,* asphaltene) and the light components (*i.e.,* C_1 - nC5) will induce the re-dissolution of the precipitated asphaltene. The experimental data for the well B-1 **(Table 3.2)** indicate that the amount of precipitation from this fluid is 0.21%.

Using the ″calculation tab″ in WinProp's main window, we select the asphaltene/wax modeling. Now, we open this newly added entry calculations tab and enter the asphaltene onset pressure (2209 psi) and temperature (250°F) as shown in **Figure 3.12**.

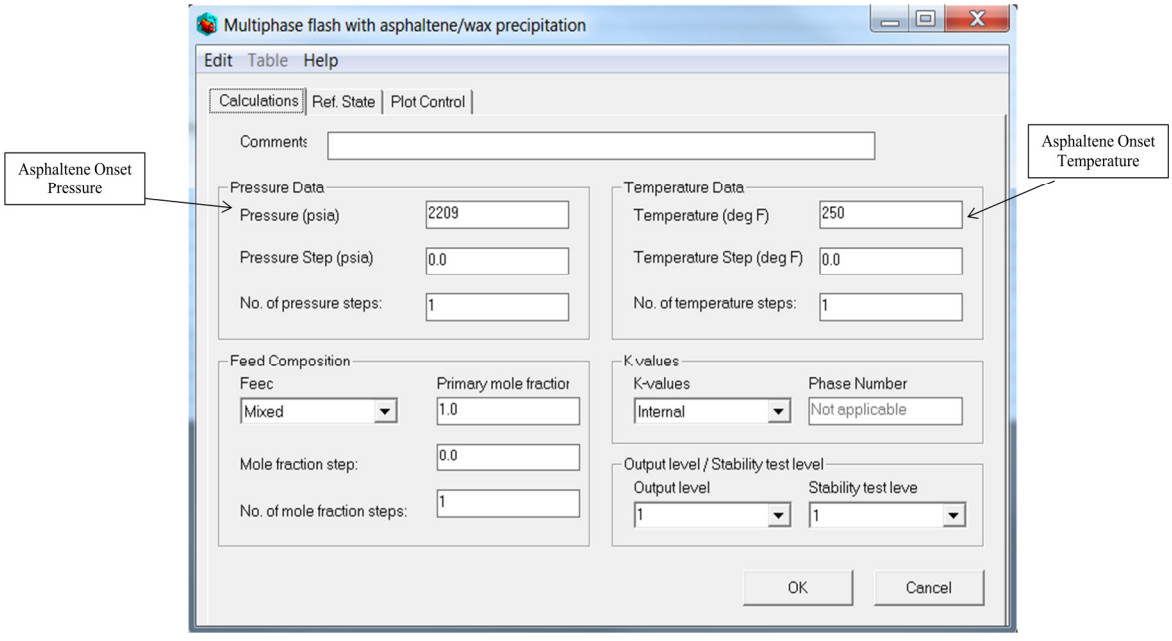

Figure 3.12: Asphaltene/Wax Modeling Calculations Tab as It Appears in WinProp

- Solid molar volume

Based on experimental observation, the solid molar volume should be set to a value slightly greater than the molar volume of the precipitating component predicted by EOS to help compensating for the volume errors (Nghiem and Dennis, 1997). The regression summary table shows that both the saturation pressure and stock tank API are matched exactly as shown in Figure 3.10. WinProp suggests that, if no experimental data exists for the solid molar volume, 1 L/mol will be a good initial value to start with as shown in **Figure 3.13**.

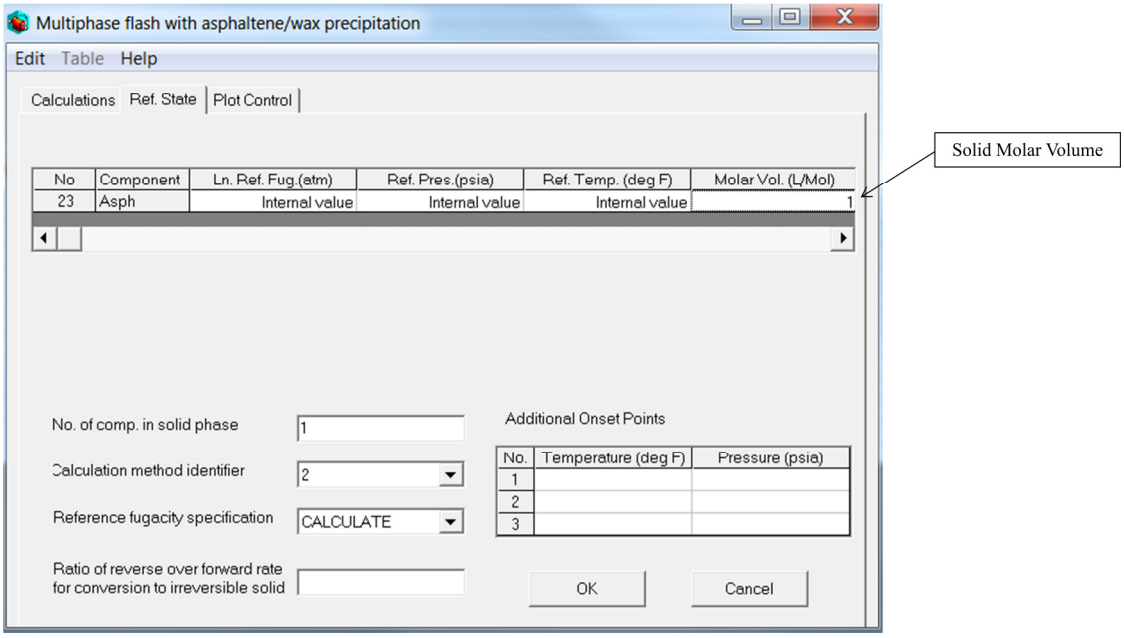

Figure 3.13: Asphaltene/Wax Modeling Reference State Tab as It Appears in WinProp

As discussed earlier, performing the regression allows the model to predict the correct fluid behavior when the interaction parameters for the asphaltene component changes, affecting the saturation pressure prediction in turn. The value of the solid molar volume

should be chosen carefully in order to achieve the desired maximum amount of precipitation. In our case, a value of 1 L/mol was gave good results.

3.2.6 Prediction of asphaltene precipitation

Asphaltene precipitation onset pressure can usually be accurately determined using asphaltene precipitation detection systems (SDS). In well B-1 data **(Table 3.3)** the amount of asphaltene precipitation is 0.21 wt% at the onset pressure of 2209 psi and 250 °F. Now, we run the WinProp to get the precipitation curve of the first trial. The shape of the resulted asphaltene precipitation curve for the first trial is shown in **Figure 3.14**.

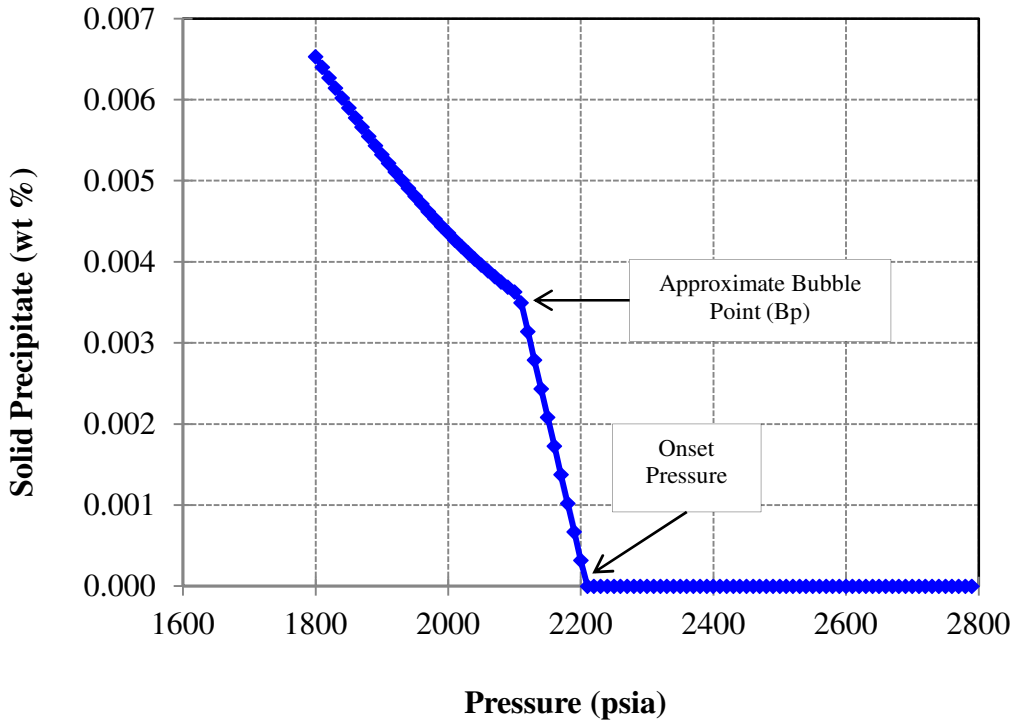

Figure 3.14: Asphaltene Precipitation (First Trial) for Well B-1 at 250°F

The shape of the precipitation curve does not seem to be correct, because it does not predict the offset pressure of asphaltene precipitation; instead, it shows the asphaltene onset pressure only. In order to fix the curve, we should consider correcting the solid model parameters, the molar volume and interaction parameters. In this case study, we focused on adjusting the interaction parameters between the asphaltene component and the light components (C_1 - nC_5) to obtain the correct shape of the precipitation curve that shows both the onset and offset of asphaltene precipitation. Interaction parameters between the asphaltene component and the components heavier than C_5 are zeros, where the great influence on the interaction coefficients is attributed to the light components.

To implement the adjustment in the interaction parameters in WinProp, we utilize the WinProp main window and select the component selection/properties **(Figure 3.1)**. Then, we select the interaction coefficients and HC-HC groups tabs as shown in **Figure 3.15** to specify pairs of binary interaction coefficients and try different interaction exponent values for each group until observing the correct asphaltene precipitation curve.

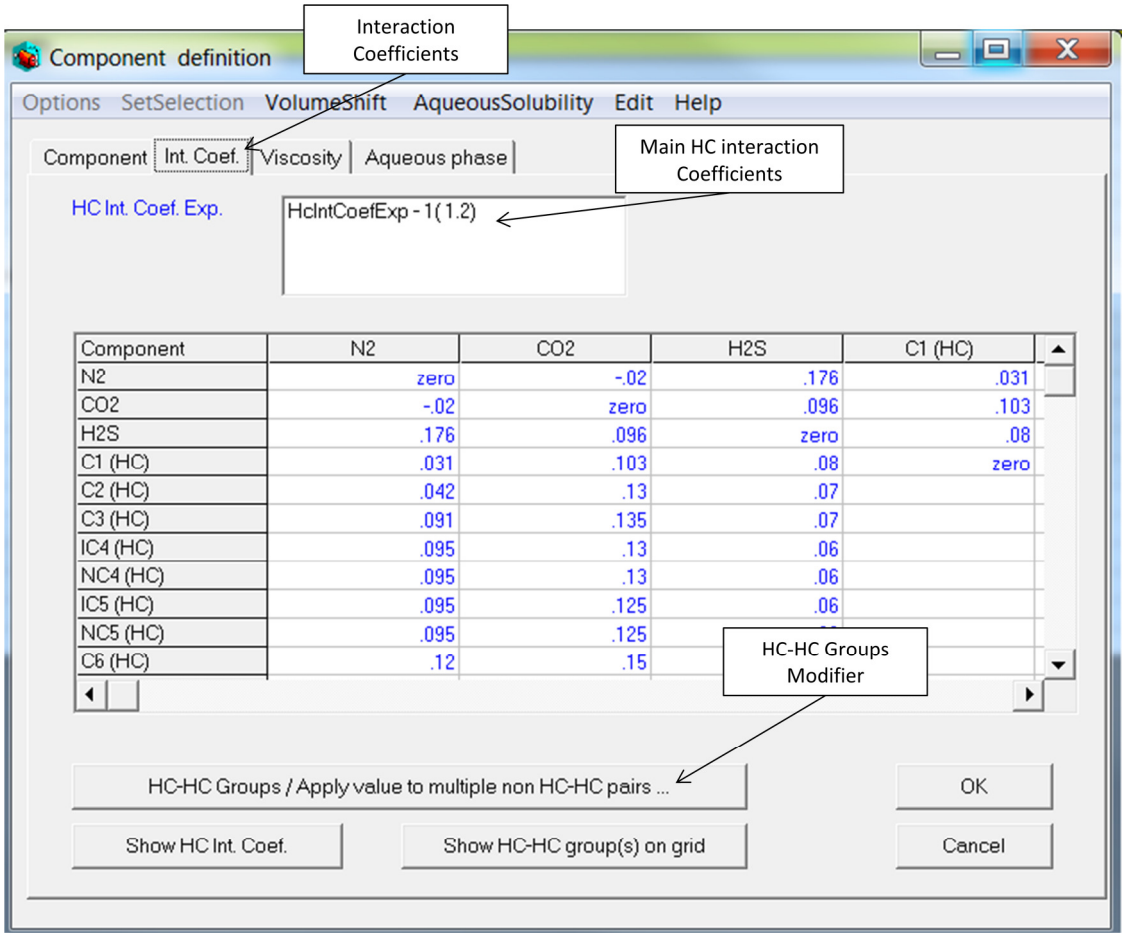

Figure 3.15: Interaction Coefficients Main Window as it Appears in WinProp.

Subsequently, we move to the interaction coefficients grouping window **(Figure 3.16)** and apply the following four steps:

- Select the HC-HC type pairs
- Create a new group
- Select the desired number of interaction parameters needed between C_n and asphaltene
- Try different exponent value until getting the correct precipitation curve

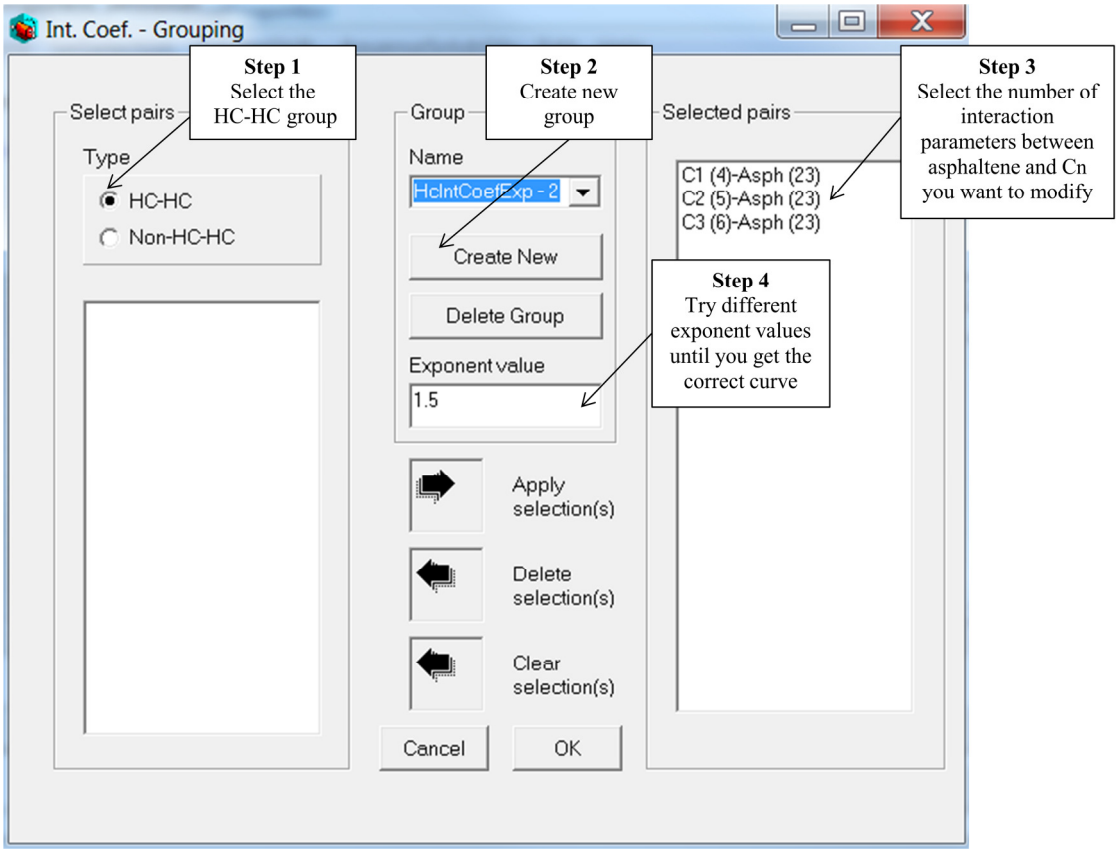

Figure 3.16: Interaction Coefficients Grouping Window

Binary interaction coefficients between two hydrocarbon components are calculated using **Equation 3.2.17**, which involves the critical volume of each component (v_{ci}) and an exponent parameter (θ) for computing interaction coefficients.

$$\delta_{ij} = 1 - \left(\frac{2 v_{ci}^{\frac{1}{6}} v_{cj}^{\frac{1}{6}}}{v_{ci}^{\frac{1}{3}} + v_{ci}^{\frac{1}{63}}}\right)^{\theta} \qquad (\mathbf{3.2.17})$$

We run the WinProp again using three interaction groups between the asphaltene component and the components C_1 through C_3 (C_4 and C_5 can be included as needed), and using an arbitrary exponent value (θ) of 1.5 as the first guess. The resulting

asphaltene precipitation curve **(Figure 3.17)** is showing much improvement than the previous curve **(Figure 3.14)**. We repeat this process using different exponent values until we get the correct asphaltene precipitation curve. The final asphaltene precipitation curve **(Figure 3.18)** was obtained using an exponent value (θ) of 1.9.

Table 3.4 shows a summary of the figures before and after adjusting the interaction coefficients along with the exponent's values. **Table 3.5** shows the final binary interaction coefficients between the different components used in the case study.

Table 3.4: Summary of the Figures Before and After Adjusting the Exponent Values

Before adjusting the interaction coefficients	
	Exponent Value (θ)
Figure 3.14	N/A
After adjusting the interaction coefficients	
	Exponent Value (θ)
Figure 3.17	1.5
Figure 3.18	1.9

Table 3.5: Binary Interaction Coefficients Between the Different Components Used in the Case Study

	CO2	C1	C2	C3	HC1	HC2	HC3	HC4	HC5	C36+	Asph
CO2	0										
C1	-0.02	0									
C2	0.031	0.103	0								
C3	0.042	0.13	0.0027	0							
HC1	0.091	0.135	0.0085	0.0017	0						
HC2	0.095	0.13	0.018	0.0069	0.0018	0					
HC3	0.12	0.15	0.0319	0.0164	0.0077	0.0021	0				
HC4	0.12	0.15	0.0471	0.028	0.0163	0.0073	0.0016	0			
HC5	0.12	0.15	0.0833	0.058	0.041	0.0261	0.0137	0.006	0		
C36+	0.12	0.15	0.1166	0.0874	0.0668	0.0479	0.0307	0.0186	0.0036	0	
ASPH	0.12	0.15	0.1329	0.1022	0.0802	0.0596	0.0404	0.0264	0.0075	0.0007	0

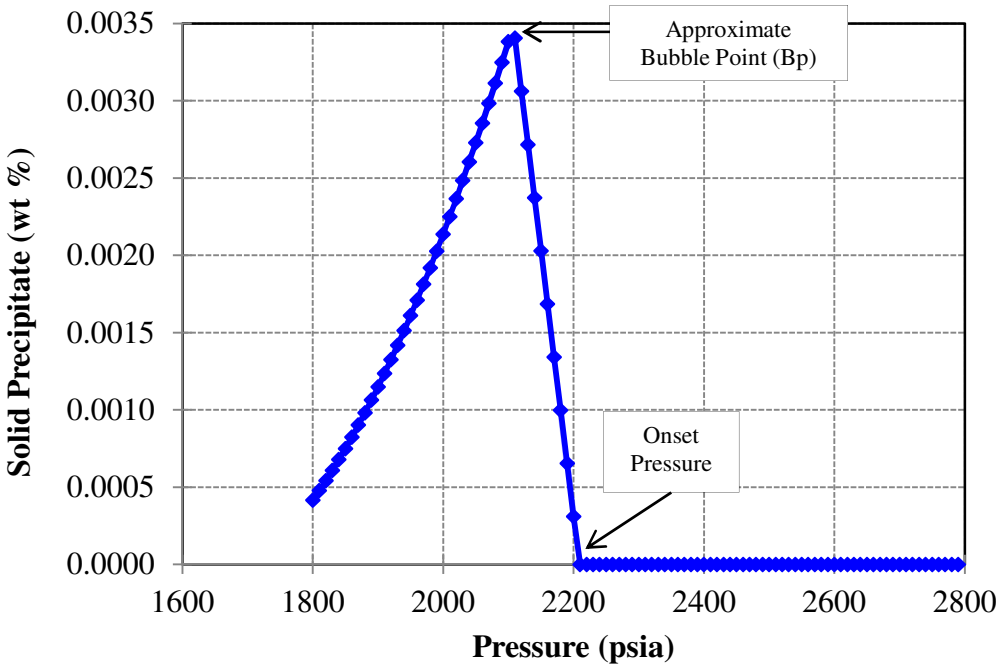

Figure 3.17: Asphaltene Precipitation Using an Exponent Value (θ) of 1.5 for Well B-1 at 250°F

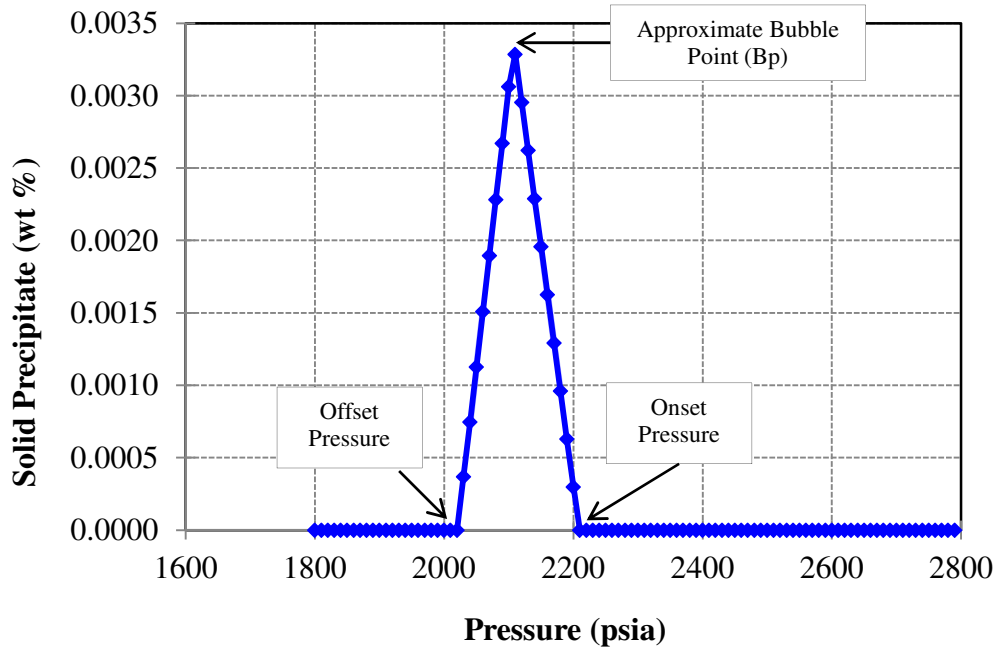

Figure 3.18: Asphaltene Precipitation Using an Exponent Value (θ) of 1.9 for Well B-1 at 250°F

It was found that the interaction coefficients between the asphaltene component and the light components have a great influence on the prediction of asphaltene precipitation. A larger value for interaction coefficient parameter between asphaltene and light components will cause a greater amount of precipitation. Also the amount of solid molar volume has influence, too, but our initial guess (1L/mol) was sufficient.

The asphaltene component is identified by splitting the heaviest component of the oil into precipitating and non-precipitating components. These two components have the same critical properties (*i.e.*, Pc and Tc) and acentric factors. The two phase envelope for well B-1 is shown in **Figure 3.19**.

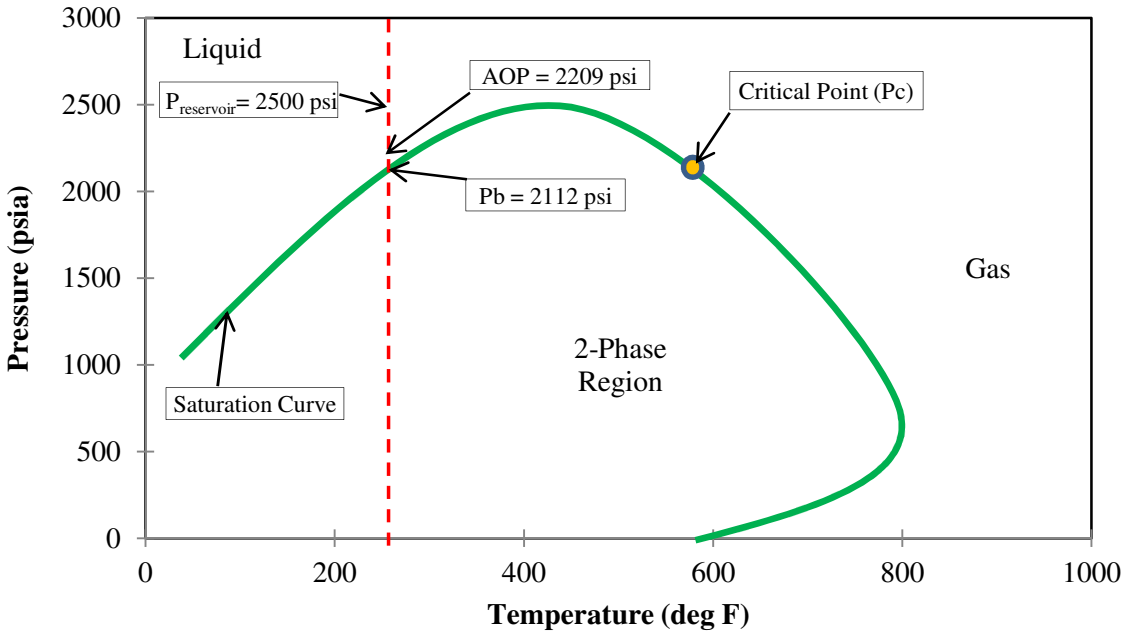

Figure 3.19: Asphaltene Phase Behavior Envelope for Well B-1

The same detailed process for modeling the phase behavior of reservoir fluids in order to predict the asphaltene precipitation was applied to the rest of the four wells (B-2, B-3, A-1, and A-2). The results of the precipitation curves for well B-2, B-3, A-1 and A-2 are shown in **Figure 3.20**, **Figure 3.21**, **Figure 3.22**, and **Figure 3.23**, respectively. The detailed compositions before and after lumping along with saturating pressures and temperatures of the four wells are shown in **Appendix A**. The final exponent values used for interaction parameters are presented in **Table 3.5**.

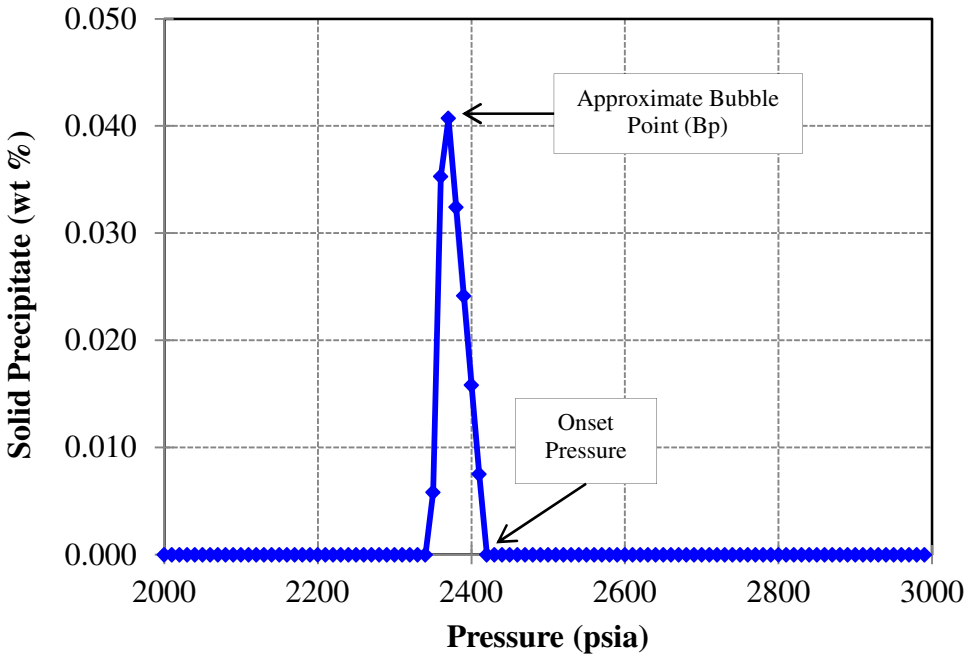

Figure 3.20: Asphaltene Precipitation for Well B-2 at 254°F

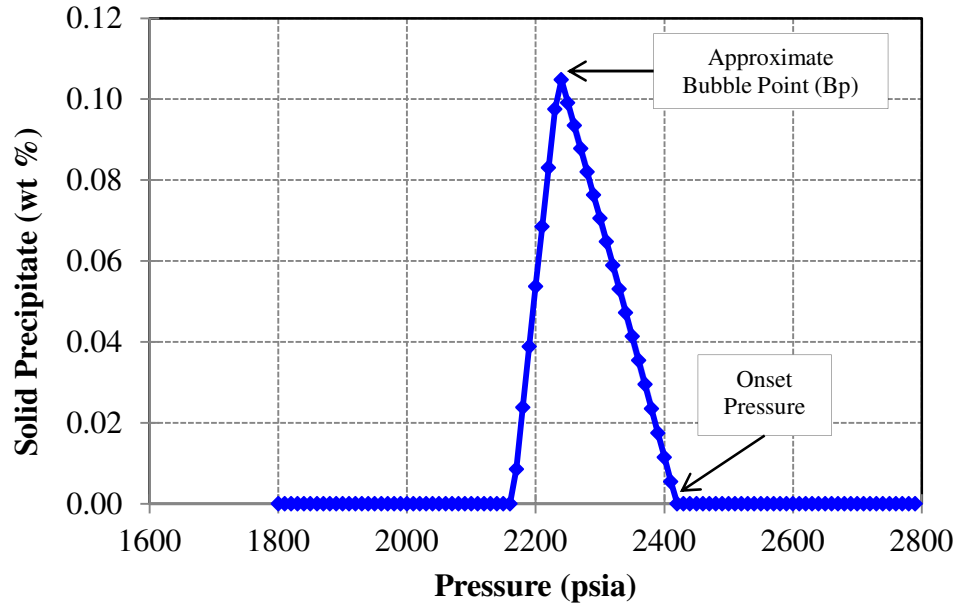

Figure 3.21: Asphaltene Precipitation for Well B-3 at 254°F

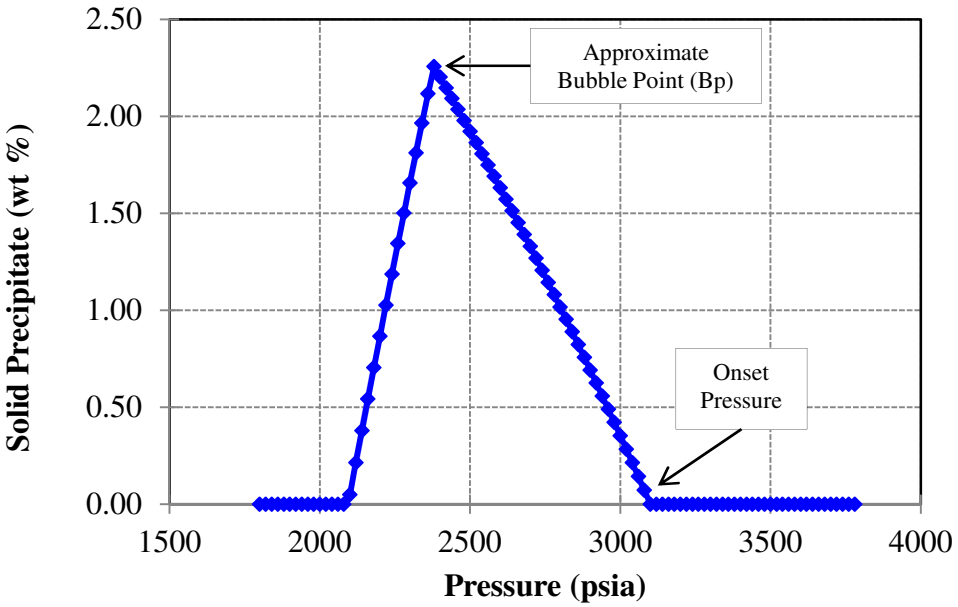

Figure 3.22: Asphaltene Precipitation for Well A-1 at 220°F

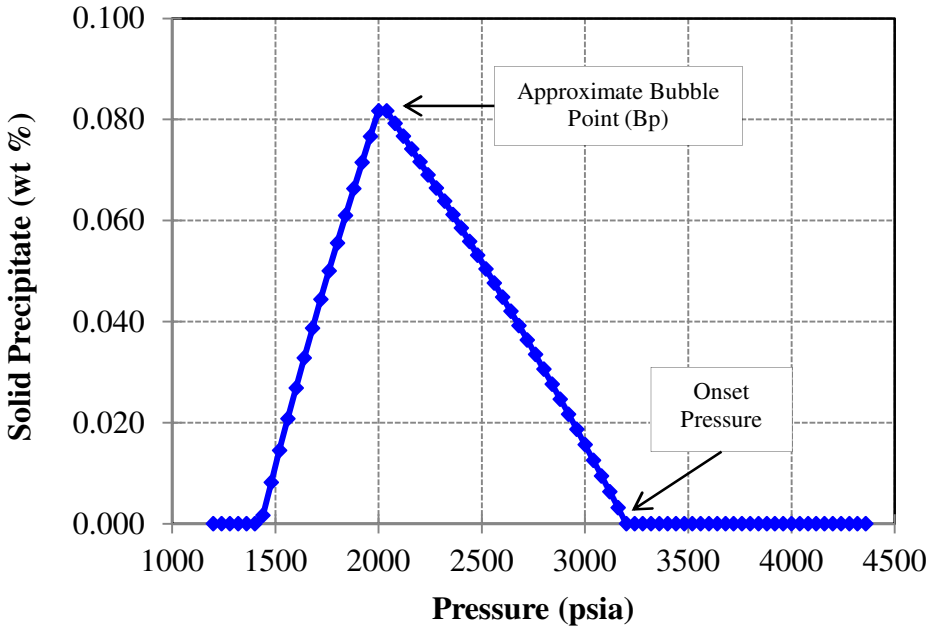

Figure 3.23: Asphaltene Precipitation for Well A-2 at 212°F

Using obtained matching parameters from sensitivity analysis along with the chosen techniques for estimation of critical properties, acentricities of SCNs, pseudo-components and binary interaction coefficients, the model showed a high sensitivity to binary interaction coefficients. This is essential for modeling the compositional effect, and by choosing the appropriate interaction coefficients, it results in a significant improvement in prediction of asphaltene precipitation curve. The volume shift of the asphaltene component in solution is an important parameter for modeling asphaltene precipitation, where it minimizes the errors related to the estimation of solid molar volume.

In summary, three main steps are required in modeling the phase behavior of reservoir fluids. In the first step, the fluid system is represented by a large number of components (*i.e.,* C_1, C_2, C_3, ..., C_{12+}). The fluid characterization and plus fraction process is followed by simple calculations such as saturation pressure calculations, which are performed on the multi-component system. In most cases, the EOS can accurately predict the saturation pressure with little adjustment to the hydrocarbon interaction coefficient exponent (HICE). The second step, involves the lumping of the multi-components group into fewer component groups. Finally, asphaltene precipitation is indicated and the differences between the experimental and simulated data are examined and the precipitation curve is plotted.

3.3 Comparison Study OF Asphaltene Precipitation Models in the Simulators of UTCOMP, CMG/GEM and ECLIPSE

3.3.1 Introduction

Solid model is used in UTCOMP, CMG/GEM and ECLIPSE simulators for asphaltene precipitation prediction. WinProp (a PVT utility from CMG/GEM) has been used to generate the data for all simulators. Section 3.2 discusses the solid model and reservoir fluid characterization using WinProp in detail. There are some differences between the three simulators in permeability reduction models, porosity reduction, and formation damage. Section 2.8.9 highlights the main differences between the models.

ECLIPSE and CMG/GEM consider that total asphaltene precipitation to consist of two parts: one part is the adsorbed portion that deposits on the formation rock, and the second part is the flowing portion precipitates (flocs) that remains in the oil phase. On the other hand, UTCOMP considers the total asphaltene precipitation to precipitate and deposit on the formation rock that does not flow with the oil. ECLIPSE assumes that the precipitation process does not change the fluid composition, whereas CMG/GEM and UTCOMP assume this damage.

ECLIPSE and UTCOMP also consider that asphaltene precipitation will cause some damages that affect the original porosity while CMG/GEM assumes the same porosity when asphaltene precipitation occurs. ECLIPSE and UTCOMP uses the same rock permeability reduction model due to asphaltene which is called the parameterized power-law relationship, whereas CMG/GEM uses the resistance factor relationship. This

relation has now been generalized such that the power-law or Carman-Kozeny (CMG/GEM, 2010) relations with adjustable exponents can be used for permeability reduction calculations, similar to ECLIPSE and UTCOMP's models. The reference fugacity is an input parameter in CMG/GEM while it is calculated automatically in ECLIPSE and UTCOMP which requires several trials to guess the matching value in CMG/GEM.

3.4 One-Dimensional Simulation Study

3.4.1 Simulation run details

This case study was developed using a simple one-dimensional model. The porosity (single model) is 0.30 and the isotropic permeabilities in all directions are 800 md and they are uniform in the whole reservoir. The reservoir fluid used in this study was presented in **Table 3.1** and **Table 3.2**. The initial reservoir pressure is 2500 psi and the bubble point pressure (Pb) is 2112 psi. The simulated one-dimensional reservoir has a grid dimension of 100 × 1 × 1. The width of each grid block in the x and y directions is a uniform 80 ft with a uniform vertical gridlock thickness of 20 ft. The injector is located at block 1 (left edge of the reservoir) and the other boundary is producer as shown in **Figure 3.24**. The producer operates under a constant bottomhole pressure (BHP) of 1000 psi. Water injection is commenced at a constant rate of 200 STB/day. The breakthrough time is 1678 days. CO_2 injection was started five months after the breakthrough time and continued for three years at a rate of 200 MSCF/day. The total simulation time is eight years.

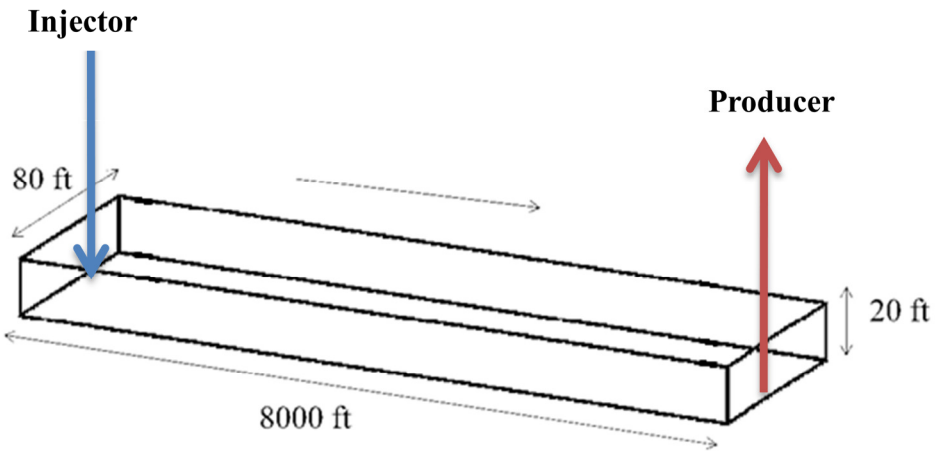

Figure 3.24: Block Dimensions of Simulated Reservoir With Grid 100 × 1 × 1

3.4.2 Input data

In Section 3.3.1 we highlighted some of the differences in the models related to asphaltene precipitation between UTCOMP, CMG/GEM, and ECLIPSE. Considering these differences, the input files for the three simulators were adjusted to allow the best possible consistent comparison between the simulators. For example, the relative permeability model used is the same for all three phases; relative permeability is plotted in **Figure 3.25** and **Figure 3.26**. Also, the reservoir fluid characterization data generated from WinProp (Section 3.2.1) is the same for all files. Furthermore, the critical compressibility factor was used in the ECLIPSE input file instead of critical volume to improve the match with the other simulators. Reference fugacity and pressure are 4.61×10^{-12} atm and 2209 psi, respectively. The same input data are applied for all simulators.

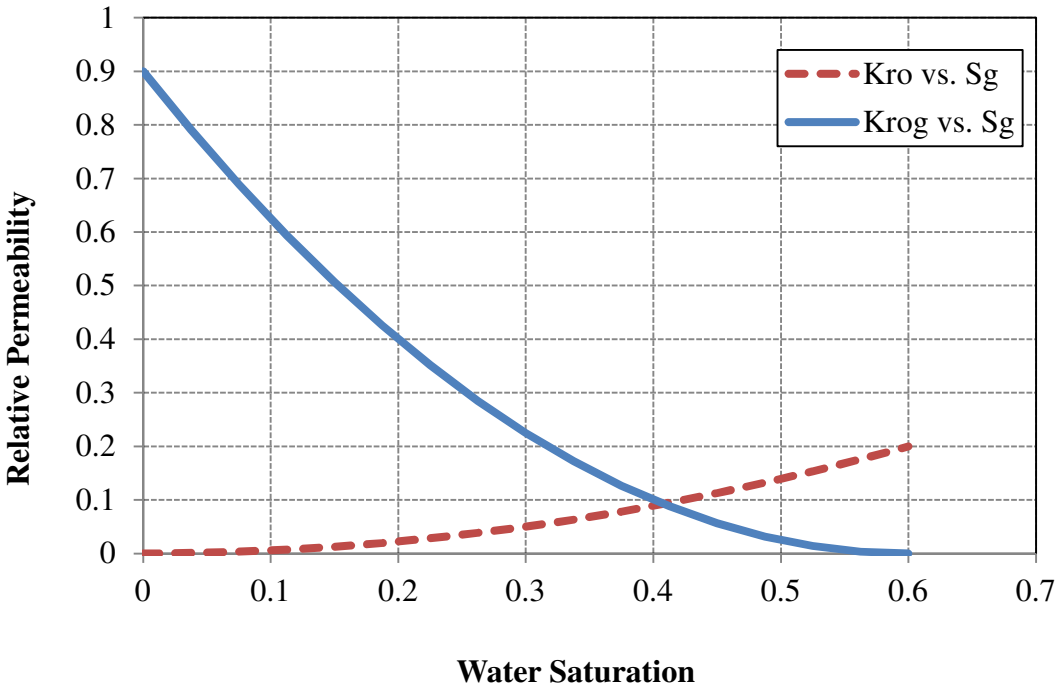

Figure 3.25: Gas-Oil Relative Permeability Curve

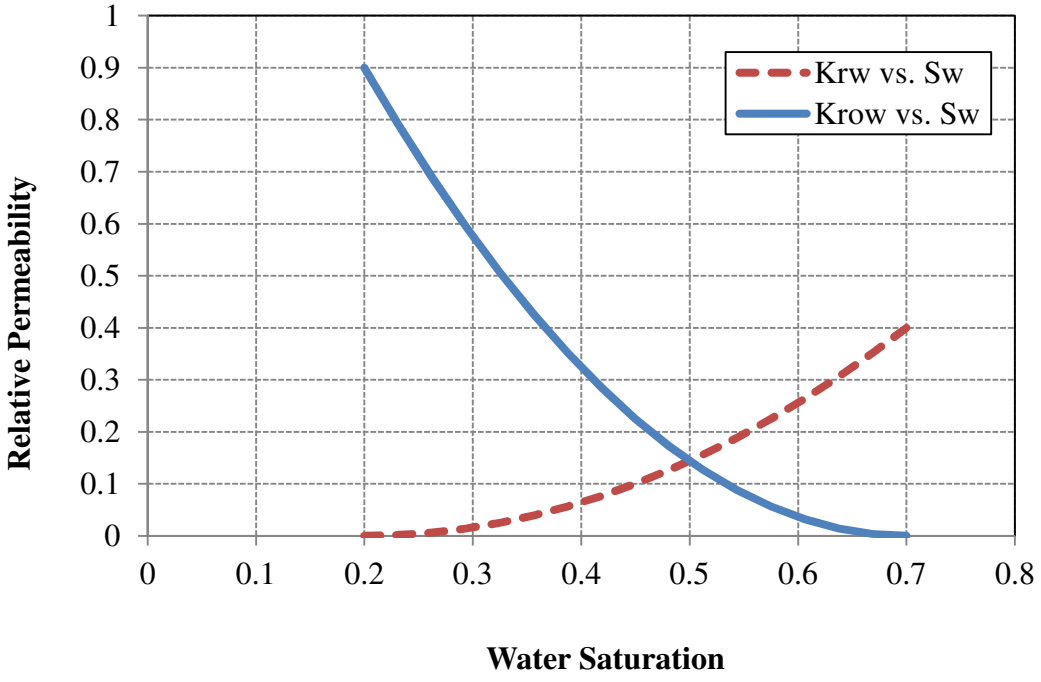

Figure 3.26: Water-Oil Relative Permeability Curve

The reservoir fluid data for well B-1 were analyzed with WinProp to generate the asphaltene precipitation curve (**Figure 3.27**). The asphaltene onset pressure (AOP), a pressure where asphaltene starts precipitating, was observed experimentally at 2209 psi; additionally, the bubble point pressure was found to be 2112 psi. The AOP is roughly 100 psi higher than the bubble point (**Figure 3.27**).

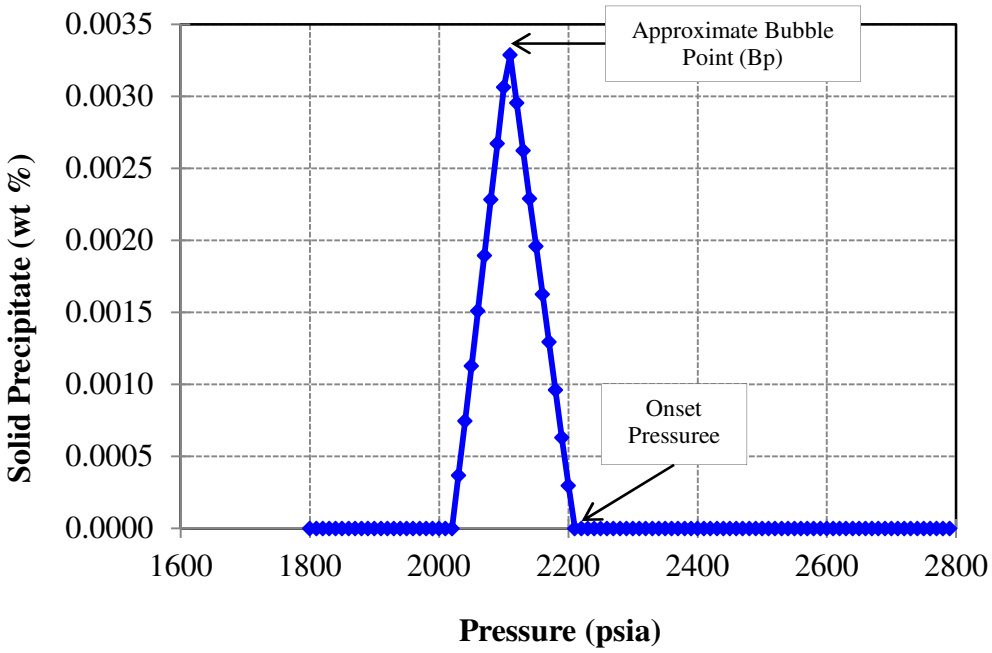

Figure 3.27: Asphaltene Precipitation Curve

3.4.3 Results and discussion

This section is a summary of the simulation results generated by three simulators; UTCOMP, CMG/GEM and ECLIPSE. Three cases (for each simulator) were run, the list of the runs is given in **Table 3.6**.

Table 3.6: The list of the runs

Simulators	UTCOMP, CMG/GEM, and ECLIPSE
1st Run	
Waterflooding without asphaltene option	**Figure 3.28**, **Figure 3.29** and **Figure 3.30**
2nd Run	
Waterflooding and Co_2 injection without asphaltene precipitation	**Figure 3.31**, **Figure 3.32**, **Figure 3.33 and Figure 3.34**
3rd Run	
Waterflooding and Co_2 injection with asphaltene precipitation	**Figure 3.35**

The UTCOMP, ECLIPSE, and CMG/GEM input files are presented in **Appendix B**, **Appendix C,** and **Appendix D,** respectively. The first case was run to investigate the production rates for the different simulators (UTCOMP, CMG/GEM, and ECLIPSE) during the waterflooding period without considering the asphaltene option. Water injection was continued for almost five years. The results show a very good match of the production rates between CMG/GEM and ECLIPSE during the waterflooding period, the breakthrough time takes place after 1678 days. **Figure 3.28**, **Figure 3.29** and **Figure 3.30** show the comparison of gas, oil and, water production rates between UTCOMP, CMG/GEM, and ECLIPSE.

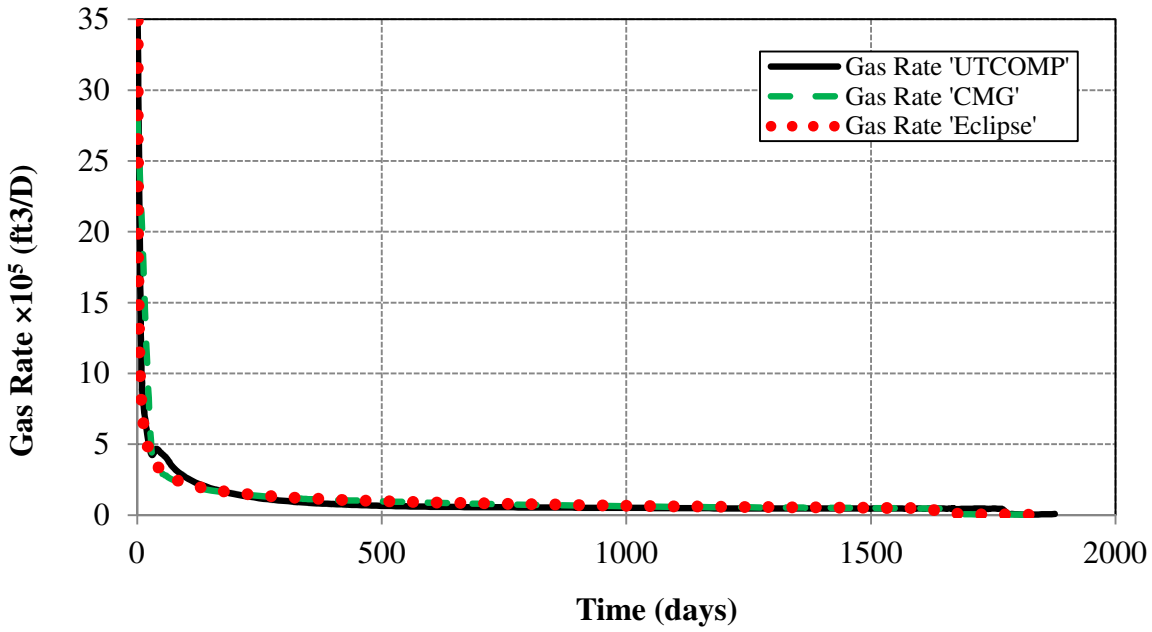

Figure 3.28: Gas Rate Comparison Between CMG/GEM, ECLIPSE, and UTCOMP (Waterflooding)

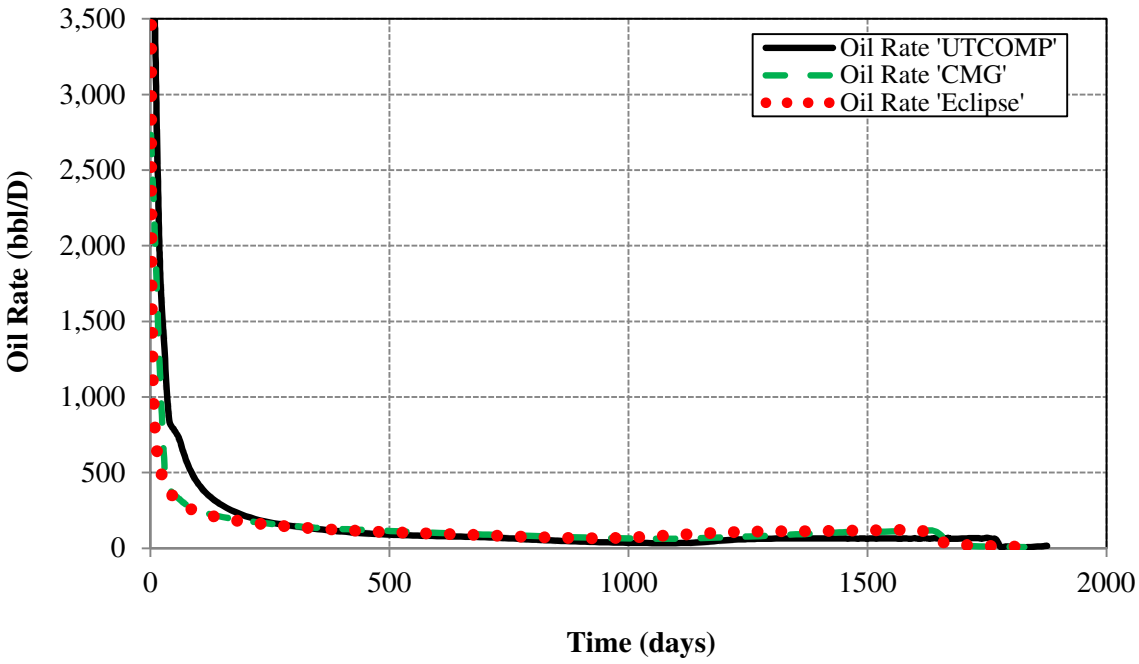

Figure 3.29: Oil Rate Comparison Between CMG/GEM, ECLIPSE, and UTCOMP (Waterflooding)

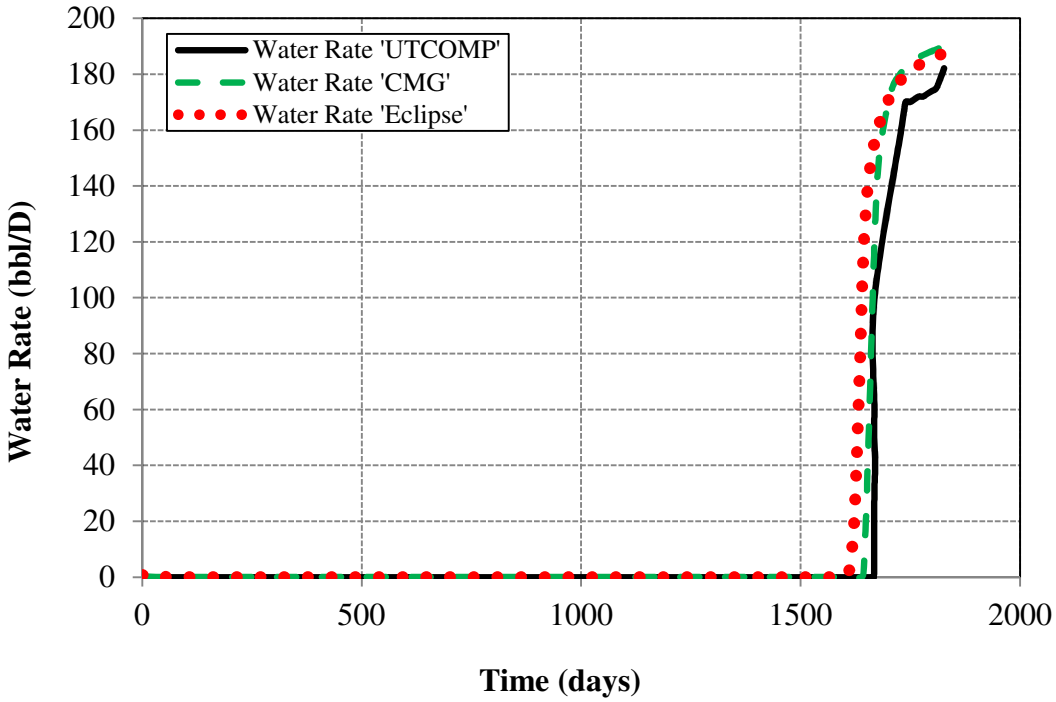

Figure 3.30: Water Rate Comparison Between CMG/GEM, ECLIPSE, and UTCOMP (Waterflooding)

The second run investigated the production rates for the different simulators (UTCOMP, CMG/GEM, and ECLIPSE) during the waterflooding and CO_2 period without considering the asphaltene option. CO_2 injection was started five months after the breakthrough time as can be seen by the increase in the oil and gas rates, the injection continued for almost three years. As for the waterflooding case, the results show a very good match of the production rates between CMG/GEM and ECLIPSE during the waterflooding period, the breakthrough time takes place after 1678 days. **Figure 3.31**, **Figure 3.32**, **Figure 3.33**, and **Figure 3.34** show the comparison of gas production rates, oil production rates, water production rates and average reservoir pressure, respectively between UTCOMP, CMG/GEM, and ECLIPSE.

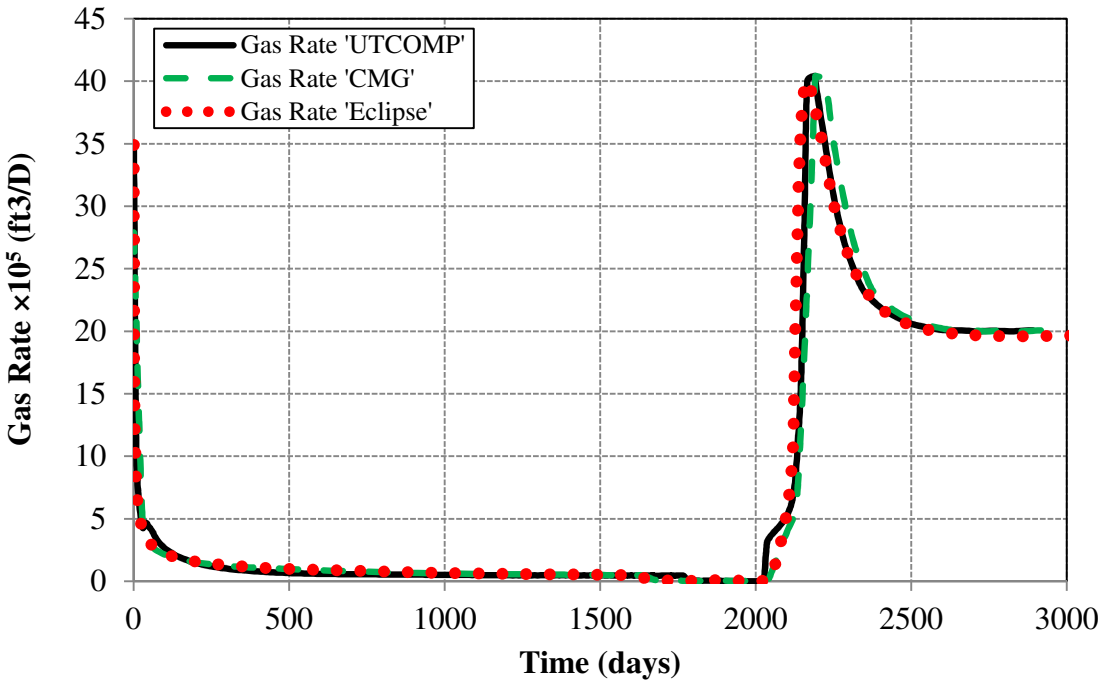

Figure 3.31: Gas Rate Comparison Between CMG/GEM, ECLIPSE, and UTCOMP (Waterflooding and CO_2 Injection)

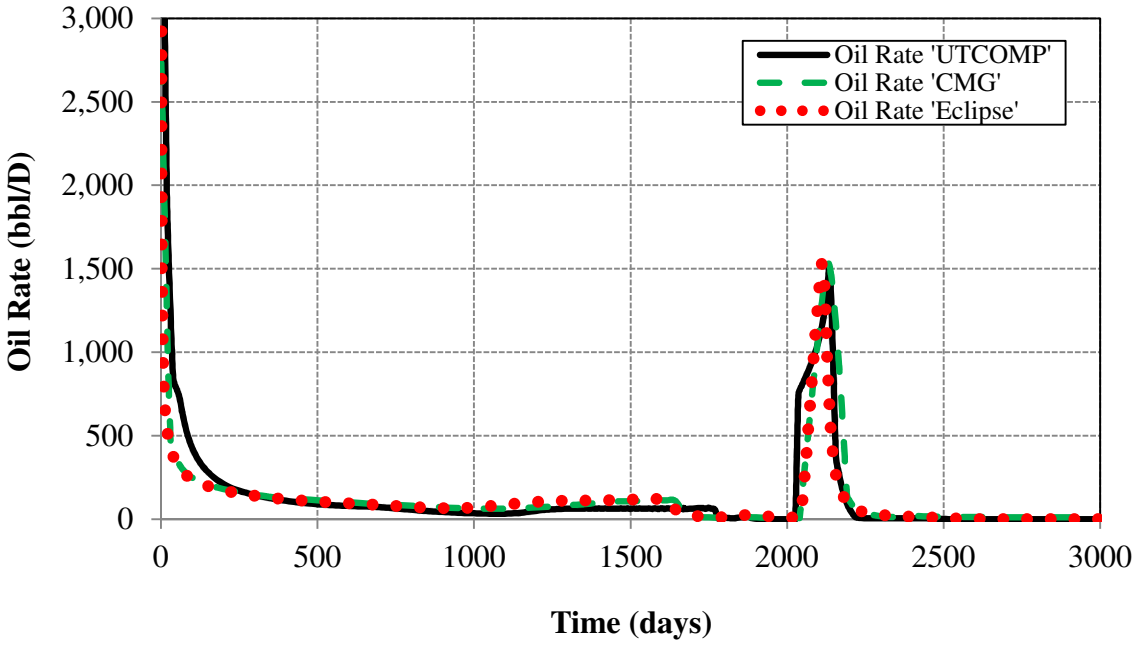

Figure 3.32: Oil Rate Comparison Between CMG/GEM, ECLIPSE, and UTCOMP (Waterflooding and CO_2 Injection)

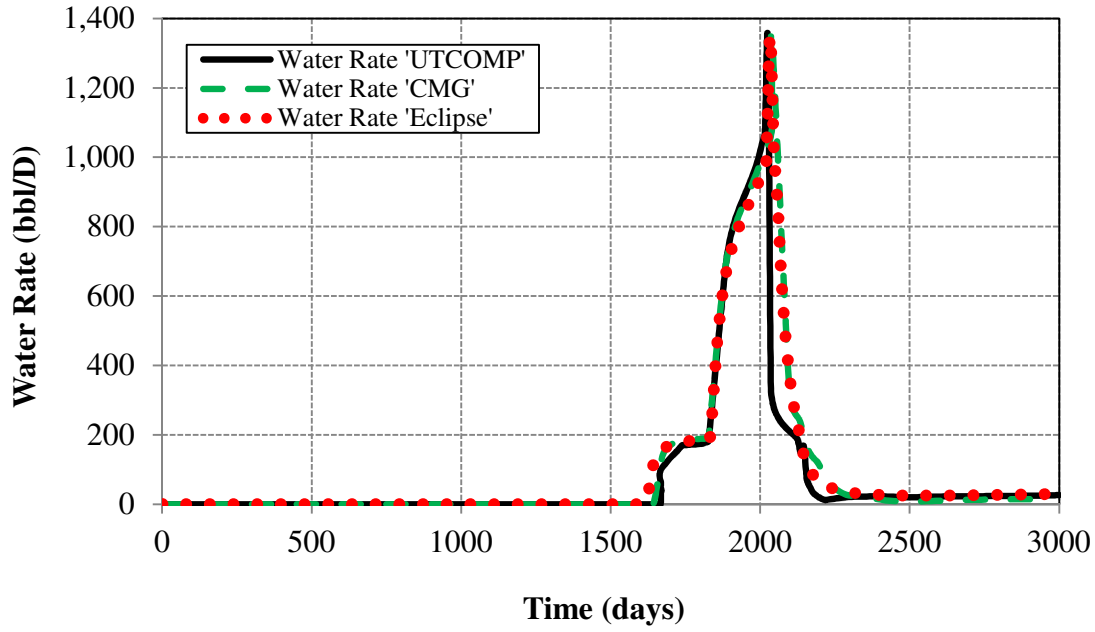

Figure 3.33: Water rate comparison between CMG/GEM, ECLIPSE and UTCOMP (waterflooding and Co_2 injection)

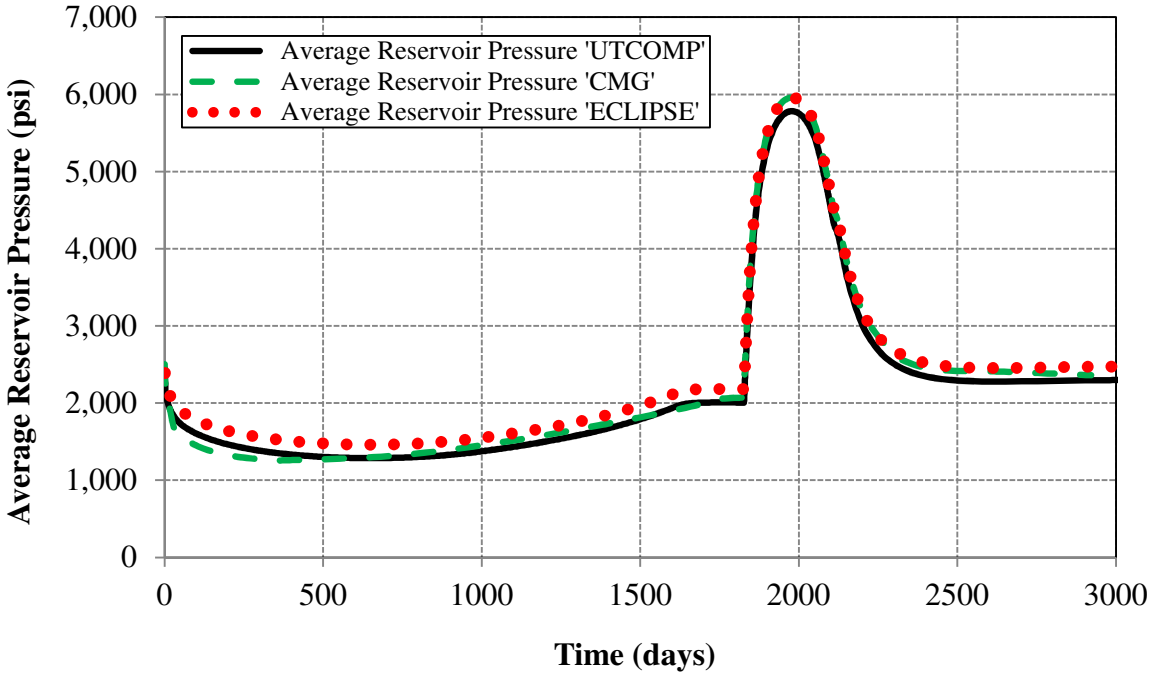

Figure 3.34: Average Reservoir Pressure Comparison Between CMG/GEM, ECLIPSE, and UTCOMP (Waterflooding and CO_2 Injection)

The excellent match between UTCOMP, CMG/GEM, and ECLIPSE in the comparison cases is attributed to the use of the same original fluid composition in all simulators. The critical properties and binary interaction coefficients (BIC) along with similar initial and constraint conditions lead to the excellent match in the predicted production rates and average reservoir pressures.

The third run investigated the effect of asphaltene precipitation on oil production rate for the different simulators (UTCOMP, CMG/GEM, and ECLIPSE) during the waterflooding and CO_2 period by considering the asphaltene option. By comparing oil rates without asphaltene considering asphaltene between CMG/GEM, ECLIPSE, and UTCOMP shown in **Figure 3.31** with the results of when considering the asphaltene option shown in **Figure 3.34**, we notice that the oil production rate obtained without asphaltene precipitation is higher than that with the asphaltene precipitation for all simulators (UTCOMP, CMG/GEM, and ECLIPSE) with different degrees from one simulator to another, **Figure 3.35** show a comparison of oil rates with and without asphaltene for the CMG/GEM simulator. In general, this would be expected since asphaltene precipitation causes a reduction in the permeability.

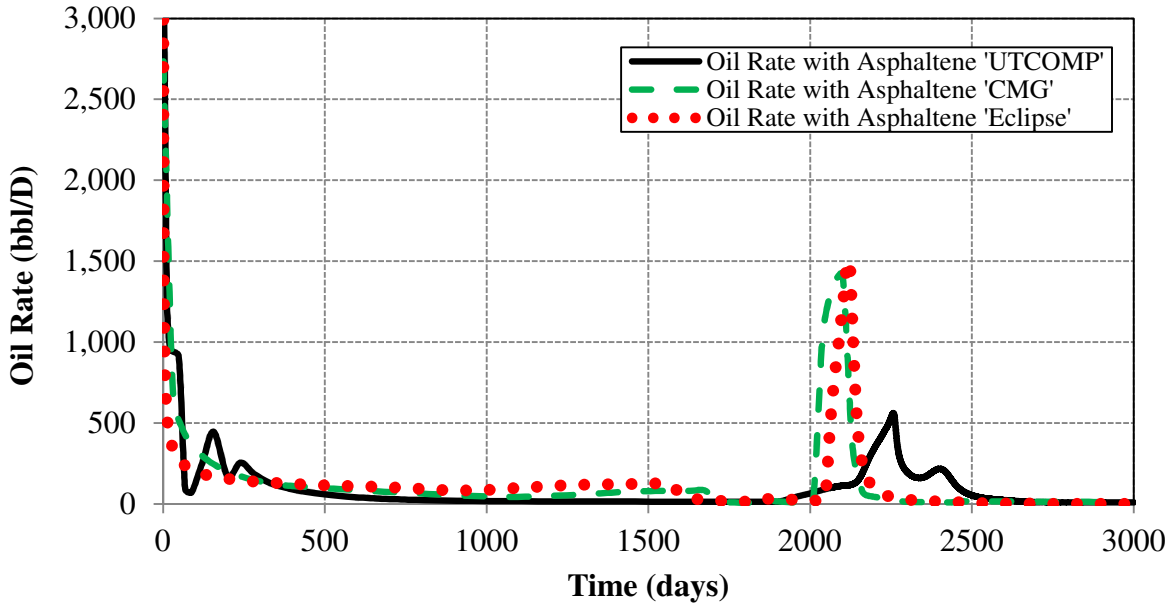

Figure 3.35: Oil Rate Comparison Between CMG/GEM, ECLIPSE, and UTCOMP (Waterflooding and CO_2 Injection) With Asphaltene Precipitation

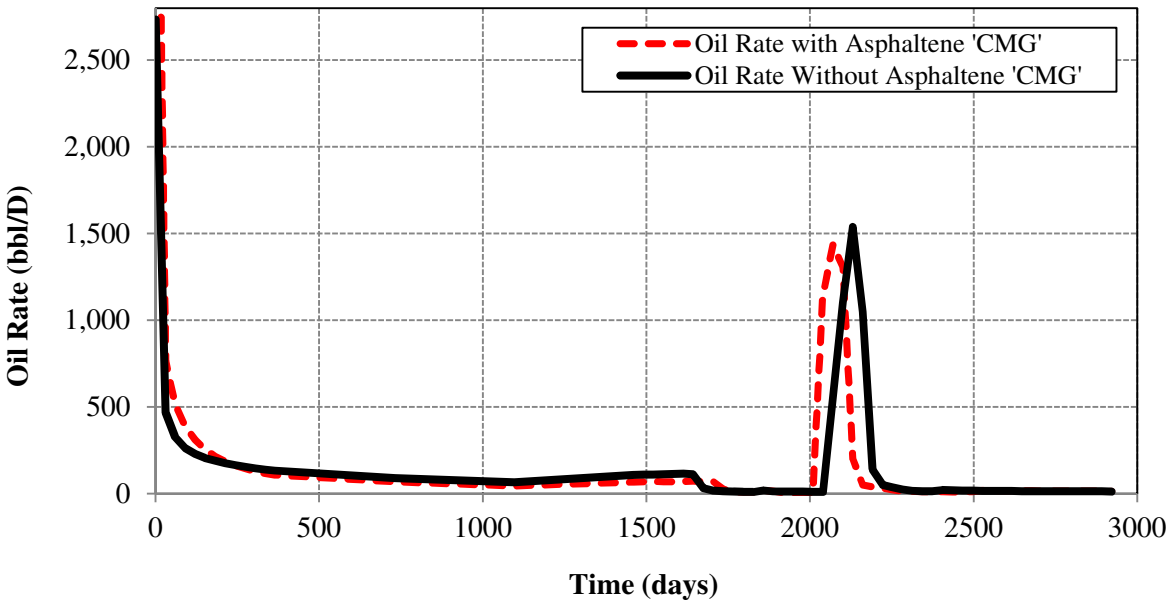

Figure 3.36: Oil Rate Comparison for CMG/GEM With and Without Asphaltene Precipitation

The sharp decline in the oil rate obtained from UTCOMP compared to the oil rate obtained from CMG/GEM and ECLIPSE may be attributed to the reason that ECLIPSE and CMG/GEM considers the total asphaltene precipitation to come from two parts: one part is the adsorbed portion that deposits on the formation rock, and the second part is the flowing portion precipitates (flocs) that remains in the oil phase. On the other hand, UTCOMP considers the total asphaltene precipitation to precipitate and deposit on the formation rock that does not flow with the oil. Also, UTCOMP considers that asphaltene precipitation will cause some damages that affect the original porosity in terms of porosity decline while CMG/GEM and ECLIPSE assumes the same porosity when asphaltene precipitation occurs.

Asphaltene precipitation is investigated for the three simulators (UTCOMP, CMG/GEM, and ECLIPSE) without considering the flocculation option. The pressure at which the asphaltene just starts to precipitate (P^*) was taken as 2209 psi for the reservoir fluid used in these runs for all simulators. However, as mentioned earlier, the fugacity is an input parameter in CMG/GEM, while it is calculated automatically in UTCOMP by equating it to the fugacity of the heaviest component in the liquid phase at P^*. f^* was calculated from WinProp (lnf^* = -26.102 atm) and used as an input for CMG/GEM simulation. **Figure 3.6**, **Figure 3.7** and **Figure 3.8** show the asphaltene precipitation for UTCOMP, CMG/GEM, and ECLIPSE, respectively. The trend of asphaltene precipitation for the three simulators show that most of the precipitation occurs close to the production vicinity, which is expected due to the pressure drop associated with the production vicinity.

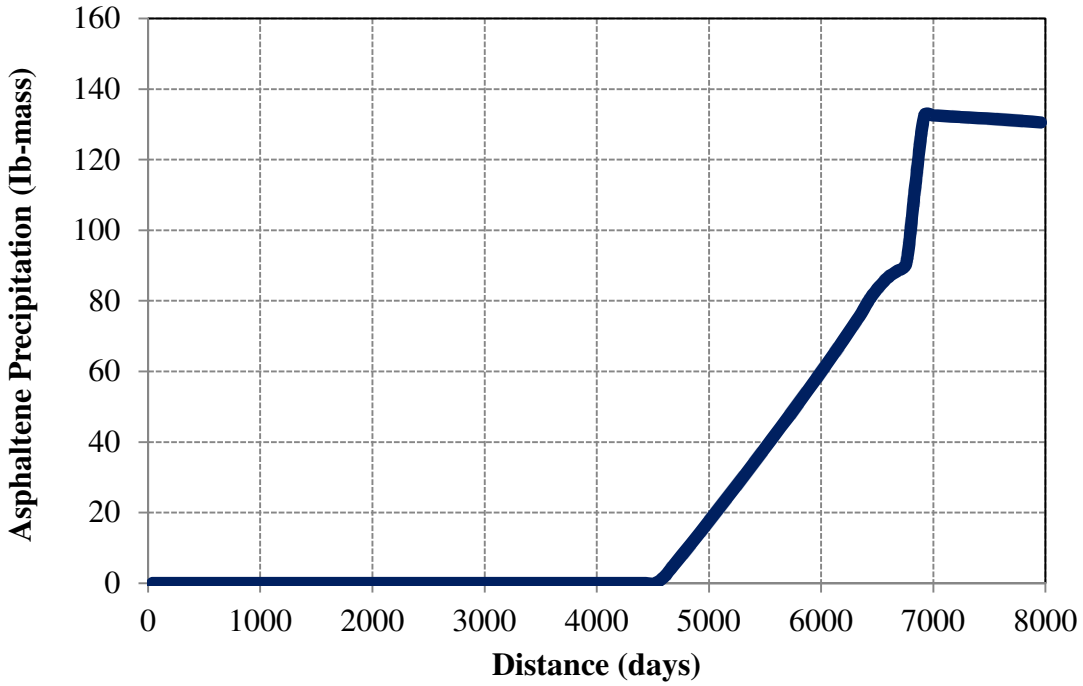

Figure 3.37: Asphaltene Precipitation Weight Fraction Using CMG/GEM

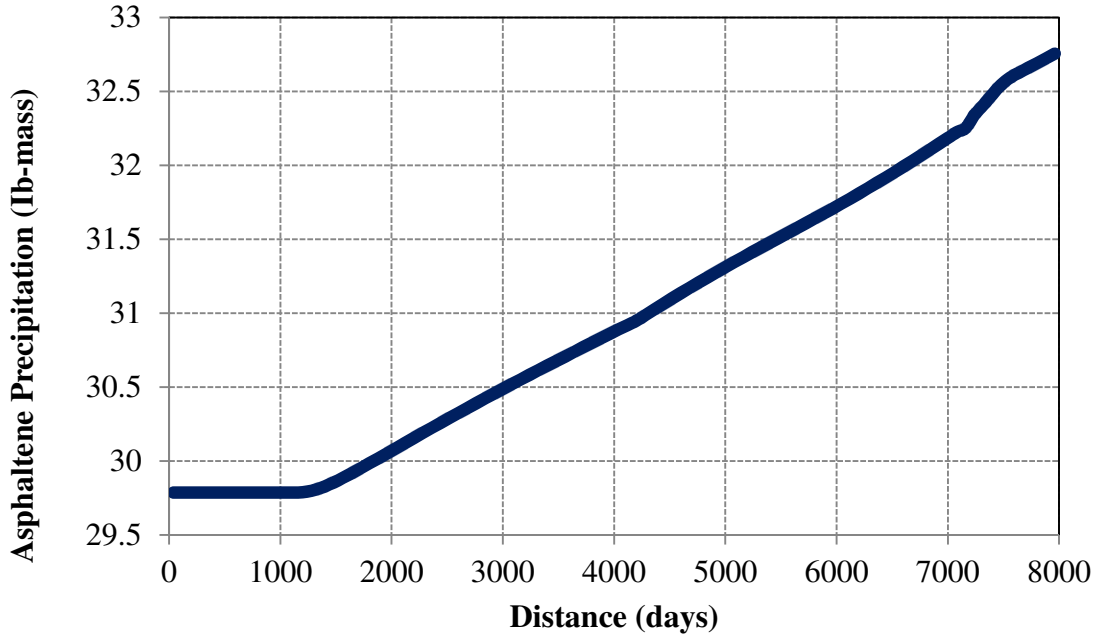

Figure 3.38: Asphaltene Precipitation Weight Fraction Using ECLIPSE

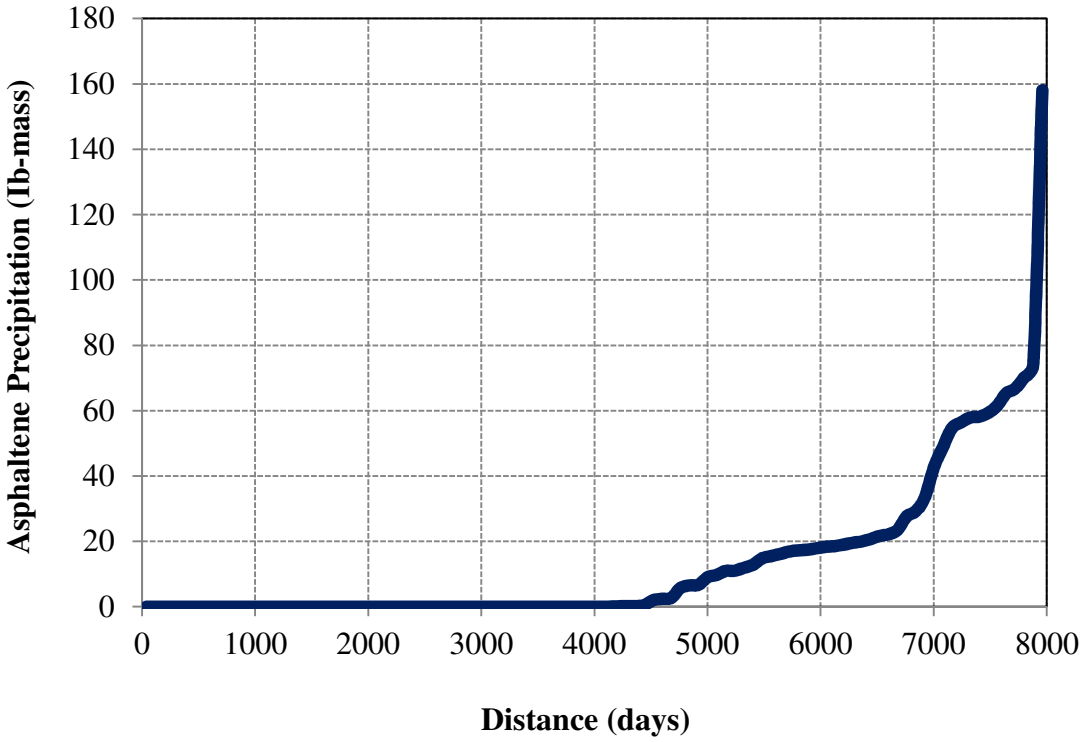

Figure 3.39: Asphaltene Precipitation Weight Fraction Using UTCOMP

3.5 Asphaltene Precipitation Sensitivity Study

Previously, we showed that the asphaltene instability region is located somewhere between the flocculation point to just below the bubble point (**Figure 2.7**), It is highly advisable to maintain reservoir pressure in the field above the bubble point where gas liberation will induce asphaltene precipitation. A field case study about asphaltene instability conducted in Saudi Arabia resulted in proposing specific criteria for flow assurance by maintaining the average reservoir pressure at 2600 psi with a production constraint of above a flowing bottomhole pressure of 2500 psi to avoid asphaltene precipitation in that specific area (Sunil *et al*., 2002). In an attempt to better understand this behavior, several simulation studies has been performed utilizing the CMG/GEM compositional reservoir simulator. The solid model was used to model the asphaltene precipitation.

- Core Scale Sensitivity Test

A simple one-dimensional simulation of near-miscible gas injection into an oil-filled core was performed to investigate the sensitivity of asphaltene precipitation as a function of pressure and temperature utilizing fluid composition data for a North Sea reservoir fluid. The fluid composition and core displacement data are given in **Table 3.7** and **Table 3.8**, respectively.

Table 3.7: Core Displacement Data for North Sea Reservoir Fluid

Length	2.25 ft
Diameter	2 in
Permeability	500 md
Porosity	30%
Water Saturation	0
Pressure	3626
Temperature	197.6 ^{o}F
Rate	2.25 ft/day
No. of grid blocks	30

Table 3.8: Fluid Composition for North Sea Reservoir Fluid

Component	**Reservoir Fluid**	**MW**
	mole %	**lb/lb$_{mol}$**
N2 + C1	8.368	16.61
C2 - C5	25.273	41.43
C6 - C9	27.014	94.63
C10 - C20	24.625	167.2
C21 - C31	9.698	354.65
C32 A+	3.654	591.68
C32 B+	1.371	591.68

The first case study was conducted to investigate the effect of asphaltene precipitation with respect to reservoir temperature at a constant reservoir pressure of 3626 psi. The result in **Figure 3.40** shows a range of reservoir temperatures between 194 F^{o} – 284 F^{o} which clearly indicate a proportional relationship between reservoir temperature and asphaltene precipitation and the effect is more pronounced near the production vicinity area as indicated by the shift of the precipitation curve when it approaches the wellbore vicinity. In the case we have control of reservoir temperature, although most of the time we do not, T = 194 F^{o} will be the optimum choice.

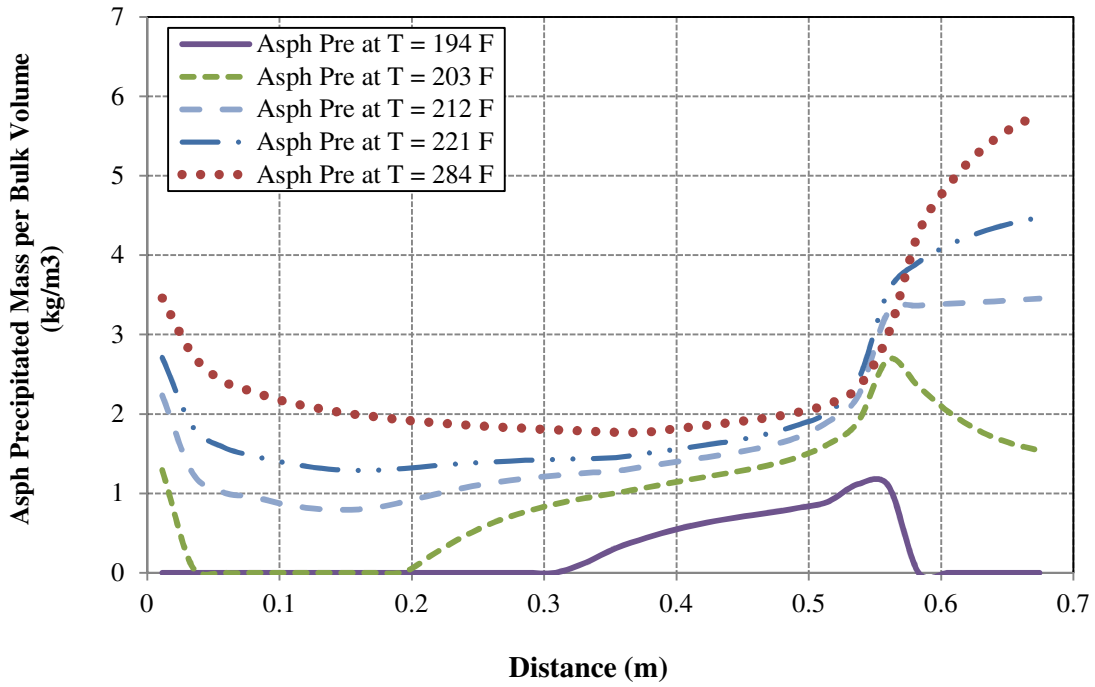

Figure 3.40: Effect of Temperature on Asphaltene Precipitation

The second case study was conducted to investigate the effect of asphaltene precipitation with respect to pressure at a constant reservoir temperature of 198 ^{o}F, the result shown in **Figure 3.41** indicates again that the effect is more pronounced near the production vicinity area as indicated by the shift of the precipitation curve when it approaches the wellbore vicinity. In Section 2.4.3, we discussed that the asphaltene instability region will be located somewhere between the flocculation point to just below the bubble point, this statement is a direct translation of the behavior of **Figure 2.7**. If we focus on the figure, we can see that the highest amount of precipitation is located at P = 3626 psi and P = 2900 psi which gives an indication that the bubble point pressure is somewhere between those pressure values, and more specifically, close to the P = 3000 psi region. This suggests maintaining the pressure either at P = 4350 psi or, if there are pressure

maintenance restrictions, a pressure slightly higher than Pb by an increment of 100 psi. This value will be a very good choice to maintain asphaltene precipitation at the minimum amount possible.

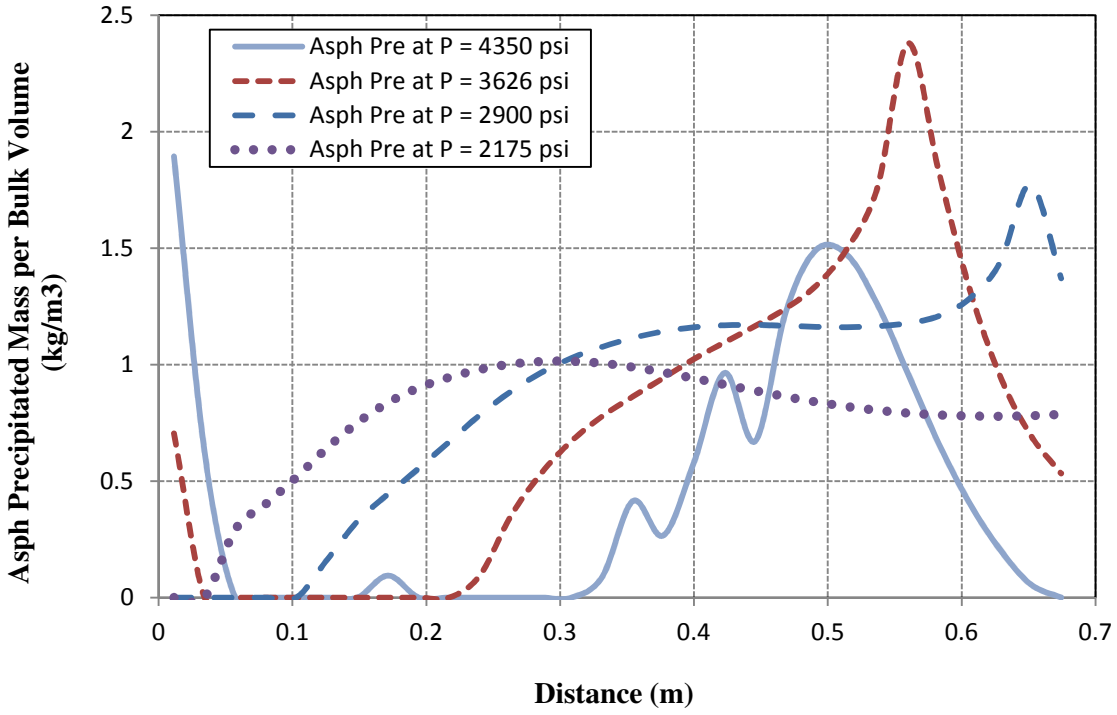

Figure 3.41: Effect of Pressure on Asphaltene Precipitation

In deep offshore fields, the operation is more challenging than land-based fields because of extreme production conditions where temperature changes and pressure drops from the reservoir to the facility are quite large. These extreme circumstances could lead to the precipitation and deposition of hydrocarbon solids, *i.e.*, waxes, asphaltenes, and hydrates.

- Field-scale sensitivity test

In order to appreciate the pronounced effect of asphaltene on field-scale tests, well B-1 data **(Tables 3.1 and 3.2)** was utilized to perform a simple one-dimensional simulation run in order to investigate the effect of asphaltene precipitation on cumulative oil recovery. The porosity and permeability are 0.30 and 800 md, respectively. The reservoir fluid used in this study is presented in **Table 3.1** and **Table 3.2**. The initial reservoir pressure is 2500 psi and the Pb is 2112 psi. The simulated one-dimensional reservoir has a grid dimension of 100 x 1 x 1. The width of each grid block in the x and y directions is a uniform 80 ft with a uniform vertical grid block thickness of 20 ft. The injector is located at block 1 (left edge of the reservoir) and the other boundary is the producer as shown in **Figure 3.24**. The producer operates under a constant bottomhole pressure of 1000 psi. Water injection is commenced at a constant rate of 200 STB/day. As expected, the result in **Figure 3.42** shows clearly the decline in cumulative oil production compared to the case simulated without an asphaltene effect. The following section includes a real field study that presents studies in details the asphaltene precipitation, deposition, and flocculation effects.

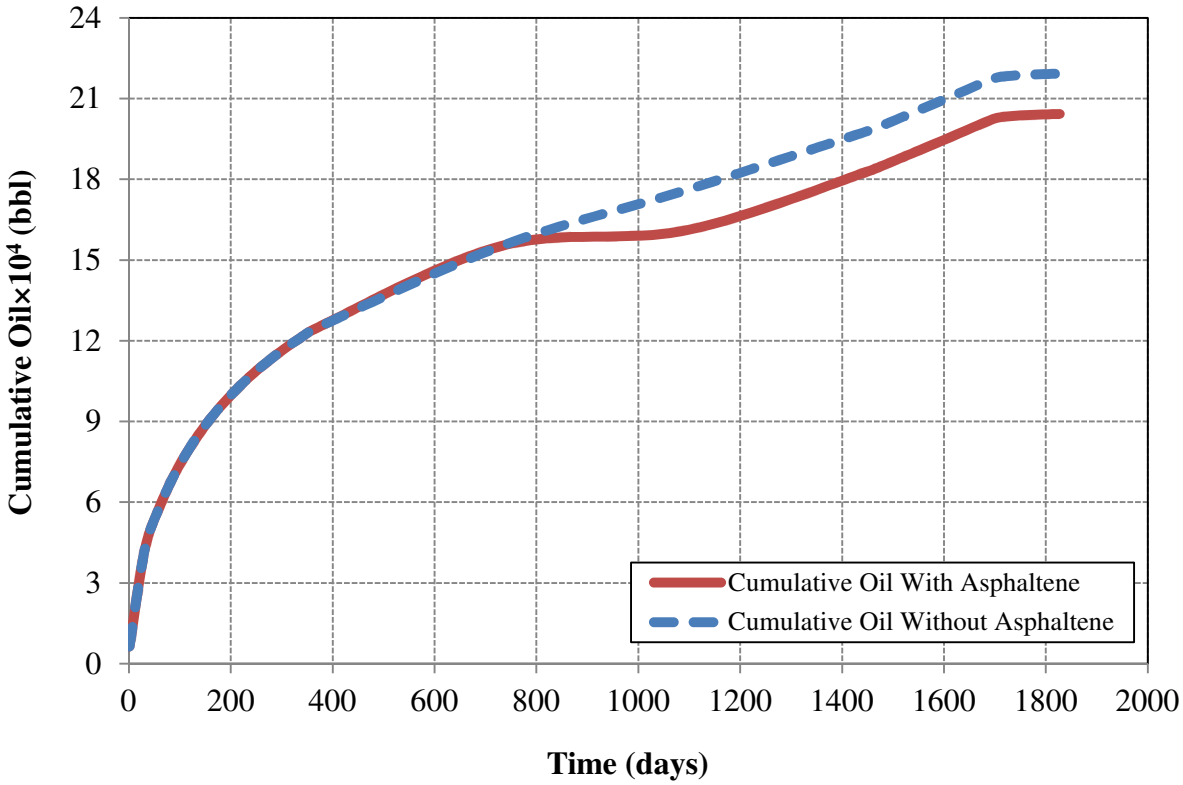

Figure 3.42: Effect of the Presence of Asphaltene on Cumulative Oil Recovery

Chapter 4: THREE-DIMENSIONAL SIMULATION MODEL

4.1 Introduction

A three-dimensional simulation was carried out to study the presence of asphaltene in oil reservoirs and near-wellbore premises. Specifically, the goal of this chapter is to evaluate the effect of asphaltene precipitation, flocculation, and deposition on reservoir performance. Several scenarios are chosen during this study. Also, comparisons of fluids' production rates at presence and absence of asphaltene is presented.

4.2 Reservoir Simulation Input Data

A synthetic three-dimensional compositional heterogeneous reservoir simulation model was built using CMG/GEM simulator to study the impact of asphaltene-related problems during the primary recovery, secondary recovery (waterflooding), and tertiary recovery (CO_2 injection) stages. The model uses well B-1 and well A-1 data. Well A-1 will be discussed in **Appendix E**. Well B-1 phase behavior data are summarized in **Table 3.1** and **Table 3.2**. The size of the reservoir is 25 ft × 25ft × 20 ft and is represented by grid numbers of 50 columns × 50 rows × 5 layers with 12 hydrocarbon components constituting the constant crude composition of this model. The model comprised a total of 12,500 grid blocks. The three-dimensional simulation employed 5-layers, incorporating all relevant production and reservoir data. **Figure 4.1** through **Figure 4.4** show the three-dimensional distribution of the heterogeneous porosity, permeability, initial water saturation data, and three-dimensional view of the injector and producer location, respectively. The average reservoir permeability and porosity is 404 md and 28%, respectively. The injector and producer are located at grid 1, 1 and 50, 50, respectively,

where they are perforated throughout all layers. The initial injection and production plan was based on flooding and draining the reservoir from the five layers. The production process lasts 14 years, with two years primary depletion, five years waterflooding, and seven years CO_2 injection. The estimated Original Oil In Place (OOIP) and Original Water In Place (OWIP) of this model is 2.7 MM STB and 4 MM STB, respectively. The initial reservoir pressure and temperature are 2,500 and 254 ^{o}F, respectively, with an asphaltene onset pressure (AOP) of 2209 psi. Additional data are shown in **Table 4.1** and **Table 4.2**.

Table 4.1: Reservoir Description

Description	**Value**
Depth of the vertical well, ft	7500
Width, length, and thickness, ft	1250 × 1250× 50
Average permeability, md	400
Average porosity, fraction	0.28
Initial reservoir pressure, psi	2500
Bubble point pressure, psi	2112
Temperature, ^{o}F	212
Asphaltene content, % (weight)	0.21

Table 4.2: Parameters Used in the Model

Grid Parameters	
$N_x \times N_y \times N_z$	50 × 50× 5
$\Delta_x \times \Delta_y \times \Delta_z$	25 × 25× 20
Well Parameters	
Wellbore Radius, ft	0.25
Skin	0

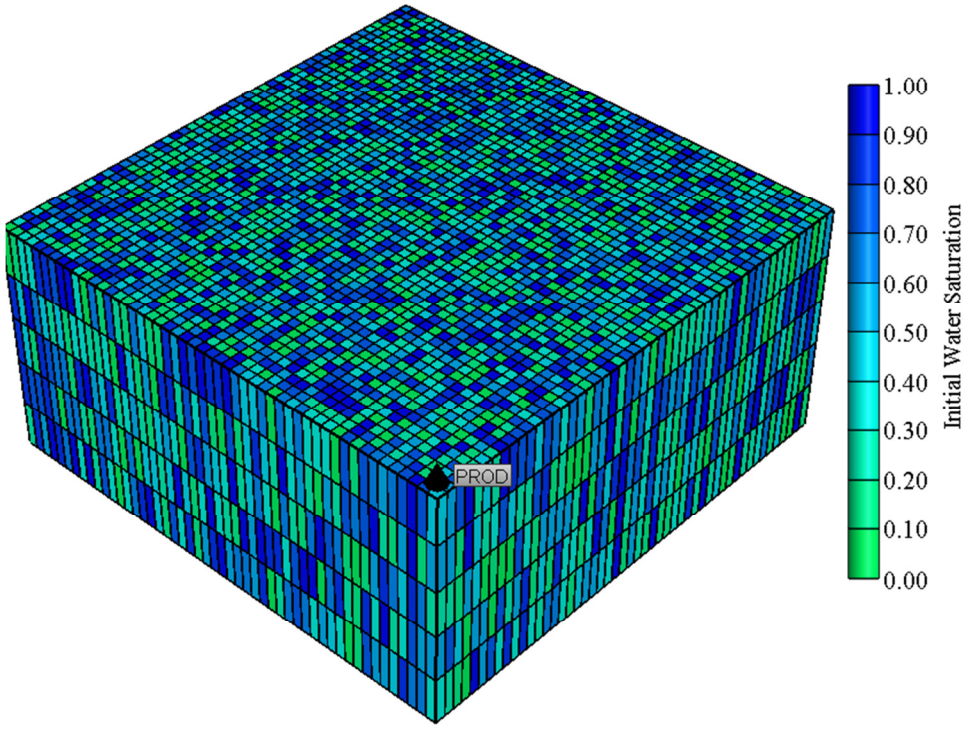

Figure 4.1: Three-Dimensional View of the Initial Water Saturation for the First Layer

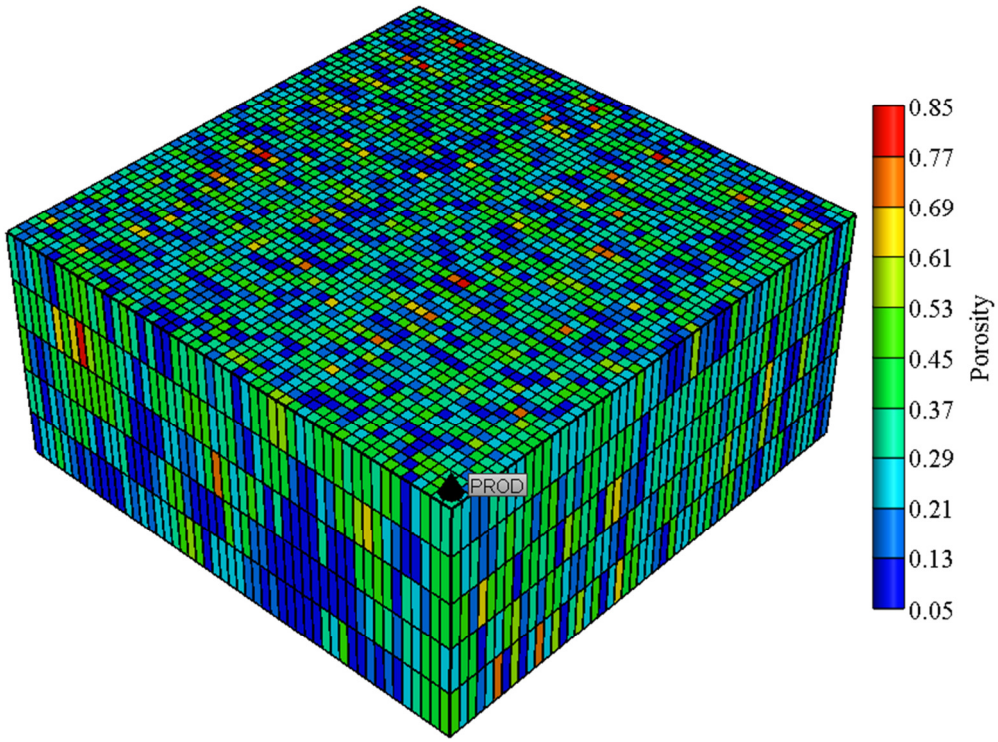

Figure 4.2: Three-Dimensional View of the Porosity for the First Layer

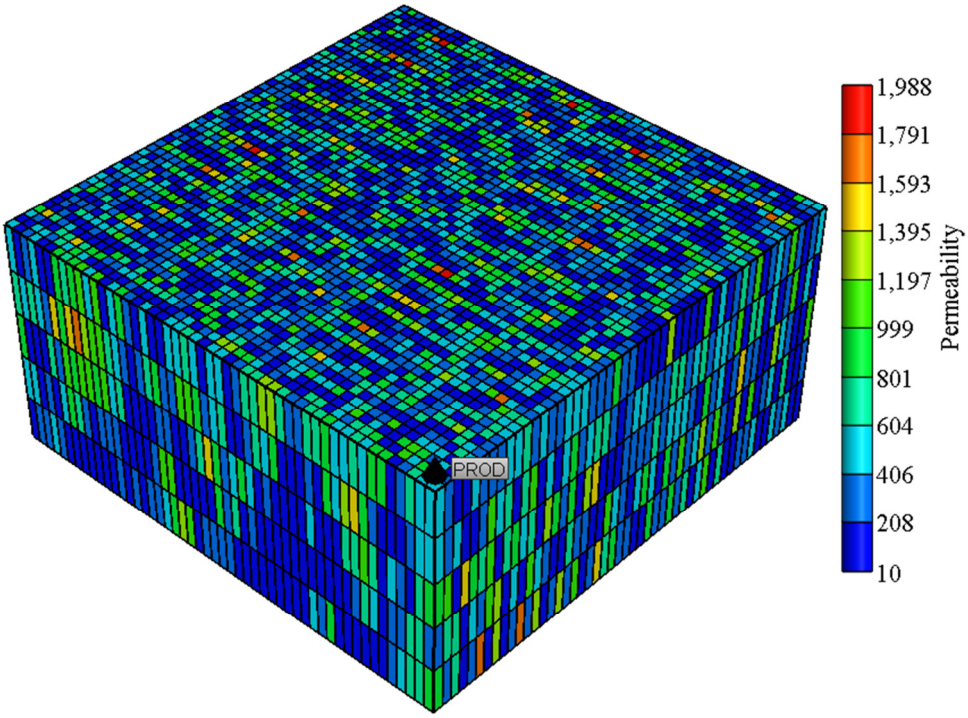

Figure 4.3: Three-Dimensional View of the Permeability Profile for the First Layer

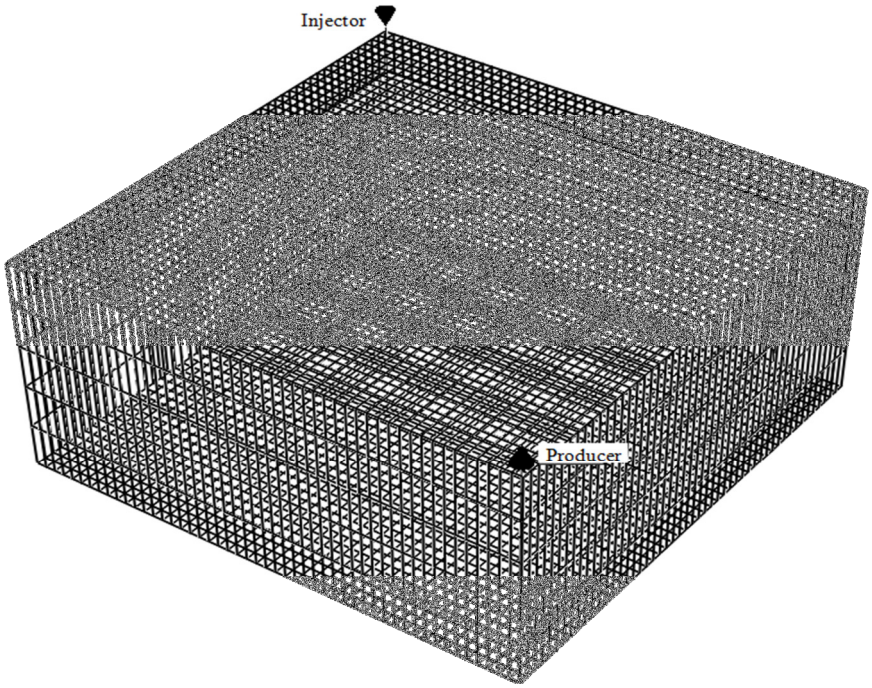

Figure 4.4: Three-Dimensional View of the Injector and Producer Location

4.3 Reservoir Simulation Results

This section is a summary of the simulation results of the effect of asphaltene precipitation, flocculation, and deposition on the productivity of well B-1 using three different bottomhole pressure (BHP) scenarios. Asphaltene precipitation has implications on production in terms of reservoir natural depletion. Generally, solubility and density parameter trends are proportional to pressure depletion. For this reason, it is crucial to investigate the behavior of asphaltene under different BHP pressure scenarios, where it is well-known that precipitation occurs in areas close to the petroleum fluid bubble point. Three different bottomhole pressures were used in this study: 1000 psi, 2100 psi, and 2300 psi. In the following sections, we label the 1000 psi, 2100 psi, and 2300 psi BHP scenarios ″Scenario 1,″ ″Scenario 2,″ and ″Scenario 3,″ respectively. Scenario 1 was selected to investigate the effect of asphaltene when a producer operates under a bottomhole pressure lower than the asphaltene onset pressure (AOP), where the average reservoir pressure in this scenario will be allowed to decrease to lower than AOP, allowing more gas to be liberated, which in turn, decreases the solubility of asphaltene and induces precipitation. Scenario 2 was selected to test the sensitivity of asphaltene precipitation when operating the well under a pressure close to the bubble point pressure (Pb =2112 psi). Scenario 3 was selected to investigate the effect of asphaltene when operating well B-1under a bottomhole pressure higher than the AOP. In Scenario 3, the average pressure will be maintained above the bubble point (Pb =2112 psi) and above the AOP, restricting gas liberation and improving the solubility of asphaltene, which is expected to have a lower precipitation amount than Scenario 1. The asphaltene

precipitation phase envelope for well B-1 is shown in **Figure 4.5** with AOP with Pb indicated in the diagram. These three different bottomhole pressure (BHP) scenarios were tested using an operating production strategy that is based on depleting the reservoir for two years, followed by five years of waterflooding, and finally CO_2 injection for seven years. Primary depletion was included to investigate the impact of pressure depletion on asphaltene precipitation and deposition. CO_2 injection was selected to improve oil production and investigate the impact of the crude alteration effect, where CO_2 injection is one of the main factors that induces asphaltene precipitation and instability.

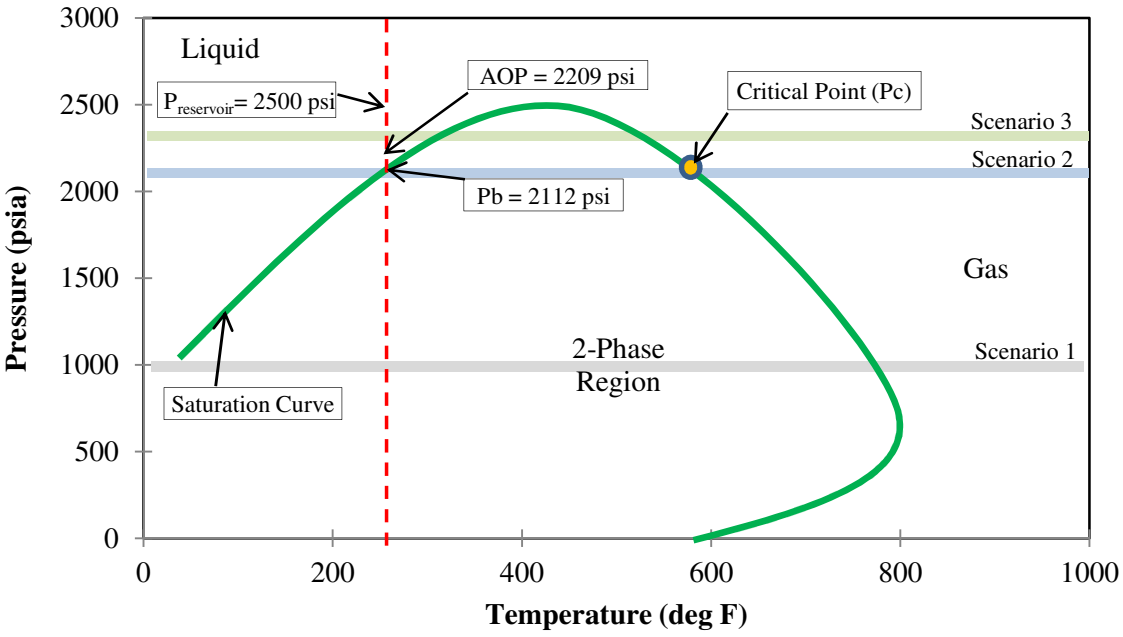

Figure 4.5: Asphaltene Phase Behavior Envelope for Well B-1

Figure 4.5 shows that as the reservoir pressure decreases below the onset point of precipitation, asphaltene begins to precipitate from crude oil. The amount of precipitation increases with the decrease of pressure until it reaches the saturation pressure. A further decrease of pressure leads to a backward dissolution of asphaltene into oil.

Case 1: Results without asphaltene precipitation

The first run was performed without considering the asphaltene option, including precipitation, flocculation, and deposition. Pressure depletion was simulated for two years followed by waterflooding and simulated for an injector for five years with a constant water injection rate of 2000 bbl/day. Carbon dioxide flooding was simulated for seven years for one injector with a constant gas injection rate constraint of 5 MM SCF/day and increasing the pressure of the reservoir to 400–600 psi more, where fluid analysis data indicated that CO_2 and hydrocarbons should be near miscible conditions. **Figure 4.6** shows the average reservoir pressure for the three different scenarios throughout the recovery stages. It shows the primary oil recovery, waterflooding recovery, and CO_2 enhanced recovery versus time. **Table 4.3** shows the result of the cumulative oil recovery and recovery break up for each recovery stage for the three scenarios. The daily injection rate of 5 MM SCF of carbon dioxide resulted in additional recovery of 0.47 MM STB, 0.68 MM STB, and 0.74 MM STB for BHP of 1000, 2100, and 2300, respectively. This is equal to 47%, 65%, and 68% of OOIP, respectively. **Table 4.3** shows that the higher final recovery performance of CO_2 (after 14 years) is achieved at the highest BHP scenario (2300 psi). The waterflooding recovery is actually

higher than the CO_2 and primary recovery stages during the stipulated 14 year period. Significant increases of cumulative oil during primary recovery stage occurs only if the BHP of 1000 psi is used as shown in **Figure 4.7**. This allows the reservoir to drain more oil due to the low restriction on the bottomhole pressure; however, the first scenario will result in 48% total recovery compared to 65% and 68% when using Scenarios 2 and 3, respectively, from the estimated original oil in place of 2.7 MM STB oil. Oil rate and gas oil ratio for the BHP scenarios are shown in **Figure 4.8** and **Figure 4.9**, respectively.

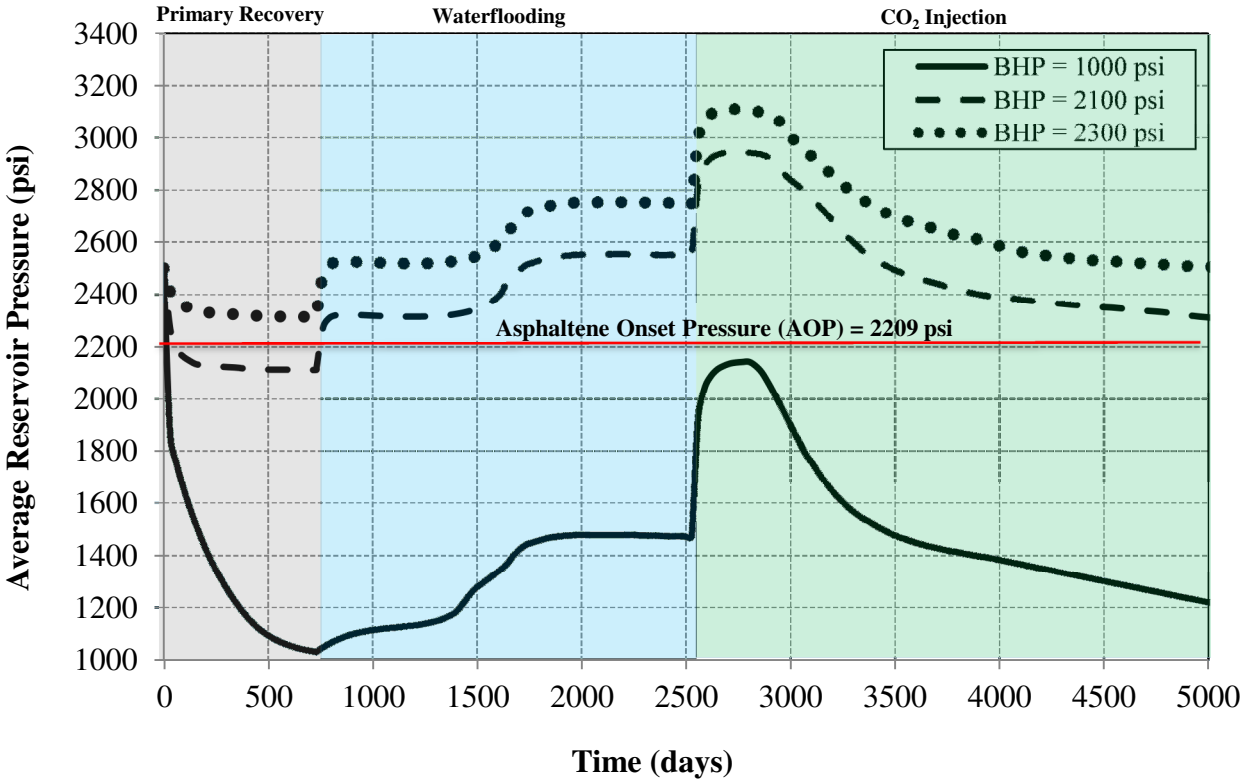

Figure 4.6: Comparison of Average Reservoir Pressure Without Using the Precipitation Option

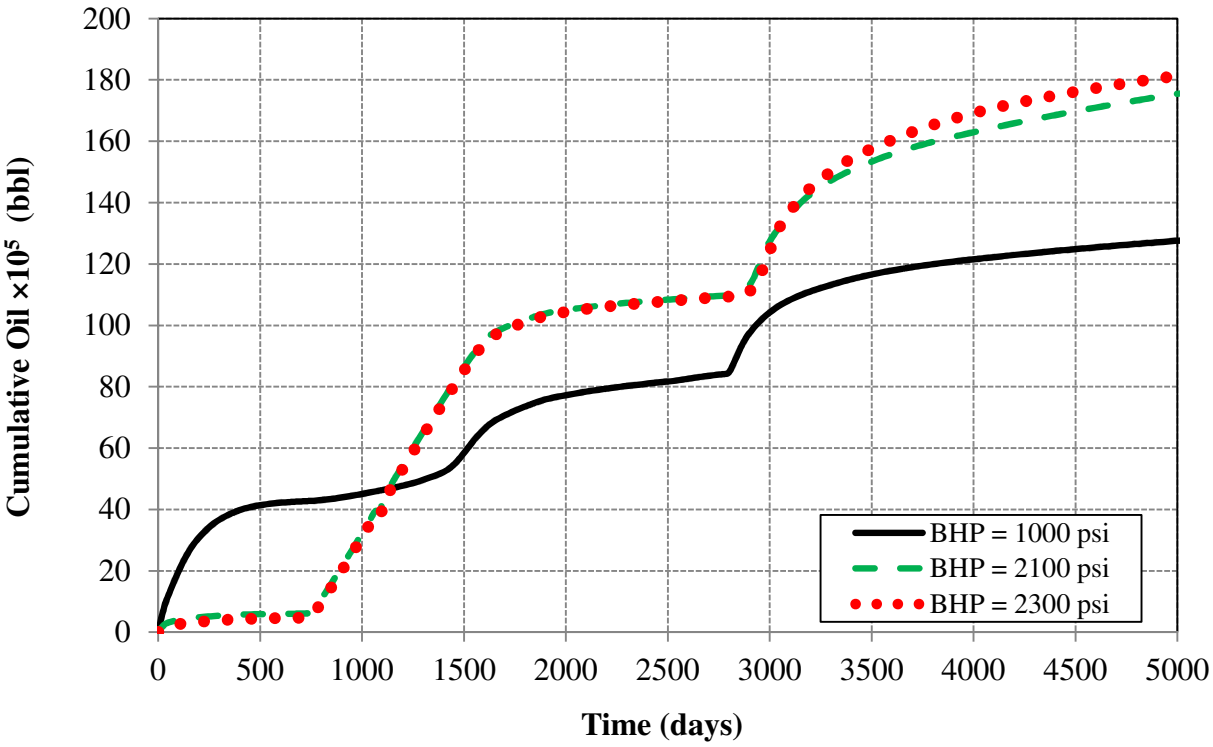

Figure 4.7: Comparison of Cumulative Oil Production Without Using the Precipitation Option

Table 4.3: Comparison of Oil Recovery at Different BHP Scenarios Without the Precipitation Option

	Oil Recovery (STB)			
	Primary Recovery	Waterflooding	CO_2 Injection	Total from IOIP
Period (years)	2	5	7	14
Scenario 1	43×10^4 (16%)	39×10^4 (14%)	46×10^4 (17%)	13×10^5 (47%)
Scenario 2	6×10^4 (2%)	10×10^5 (38%)	68×10^4 (25%)	18×10^5 (65%)
Scenario 3	5×10^4 (2%)	10×10^5 (38%)	74×10^4 (28%)	18×10^5 (68%)

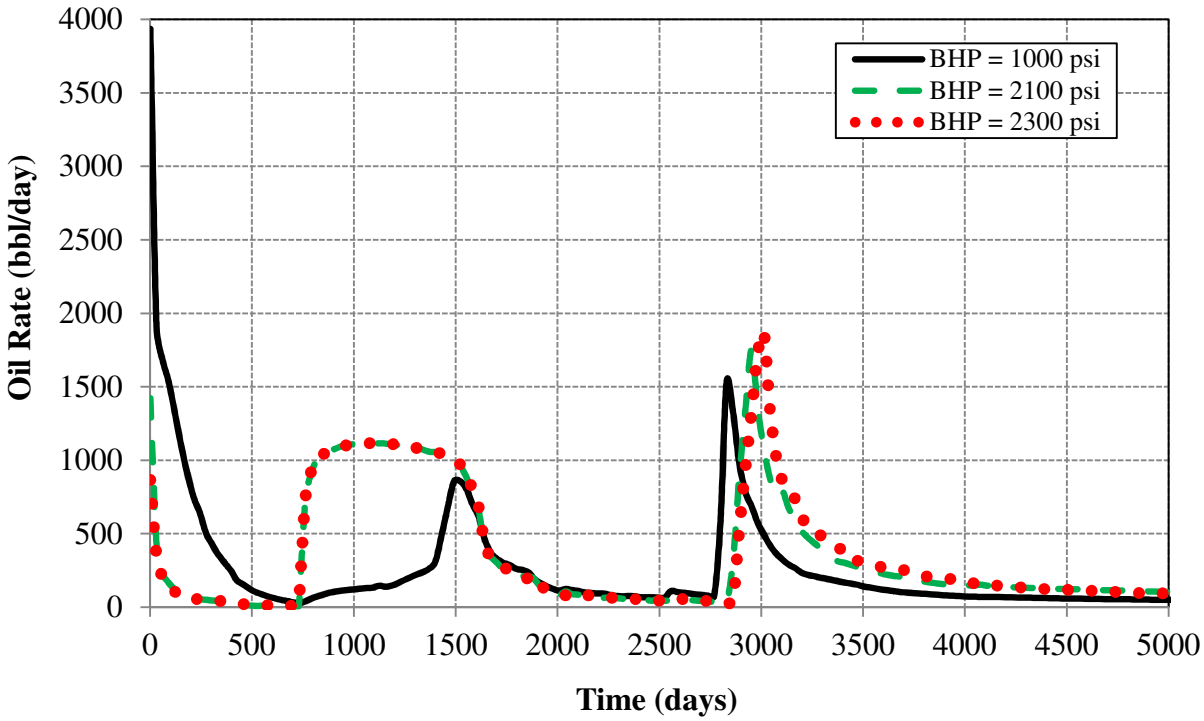

Figure 4.8: Comparison of Oil Rate Without Using the Precipitation Option for Different Scenarios

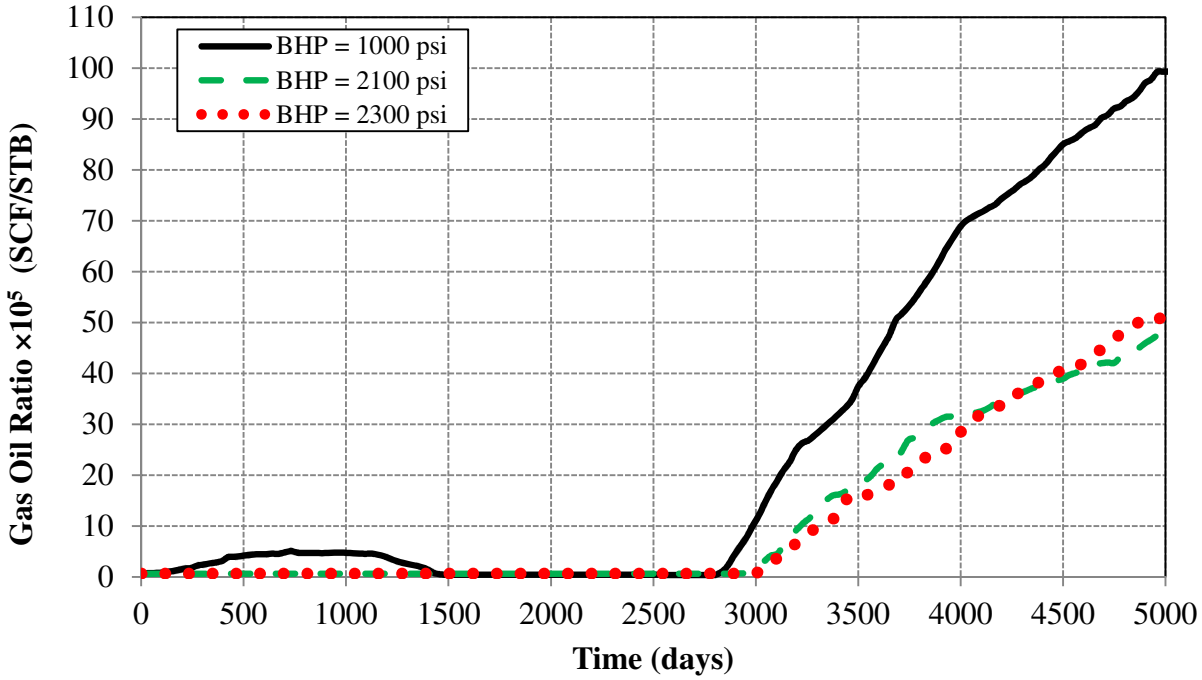

Figure 4.9: Comparison of Gas Oil Ratio Without Using the Precipitation Option for Different Scenarios

Case 2: Results with asphaltene precipitation

The same model and procedure used in Case 1 was repeated for the three scenarios considering the asphaltene option. In this case study, asphaltene precipitation was considered in the model without including the flocculation and deposition options. The fugacity of asphaltene and solid molar volume parameters used in the asphaltene precipitation model simulation are shown in **Table 4.4**.

Table 4.4: Asphaltene Precipitation Parameters

Solid Model Parameters	
Fugacity (f_s), atm	4.62×10^{-12}
Solid molar volume (v_c), L/mol	1

The results show that oil rate with the asphaltene precipitation is almost the same as the cases without asphaltene precipitation for all of the different scenarios. The reason is due to neglecting asphaltene deposition, which means there will be no pore plugging, no porosity reduction, and no permeability reduction. Also, neglecting the flocculation will result in assuming the asphaltene precipitation as an irreversible process, which is not accurate. **Figure 4.10** shows the result of oil rate comparison with and without the asphaltene precipitation option for Scenario 3.

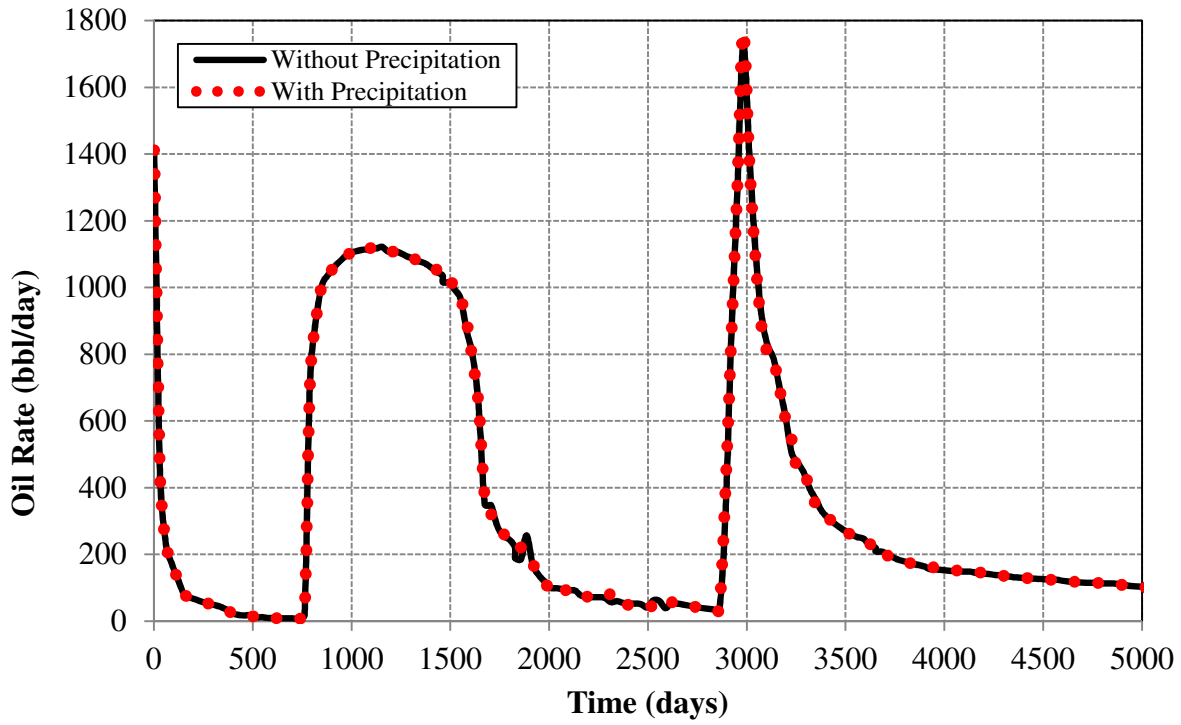

Figure 4.10: Comparison of Oil Rate With and Without the Precipitation Option for Scenario 3

Case 3: Asphaltene flocculation at different scenarios

This case study discusses the effect of the forward and backward reaction rates on oil rate and compares the flocculated mass and the precipitation at the production cell for the different scenarios**.** The re-dissolution of precipitated asphaltene can be modeled by allowing solid s_1 to be transformed via a simple reversible reaction into another solid s_2, which means that smaller asphaltene particles will be flocculated into larger aggregates (Nghiem *et al.*, 2000). The reaction may be written as $s_1 \leftrightarrow s_2$.

The reaction rate for s_2 is

$$r = k_{12} C_{s_1,o} - k_{21} C_{s_2,o}. \qquad \textbf{(4.3.1)}$$

If k_{21} is zero, the reaction is irreversible and s_2 will not go back into the solution whereas if $k_{21} << k_{12}$, the precipitation of s_2 is reversible, but may take a long time to complete (Nghiem *et al.*, 2000).

Figure 4.11 shows the history of asphaltene flocculated mass (lb) entering the producer (five layers) using Scenarios 1, 2, and 3. **Figure 4.12** shows that asphaltene flocculated mass (lb) entering the producer decreases as BHP lowers. The flocculated mass (lb) decreased from an average of 20 lb for Scenario 1 at the production cell during primary and waterflooding to an average of 15 lb an 10 lb for Scenarios 2 and 3, respectively, for the five layers. This high amount of flocculation shown in **Figure 4.12** was obtained at a forward reaction rate (k_{12}) of 100 and backward reaction rate of (k_{21}) of 0, where this scenario will lead to flocculating all the asphaltene without any fraction going back to the solution. In this case, the asphaltene precipitation will be zero. **Figure 4.13** shows an example of the asphaltene precipitation at different possible flocculation rates. **Figure 4.14** compares the oil rate at a different flocculation rate. The result shows that the oil rate is the same at the different forward and backward reaction rate combinations. However, when the backward reaction is irreversible (K_{21} =0), the oil rate showed higher fluctuation during the waterflooding stage, where this backward reaction rate assumes no precipitated particle will return to the solution.

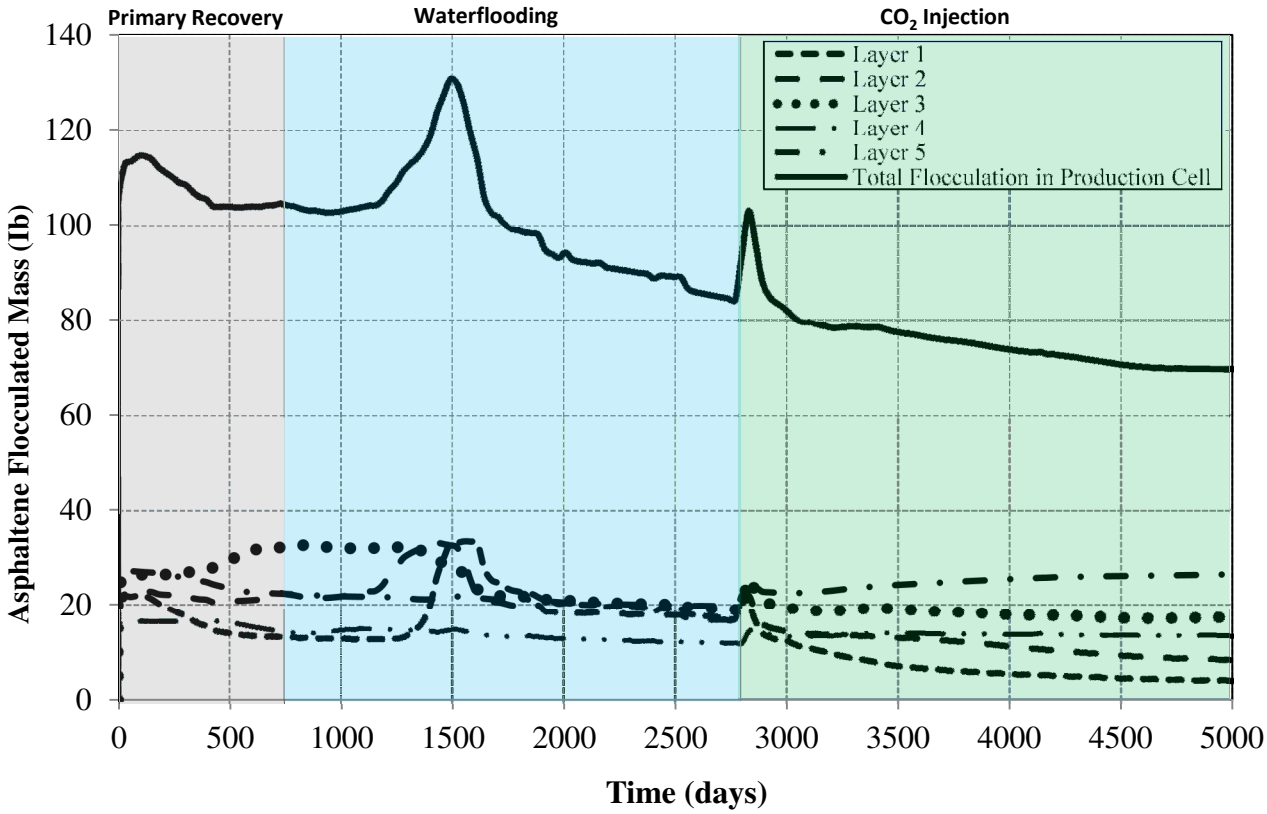

Figure 4.11: Asphaltene Flocculated Mass (lb) at the Production Cell for Scenario 1

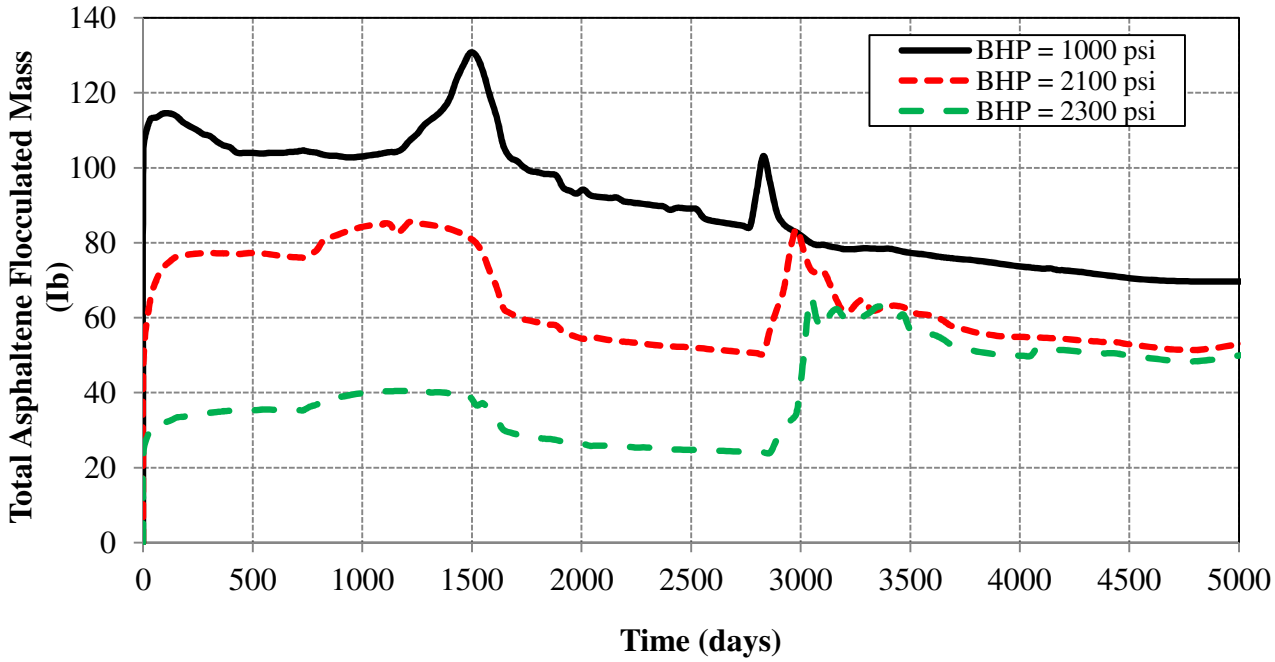

Figure 4.12: Total Asphaltene Flocculated Mass (lb) at the Production Cell for $k_{12} = 100$ and $K_{21} = 0$

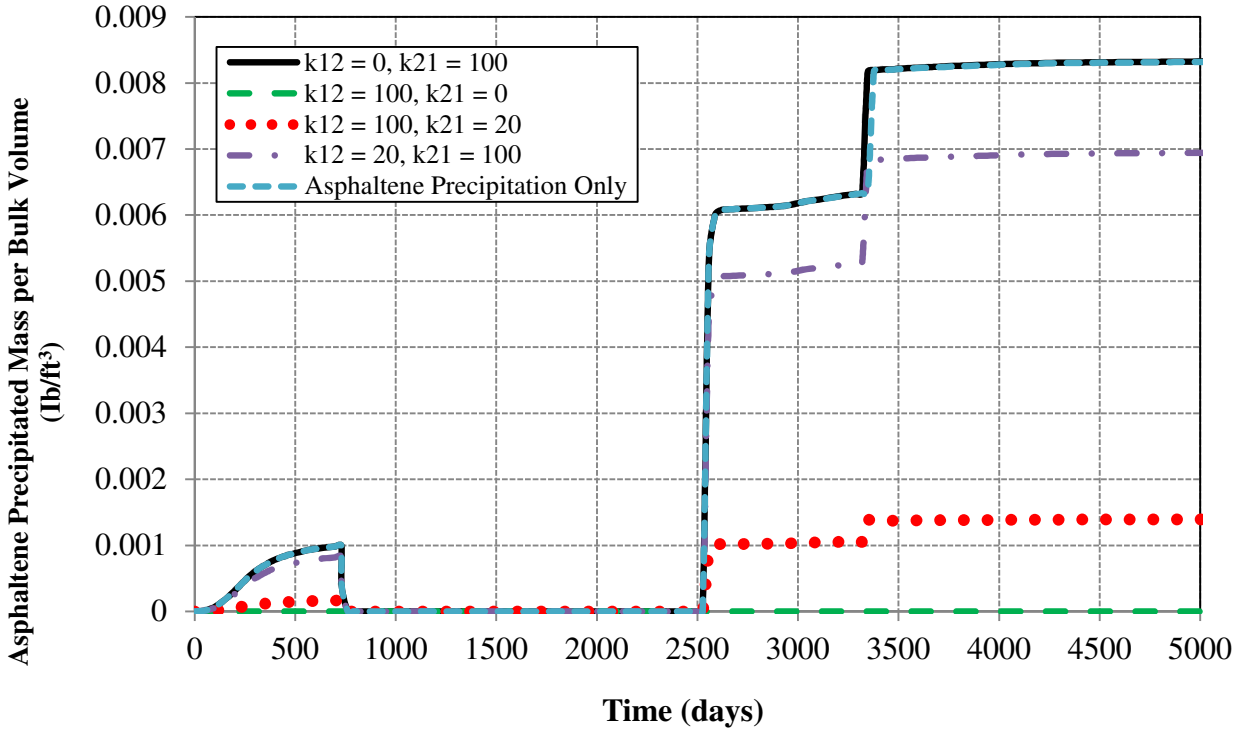

Figure 4.13: Asphaltene Precipitated Mass per Bulk Volume (lb/ft^3) at Different Flocculation Parameters (k_{12} and K_{21}) for Scenario 3

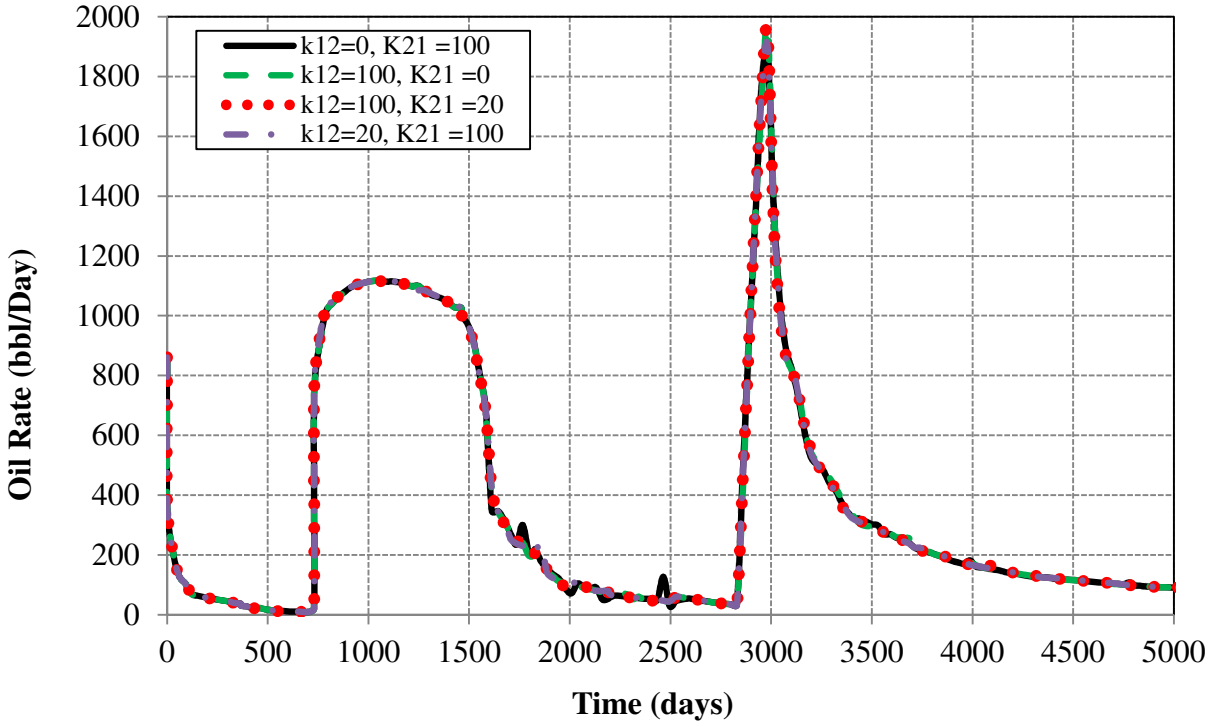

Figure 4.14: Oil Rate at Different Flocculation Parameters (k_{12} and K_{21}) for Scenario 3

Case 3: Asphaltene deposition at different BHP scenarios

The deposition of asphaltene during oil recovery has large economic and technical impacts on the production. During oil recovery, the occurrence of solid organic deposits such as asphaltenes in wells have been well-documented in the literature. The fugacity of asphaltene and solid molar volume used in this case study is the same as Case 1 (**Table 4.4**). The deposition parameters used in the asphaltene solid model simulation are shown in **Table 4.5.** Two runs were performed using two different sets of deposition parameters. Run 1 was performed utilizing deposition parameters from Figuera *et al*., 2010, and Run 2 was performed utilizing deposition parameters from Wang, 2000.

Table 4.5: Deposition Parameters (Figuera *et al*., 2010) and (Wang, 2000)

Deposition Parameters		
	Run 1	Run 2
Surface Deposition rate (α), day^{-1}	1	2419.2
Entrainment rate (β), ft^{-1}	0.5	0
Critical interstitial velocity (v_{cr}), ft/day	18	0
Pore throat plugging rate (γ), ft^{-1}	5	0
Forward reaction rate (K_{12}), day^{-1}	100	100
Backward reaction rate (K_{21}), day^{-1}	0	0

Deposition data used in Run 1 were chosen to reflect a closer behavior to the one observed in a field (Figuera *et al*., 2010). **Figure 4.15** and **Figure 4.16** show the comparison of the oil rate and cumulative oil production with and without the asphaltene deposition option, respectively, for Scenario 3, Run 1. The results show that cumulative oil production with the asphaltene deposition is more than that without asphaltene deposition. It is interesting that asphaltene precipitation and deposition increased the

cumulative oil production; however, **Figure 4.17** shows that the average pressure drop is faster in the case with no asphaltene deposition, which leads to more gas liberation from the crude as shown in **Figure 4.18**, which decreases the oil production. Also, the lower average reservoir pressure decreases the driving force for the oil mobility, which leads to lowering the oil production. It is worthy mentioning that, considering entrainment in the deposition model resulted in reducing the effect of asphaltene deposition, removing the deposited asphaltene around the well, and improving the well productivity (Figuera *et al.*, 2010). Also, asphaltene precipitation in a reservoir with a moderate permeability ($\bar{k} = 404\ md$) helps prevent pressure from dropping too fast, thus in turn improves oil production (Wang, 2000).

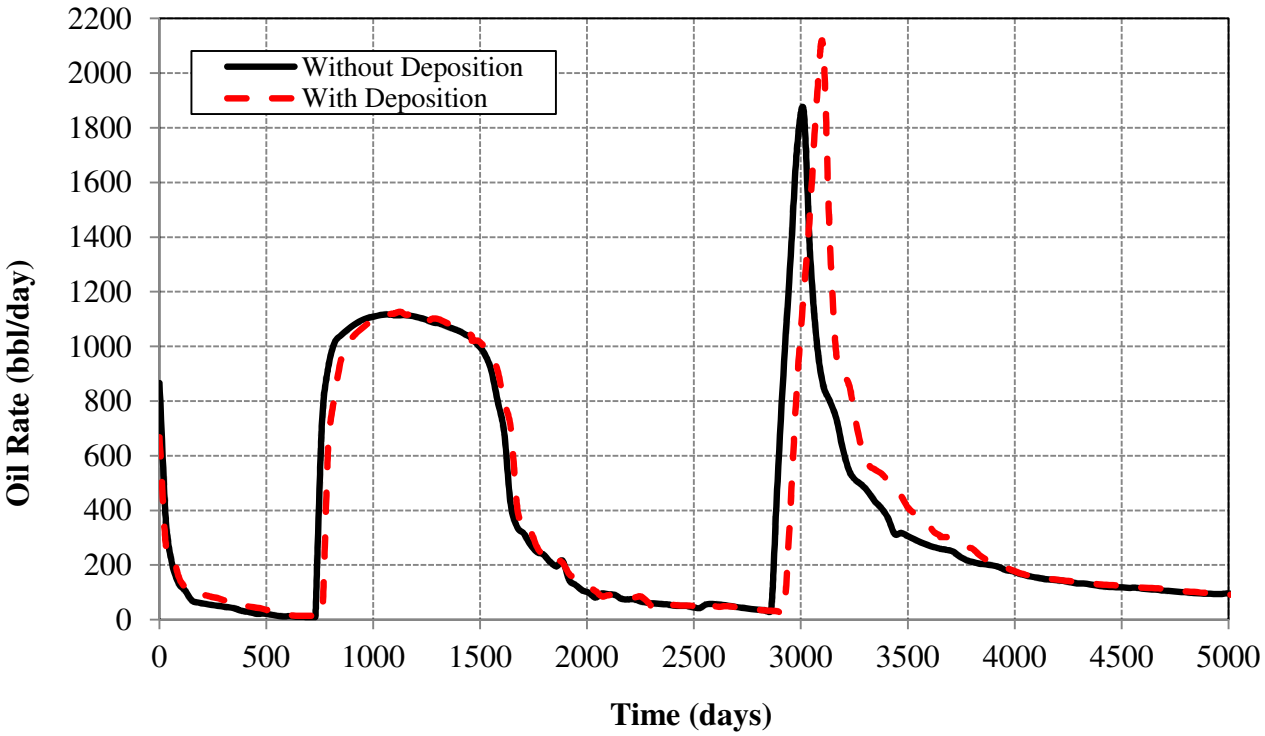

Figure 4.15: Comparison of Oil Rate With and Without the Deposition Option for Scenario 3, Using Run 1

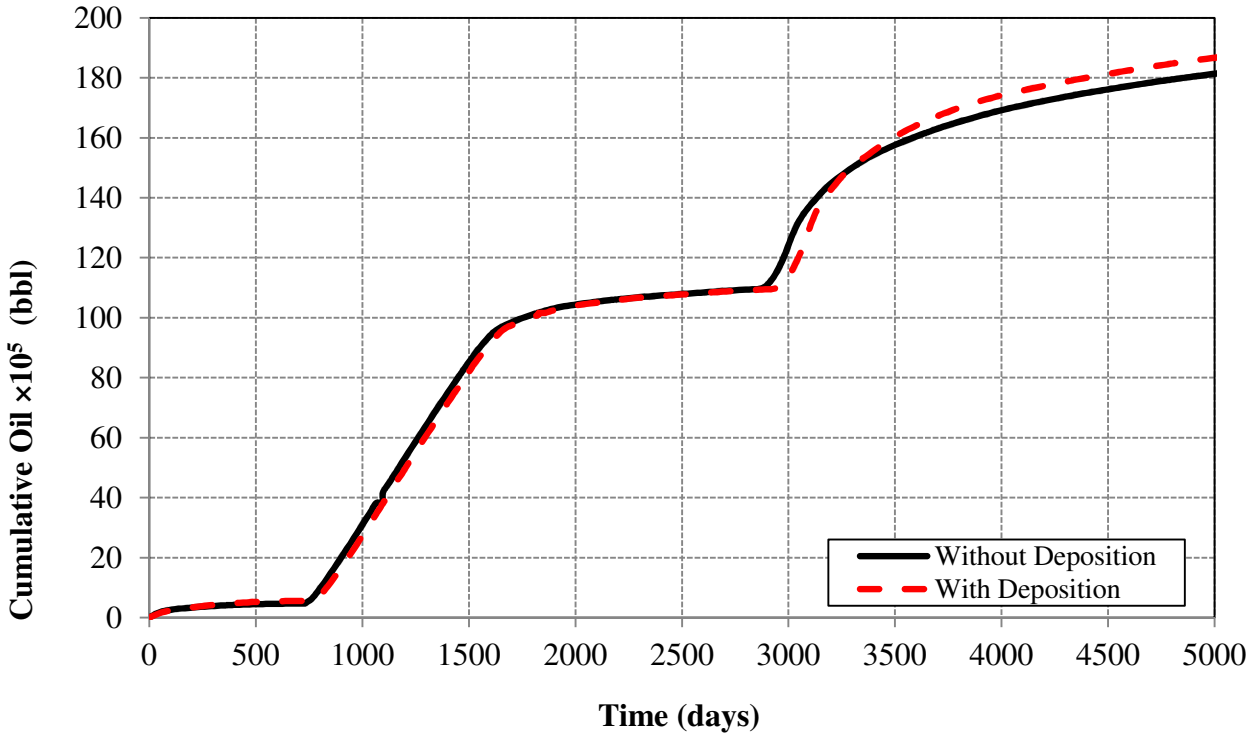

Figure 4.16: Comparison of Cumulative Oil With and Without the Deposition Option for Scenario 3, Using Run 1

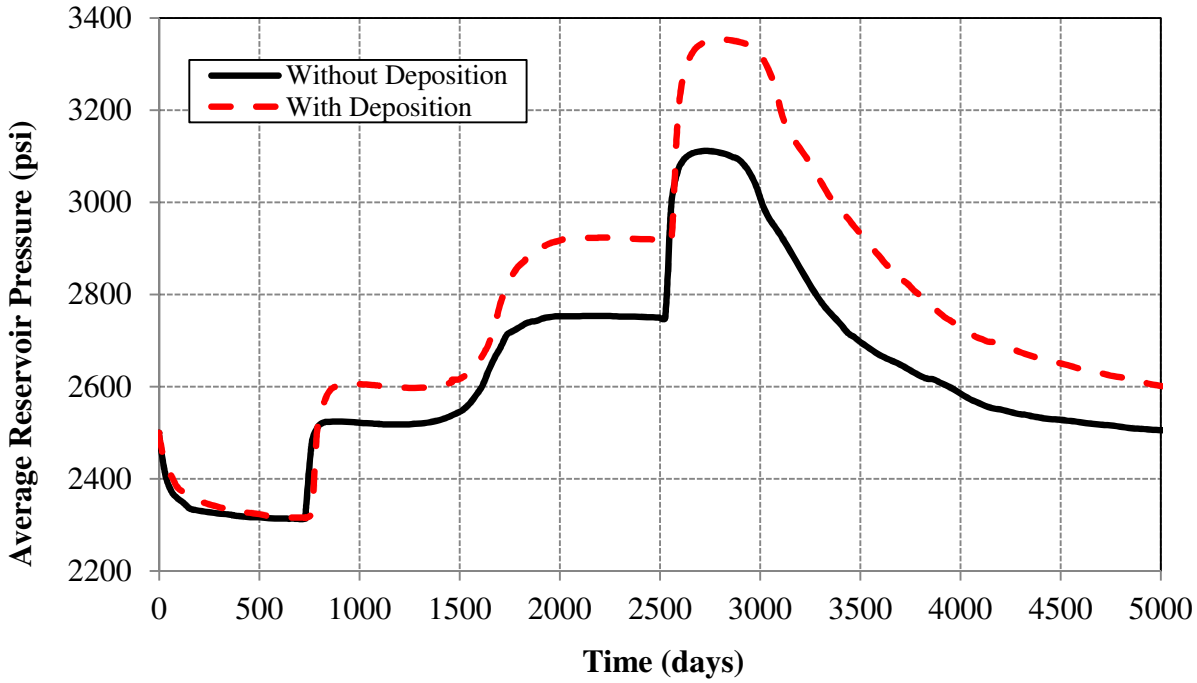

Figure 4.17: Comparison of Average Pressure With and Without the Deposition Option for Scenario 3, Using Run 1

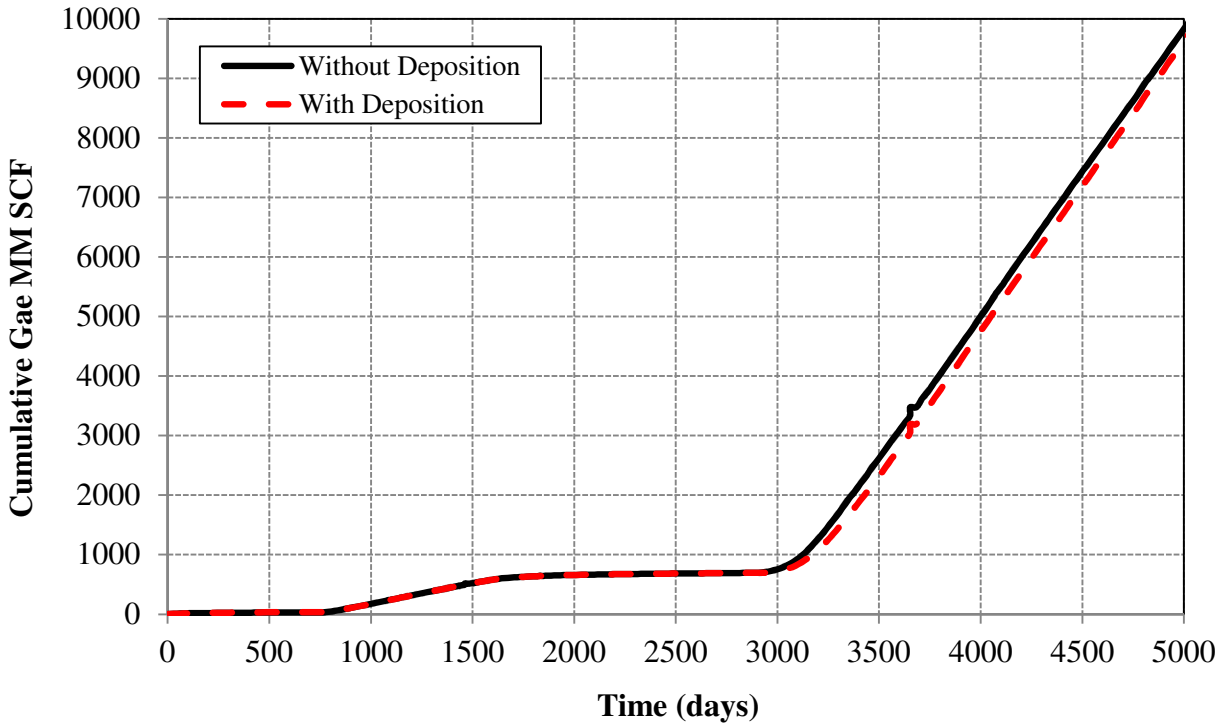

Figure 4.18: Comparison of Cumulative Gas With and Without the Deposition Option for Scenario 3, Using Run 1

Run 2 uses a surface deposition rate of 2419.2 day^{-1}, a pore throat plugging rate of 0 ft^{-1} , and an entrainment rate of 0 ft/day in the solid model. **Figure 4.19** and **Figure 4.20** show the comparison of the oil rate and cumulative oil production with and without asphaltene precipitation, respectively, for Scenario 3, Run 2. The results show that cumulative oil and production rate with the asphaltene precipitation is less than the same case without asphaltene precipitation. At the very beginning, these two curves are almost the same. At the beginning of CO_2 injection, they diverge from each other. With asphaltene precipitation, gas mobility will not change much. However, the average reservoir pressure stays lower as shown in **Figure 4.21**, contrary to results obtained in Run 1. **Table 4.6** shows the comparison of oil recovery, with deposition, between Run 1 and Run 2 deposition parameters for Scenario 3.

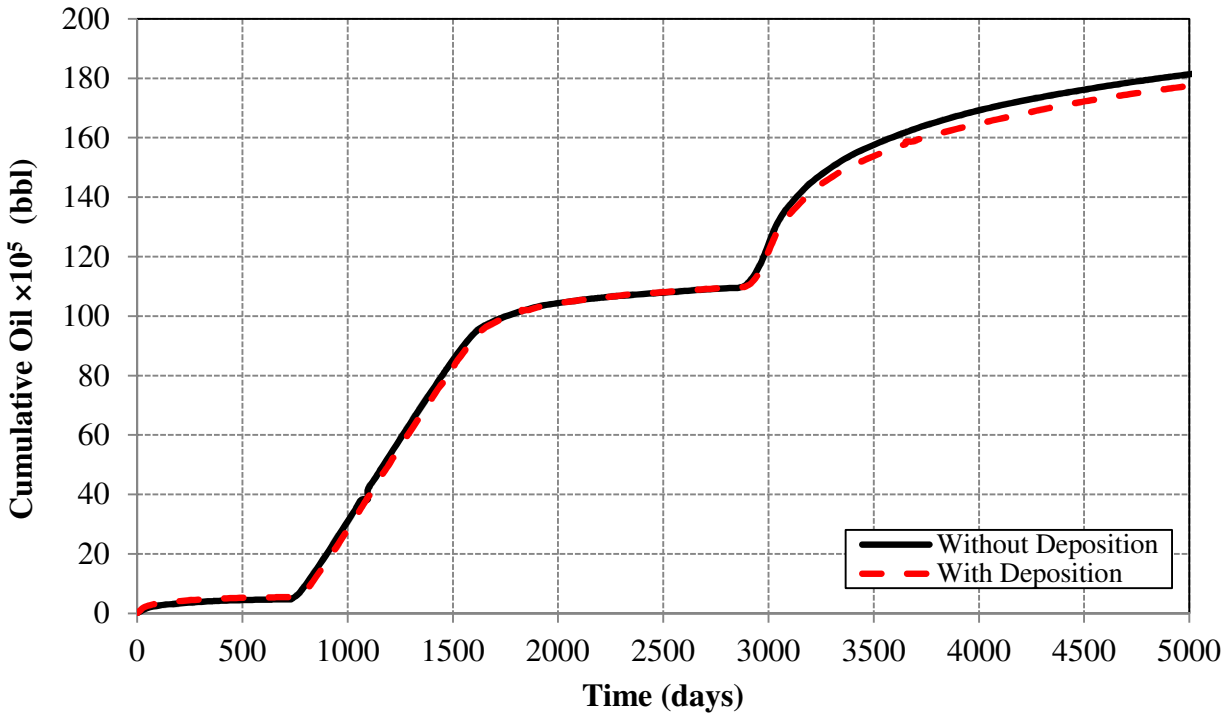

Figure 4.19: Comparison of Cumulative Oil Production With and Without the Deposition Option for Scenario 3, Using Run 2

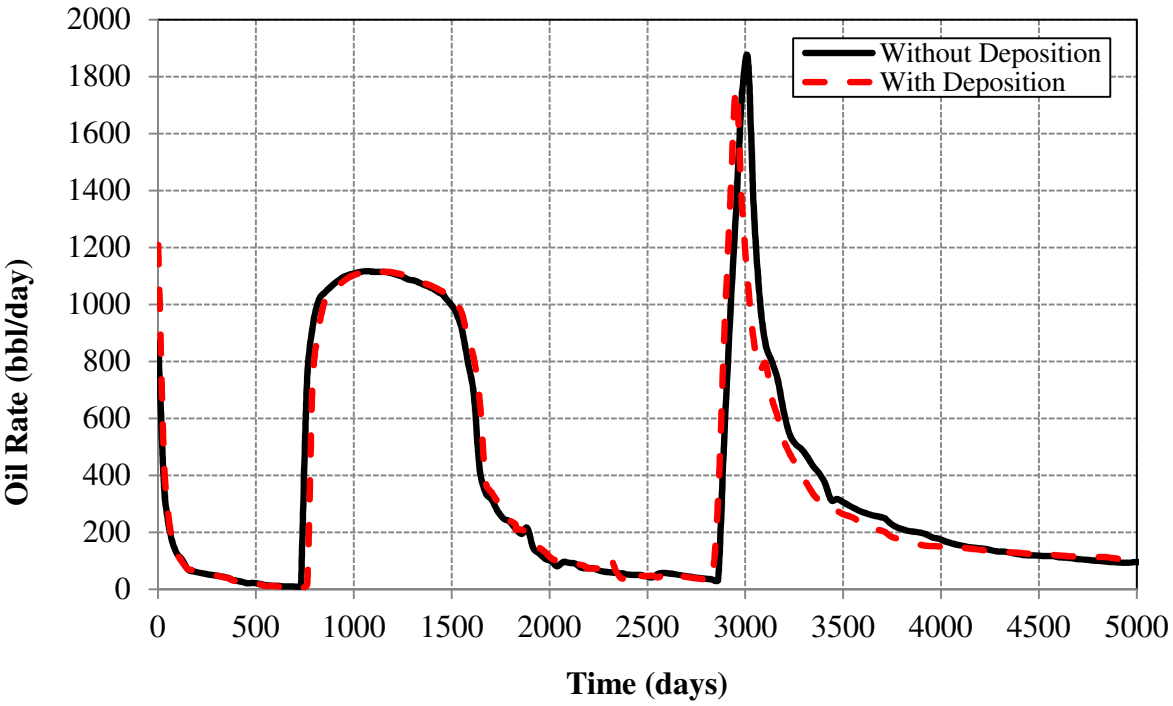

Figure 4.20: Comparison of Oil Rate With and Without the Deposition Option for Scenario 3, Using Run 2

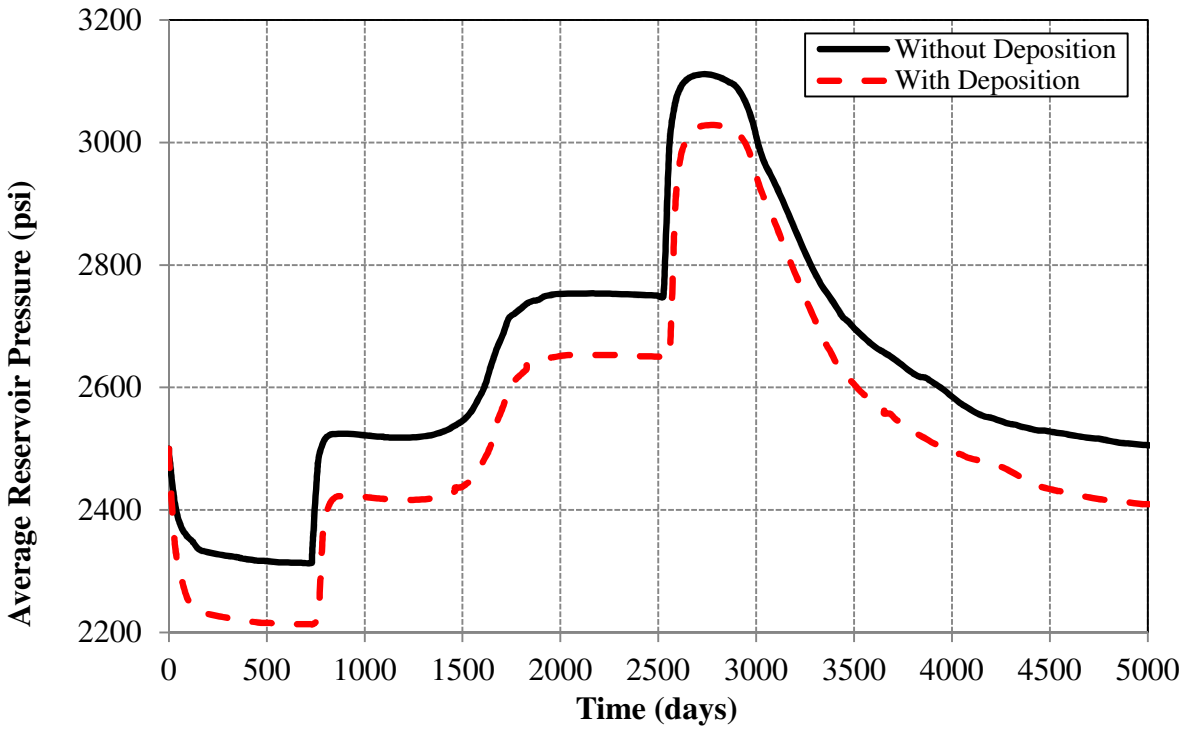

Figure 4.21: Comparison of Average Pressure With and Without Deposition for Scenario 3, Using Run 2

Table 4.6: Comparison of Oil Recovery With the Deposition Option for Scenario 3, Using Runs 1 and 2

	Cumulative Oil Recovery (STB)			
	Primary Recovery	Waterflooding	CO_2 Injection	Total from IOIP
Periods (years)	2	5	7	14
Run 1	6×10^3 (2%)	10×10^5 (38%)	80×10^5 (30%)	19×10^5 (70%)
Run 2	5×10^3 (2%)	11×10^5 (38%)	18×10^5 (26%)	19×105 (66%)

Figure 4.22 shows the distributions of the asphaltene deposited mass throughout the three recovery stages (primary recovery, waterflooding, and CO_2 injection) for the first layer in the reservoir for Scenario 1 and Scenario 3. It shows that, for both scenarios, asphaltene deposited mass during the primary recovery and waterflooding stages is small compared to the high amount of asphaltene deposited mass for the CO_2 injection stage. The explanation of this is linked to the asphaltene instability caused by the increased amount of aliphatic components during CO_2 injection, which induces precipitation and deposition, and may cause pore throat plugging. This figure also shows that there is a considerable difference in the asphaltene deposited mass between Scenario 1 and Scenario 3 in all recovery stages to a great extent in the CO_2 injection stage. This result confirmed that CO_2 injection is the main contributing reason to asphaltene precipitation.

Figure 4.23 shows the total asphaltene deposited mass versus time at the production well for all scenarios. For Scenario 1, it shows that the total deposited asphaltene mass is about 368 lb for all layers during primary and waterflooding stages compared to 415 lb for the CO_2 injection stage. The highest amount of deposition was obtained at a forward reaction rate (k_{12}) of 100 and at a backward reaction rate of (k_{21}) of 0, where this scenario will lead to depositing all the precipitated asphaltene without any returning to the solution. The figure shows much lower deposited asphaltene mass in Scenario 3 compared to Scenarios 1 and 2. **Table 4.7** shows the comparison of the total deposited asphaltene mass between all scenarios.

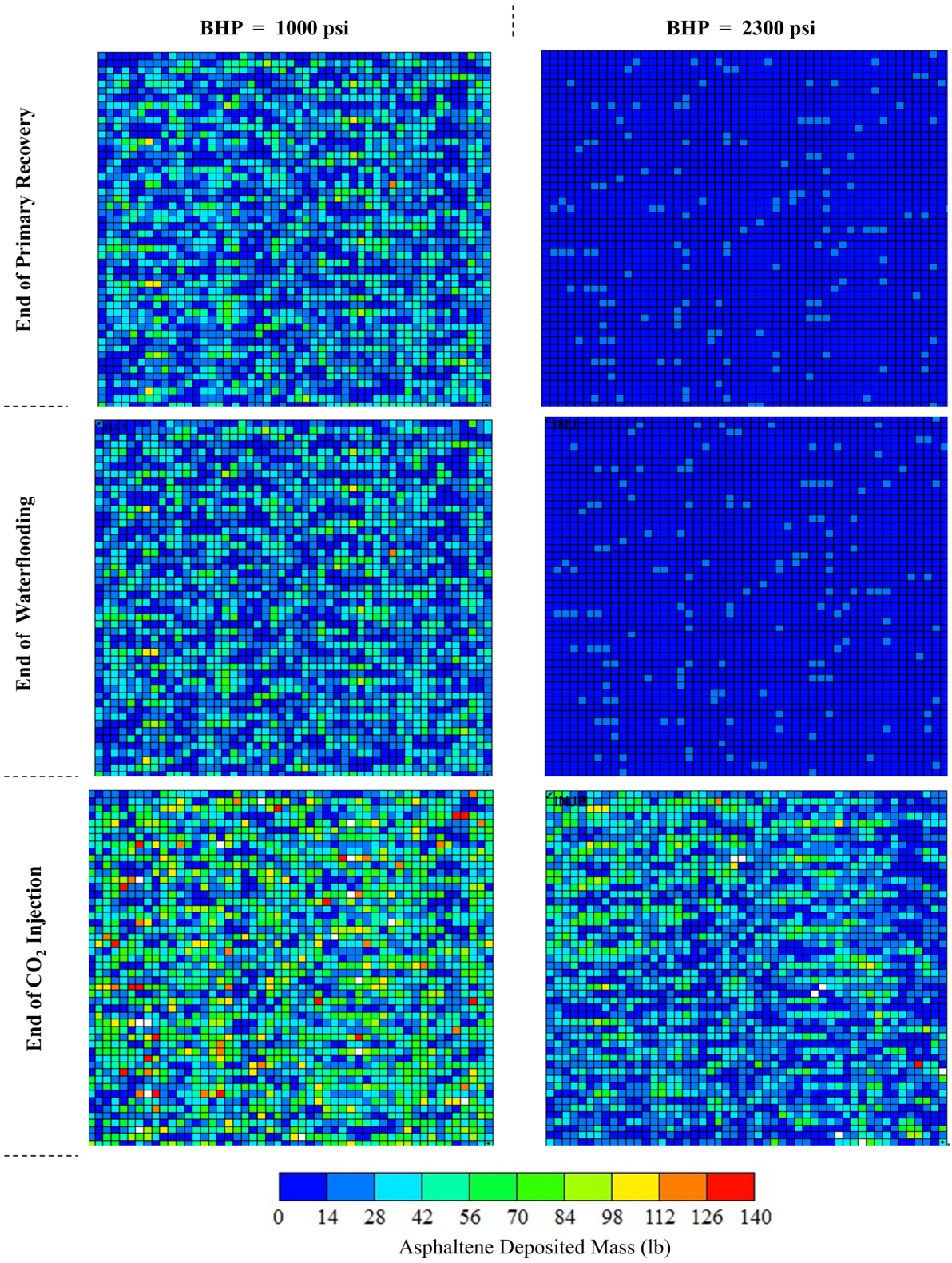

Figure 4.22: Two-Dimensional View Comparison of Asphaltene Deposited Mass (lb) Between Scenarios 1 and 3

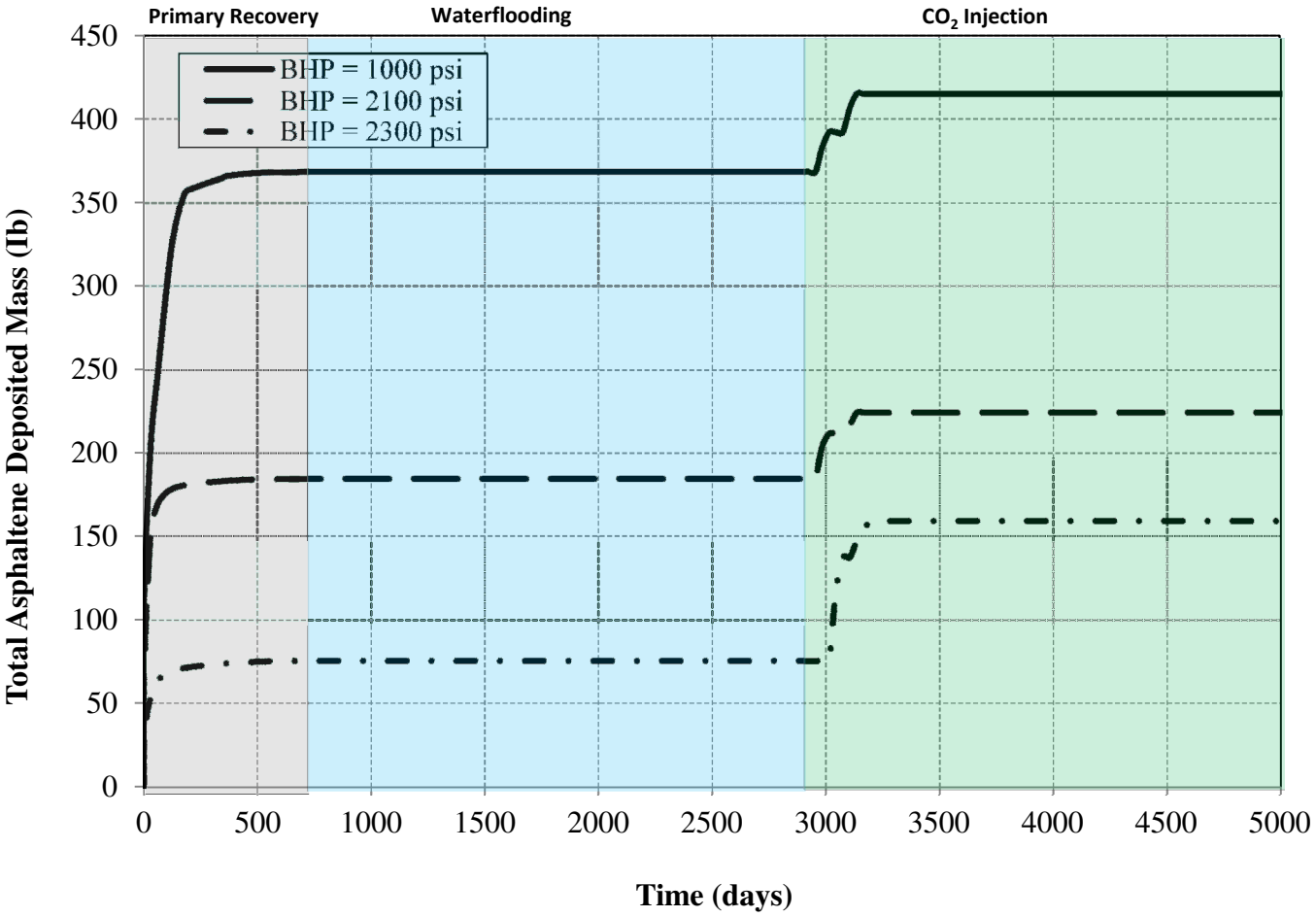

Figure 4.23: Asphaltene Deposited Mass (lb) During all Recovery Stages for Different Scenarios

Table 4.7: Comparison of Total Deposited Asphaltene Mass for Different Scenarios

Total deposited asphaltene mass (lb)			
	Primary Recovery	Waterflooding	CO_2 Injection
Scenario 1	368	368	415
Scenario 2	184	184	224
Scenario 3	75	75	159

Case 5: Production and completion optimization

This section is a summary of the simulation results of the benefits of selecting the optimum completion zone, injection strategy, and the operating production strategy for pressure depletion, waterflooding, and CO_2 injection stages that reduce asphaltene deposition and enhance the productivity of well B-1. Six runs were performed for this purpose. In this case, we will investigate the effect of asphaltene precipitation and deposition on oil reservoir parameters and performance including wettability alteration during the water alternating gas process (WAG). The WAG process will be investigated for the effects of asphaltene presence on oil recovery during its application. The operating and completion procedure to minimize the asphaltene problem is not well studied. It is believed a better understanding of the fundamental processes leading to solids precipitation is a prerequisite to the management and prevention of production problems. Based on the comparison studies performed earlier for the optimum BHP pressure, it was realized that the 2300 psi BHP scenario is the best and for this reason it will be used in this optimization study. The default completion and perforation design used in the simulation model earlier was used as the base for this comparison study. **Table 4.8** shows a summary of the runs used for the production assurance optimization and their associated recovery.

Table 4.8 Summary of the Runs

	Water injection Scheme	CO_2 injection Scheme	Production Scheme	Recovery
Base Case	Inject from all layers	Inject from all layers	Produce from all layers	68.00%
Case 1	Inject from all layers	Inject from the bottom three layers (3 - 5)	Produce from all layers	68.05%
Case 2	Inject from all layers	Inject from the upper three layers (1 - 3)	Produce from all layers	67.29%
Case 3	Inject from the bottom three layers (3 - 5)	Inject from the upper three layers (1 - 2)	Produce from the bottom three layers (3 - 5)	66.77%
Case 4 (WAG)	Inject from all layers	Inject from all layers	Produce from the bottom three layers (3 - 5)	65.42%
Case 5 (WAG)	Inject from all layers	Inject from all layers	Produce from the bottom three layers (3 - 5)	65.83%
Case 6 (WAG)	Inject from all layers	Inject from all layers	Produce from all layers	64.01%

The default design was to inject water and CO_2 and produce from the five layers. The first run (Case 1) was the same as the default setup (Base Case) except that CO_2 injection was to be through the bottom three layers. The second run (Case 2) was the same as the default setup (Base Case) except that CO_2 injection was to be through the upper three layers. The third run (Case 3) set up was to inject water from the bottom three layers, inject CO_2 from the upper three layers, and produce from the bottom three layers.

Cases 4, 5, and 6 were performed to test the sensitivity of asphaltene deposition with the use of WAG. Case 4 and Case 5's set up is the same as the base case except that the production was allowed from the bottom three layers, however; the WAG cycle in Case 4 was based on two-year alterations (2 years of CO_2 followed by water for the same period), whereas Case 5 was based on year to year (1 year of CO_2 followed by water for one year, etc.). Case 6 is the same as the base case, but with the use of WAG based on two-year alterations as in Case 4. **Figure 4.24** and **Figure 4.25** show a comparison of

average reservoir pressure between the base case and the rest of the cases. Both figures show clearly that the WAG process will result in a high average reservoir compared to the base case, especially in Cases 4 and 5 where the production was coming from the bottom three layers instead of all layers as in Case 6. However, **Figure 4.26** and **Figure 4.27** show that Cases 1, 2, and 3 result in the higher recovery than Cases 4, 5, and 6. The recovery for each case is shown in **Table 4.7**. The reason for this difference between the cases with WAG and the cases without is due the fact that WAG process will introduce instability more frequently than the cases without WAG. **Figure 4.28** and **Figure 4.29** show a comparison of gas oil ratio between the base case and the rest of the cases. **Figure 4.29** indicates an unstable gas-oil ratio during the WAG cycle compared to a stable gas-oil ratio for the cases without. To understand this more, asphaltene deposition was investigated for all cases. **Figure 4.30** shows two-dimensional distributions of the asphaltene deposited mass throughout the CO_2 injection stage for layer 1 in the reservoir using the 2300 psi BHP constraint. As can be seen that asphaltene deposited mass in Cases 1, 2, and 3 is much lower than Cases 4, 5, and 6 which uses the WAG process. High asphaltene deposited mass is associated with the WAG process, which may cause pore throat plugging and reduce oil recovery. Based on the results obtained, the best way to complete a well in areas where asphaltene is anticipated is to place the well at higher horizon, where in lower horizons it is expected to show more asphaltene problems than wells that are higher in the structure. Thus, it is advisable to place the wells in such cases as high as possible. Also, it is suggested to inject CO_2 through the bottom layers in order to push the oil upward and mobilize more oil rather injecting from the top which applies

more restriction to the oil flow, especially when the well has a low average reservoir pressure. Also, it is suggested to apply a bottomhole pressure constraint that is higher than the asphaltene onset pressure. The results discussed in this section are supported by multiple simulation runs, field observations and by reported cases in Chapter 2's literature review.

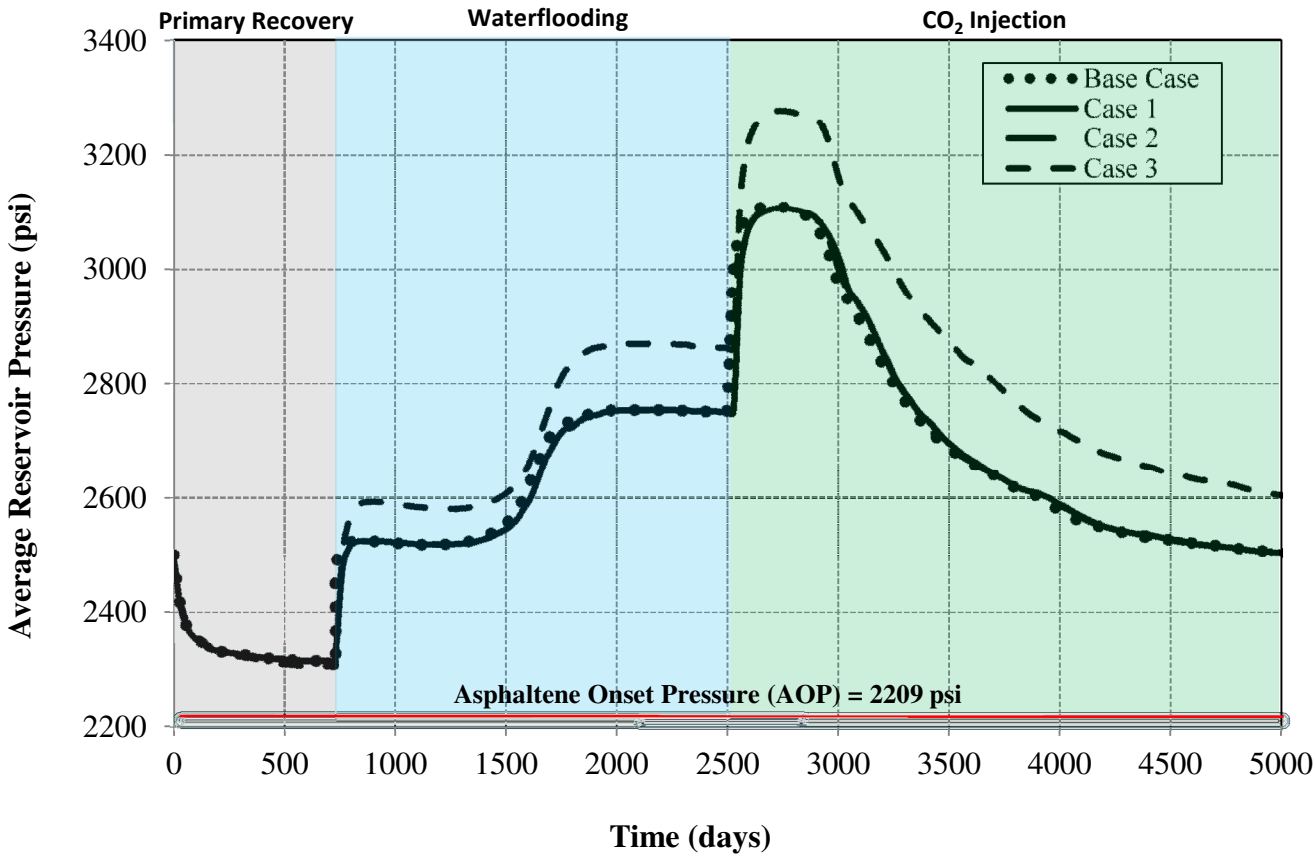

Figure 4.24: Comparison of Average Pressure for Cases 1, 2, and 3 With the Base Case

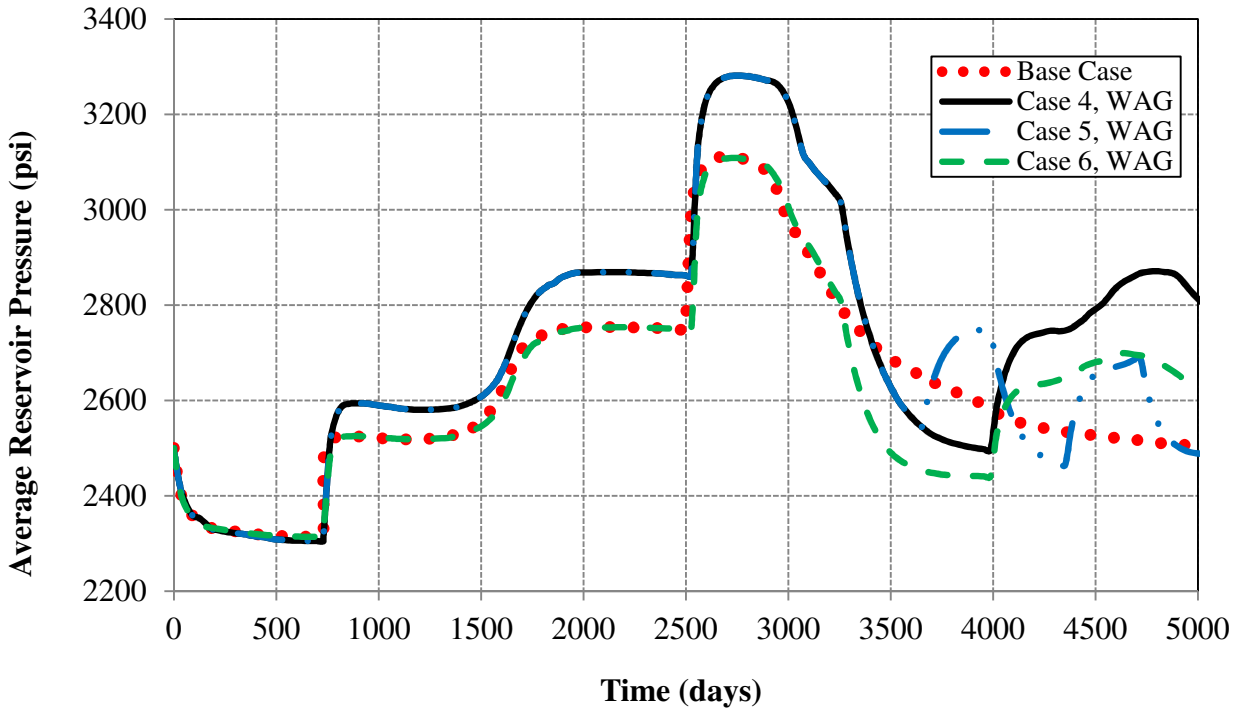

Figure 4.25: Comparison of Average Pressure for Cases 4, 5, and 6 With the Base Case

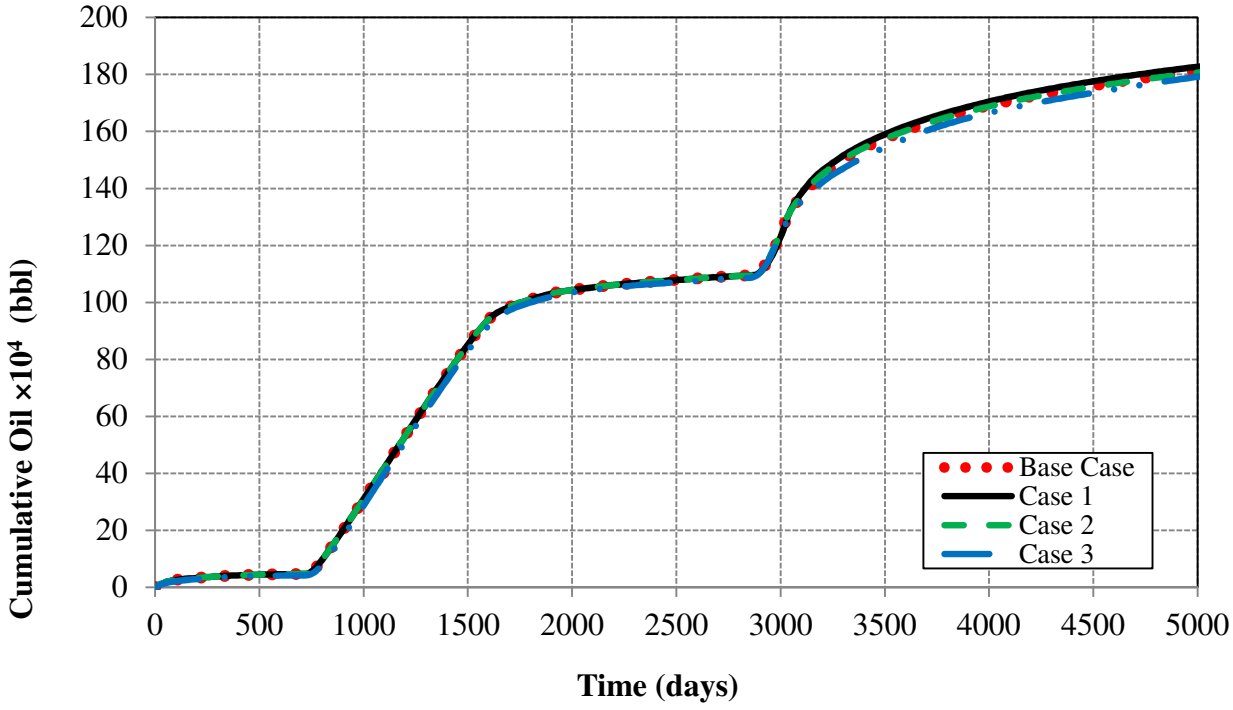

Figure 4.26: Comparison of Cumulative Oil Production for Cases 1, 2, and 3 With the Base Case

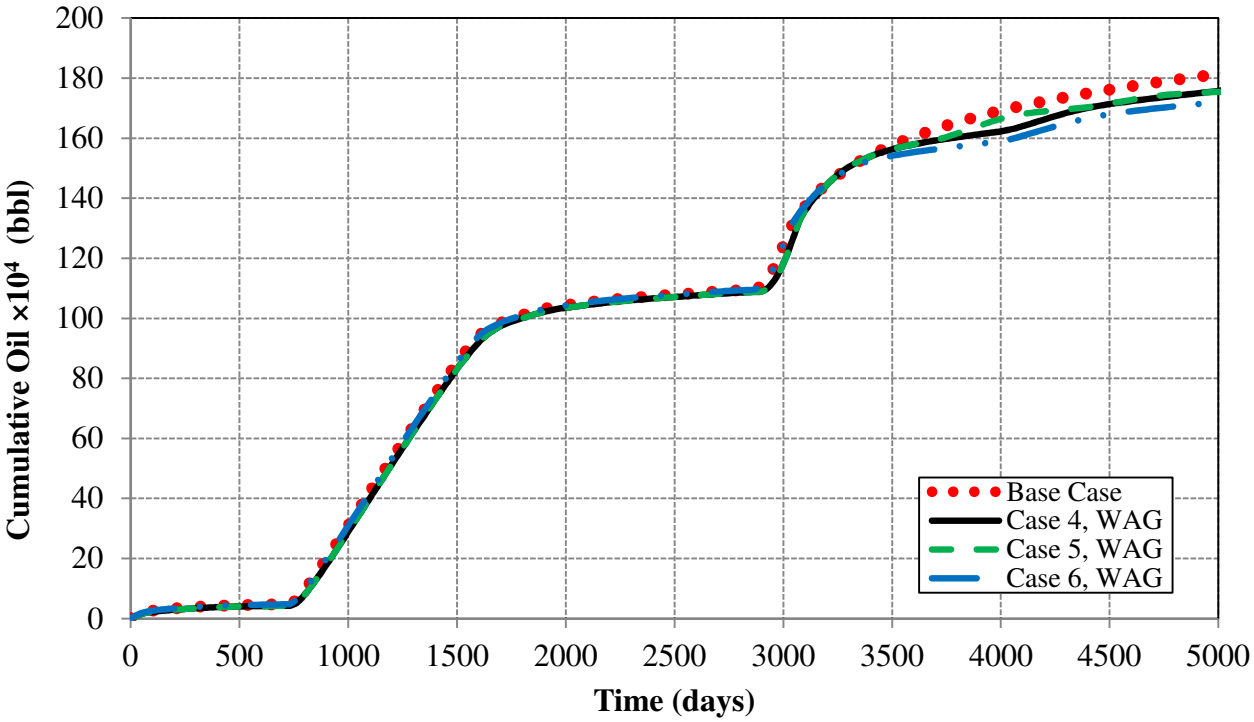

Figure 4.27: Comparison of Cumulative Oil Production for Cases 4, 5, and 6 With the Base Case

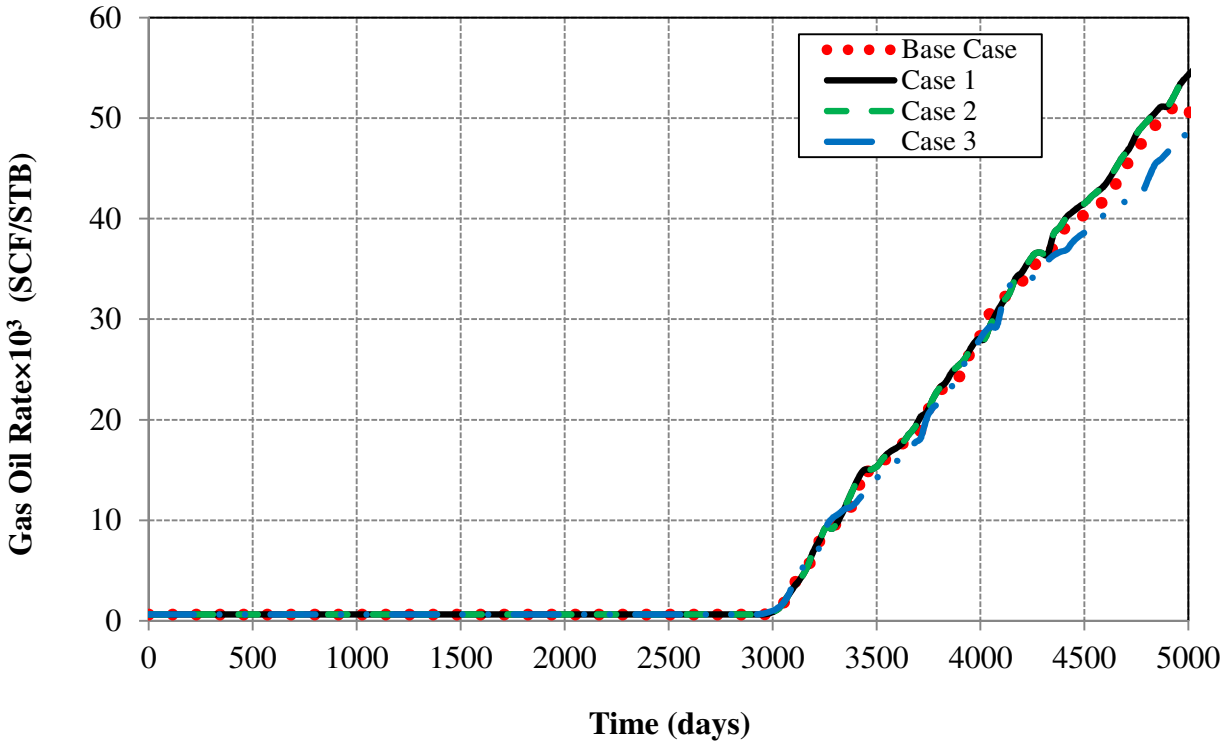

Figure 4.28: Comparison of the Gas-Oil Ratio for Cases 1, 2, and 3 With the Base Case

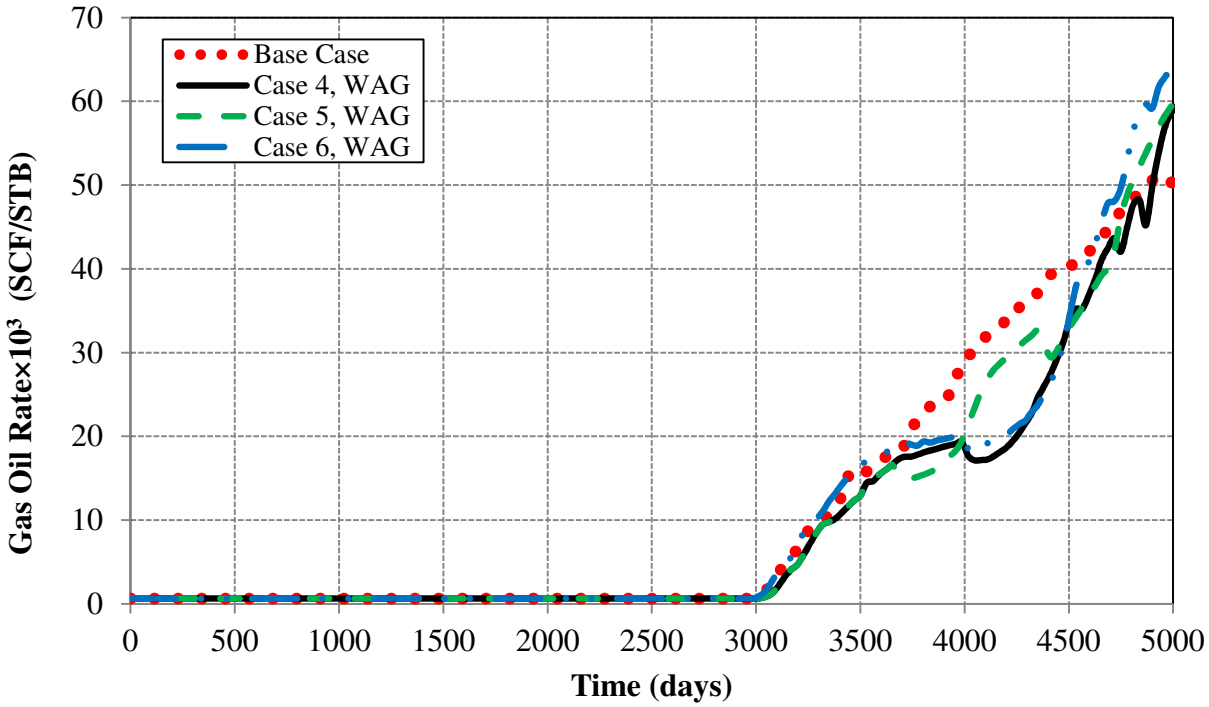

Figure 4.29: Comparison of the Gas-Oil Ratio for Cases 4, 5, and 6 With the Base Case

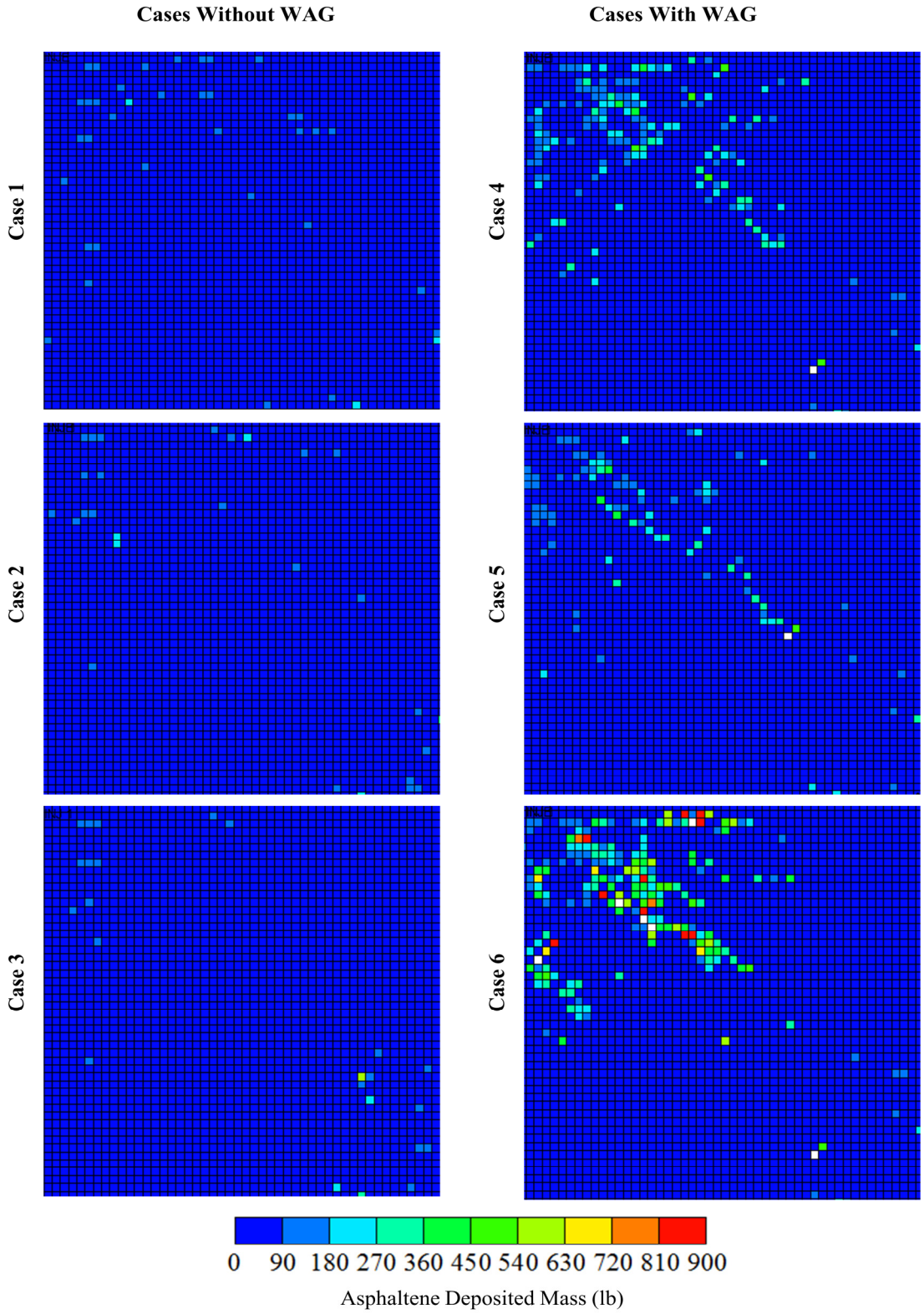

Figure 4.30: Two-Dimensional View Comparison of Asphaltene Deposited Mass (lb) for Cases 1 to 6

Chapter 5: SUMMARY, CONCLUSION, AND RECOMMENDATIONS

Summary, Conclusions, and Future Work

This chapter presents a summary of the research performed followed by some of the conclusions drawn based on this work. Some recommendations for future work are discussed at the end of the chapter.

5.1 Summary

Asphaltene precipitation is a complex and serious problem that affects oil recovery and induces formation damage. Many thermodynamics models have been developed to model asphaltene precipitation. They are divided into three groups: the real solution model (solubility model and solid model), the colloidal solution model, and the association equation-of-sate model. This thesis discusses different techniques related to preventing or delaying asphaltene precipitation problems. It presents summarized production and completion strategies that help delay asphaltene problems and also suggests precautionary procedures in dealing with asphaltene potential areas. A comprehensive phase behavior study for five wells from the Middle East was performed as part of an asphaltene precipitation study. The study outlined several important concepts and detailed procedures for modeling asphaltene phase behavior using WinProp, which uses the Nghiem model for asphaltene precipitation. The predictions showed good agreement with the experimental results obtained from the five Middle-Eastern wells. The model showed the ability to generate acceptable predictions of precipitated asphaltene at a wide range of conditions to address various aspects leading to asphaltene precipitation.

UTCOMP, CMG/GEM, and ECLIPSE simulators were used mainly to predict asphaltene precipitation and compare their results. The study compared the average pressure, oil rate, and WOR and resulted in an acceptable match between the three simulators. The asphaltene precipitation was then compared between the three simulators and showed that the three simulators generate similar trends of asphaltene precipitation behavior with different amounts. This behavior was attributed to some differences in asphaltene modeling set up between the three simulators, especially the assumption in CMG/GEM and ECLIPSE. This assumption states that the same porosity values exist before and after the precipitation process, whereas UTCOMP suggests that asphaltene precipitation will cause some damages that affect the original porosity in terms of porosity decline. An asphaltene sensitivity study was performed to investigate the asphaltene precipitation on core-scale and field-scale levels.

The results of the heterogeneous three-dimensional simulation study confirmed the reported behavior of asphaltene as a function of pressure. It showed that as pressure decreases (at above Pb), the asphaltene content in oil decreases and the amount of precipitated asphaltene increases. In decreasing pressure (at below Pb) the asphaltene re-dissolves back into the oil (amount of precipitated asphaltene decreases). The simulation study also showed that asphaltene deposition moves along the displacement front. This is because deposition is related to the development of miscibility of CO_2 flooding, whereas a much lower amount of asphaltene deposited mass has been observed during water flooding. Different production practices were applied to define the most

appropriate and efficient production strategy. The outcomes generated by the model can be used to identify favorable operating conditions to asphaltene precipitation. This information is useful to be used in designing production strategies and EOR projects especially CO_2 injection. This study includes a comprehensive discussion and comparison of production rates with and without asphaltene precipitation, flocculation, and deposition and a comparison of asphaltene precipitation, flocculation, and deposition at different times using different bottomhole and production rate constraints. Several cases were tested to suggest an optimum completion and operating strategy in the presences asphaltene.

5.2 Conclusion

The following conclusions can be presented on the basis of this study:

- Asphaltene phase behavior study for five wells from the Middle East was performed as part of modeling asphaltene precipitation using the Nghiem model. The predictions of the proposed model showed good agreements with the experimental results obtained from the five Middle-Eastern wells. The model showed the ability to generate acceptable prediction asphaltene precipitation at a wide range of conditions to address various aspects leading to asphaltene precipitation.
- A one-dimensional simulation study was performed to compare the precipitation model in UTCOMP, CMG/GEM, and ECLIPSE simulators. The result, including asphaltene precipitation, showed an acceptable match between simulators.

- A three-dimensional compositional simulation model was run to investigate the effect of asphaltene precipitation, flocculation, and deposition on oil recovery during pressure depletion, waterflooding, and CO_2 injection stages. The results showed how these parameters affect the flooding efficiency and well productivity. It has been shown that the effect of asphaltene deposition is more pronounced during CO_2 injection, which agrees with field observations reported in the literature.

- The three-dimensional compositional simulation study showed the importance of modeling asphaltene precipitation during the early design of production strategies, where it impacts oil recovery.

- The precipitated asphaltene may deposit throughout the reservoir and not only in the near-wellbore vicinity.

- Deposition parameters showed high sensitivity to the asphaltene model. In order to obtain accurate prediction to the filed behavior, experimental data for entrainment rate, critical interstitial velocity, deposition parameters, and pore plugging coefficients are required.

- Including entrainment helped reducing the effects of asphaltene deposition, removing the deposited asphaltene around the well and improving productivity in turn.

- Six runs were conducted to test the optimum production and operating strategies, and completion design. The results suggest using a bottomhole pressure higher than the asphaltene onset pressure. The result showed also that the WAG process will provide higher pressure support to the reservoir; however, it decreases the oil

recovery and induces asphaltene deposition to a great extent compared to the cases without using WAG cycles. The study suggested completing the well at the upper layers rather than at the lower layers in wells where asphaltene exist. These mechanisms are extremely important, especially in offshore development with subsea wells, where the cleaning of plugged wells is very costly.

5.3 Recommendations for Future Work

More studies are needed to consolidate the findings of this thesis and to enhance our understandings of asphaltene precipitation. This thesis focused on comparing three different softwares (UTCOMP, CMG/GEM, and ECLIPSE) for homogenous reservoirs, and the comparison may be extended to account for reservoir heterogeneity, faults, and other naturally occurring properties. The effect of asphaltene deposition on wettability alteration should be molded and incorporated in compositional simulators to help explain the effect of asphaltene deposition during the WAG process, where the formation wettability changed from water-wet to oil-wet. This three-dimensional study was conducted on vertical wells, and it is important to extend it to horizontal wells where pressure drop is higher and asphaltene remediation is much more expensive than in vertical wells.

APPENDIX A

Reservoir Data for Wells: B-2, B-3, A-1, and A-2

Table A1: Well B-2 Molecular Weight and Composition Data

Component	Reservoir Fluid	MW	Std. Density
	mole %	lb/lbmol	lb/ft^3
N2	0.163	28.01	
CO2	1.941	44.01	
H2S	0	34.08	
C1	33.532	16.04	
C2	7.659	30.07	
C3	7.271	44.1	
i-C4	1.884	58.12	
n-C4	4.695	58.12	
i-C5	2.195	72.15	38.5
n-C5	2.984	72.15	38.8
n-C6	5.049	85.58	41.5
C7	4.377	94.9	44.6
C8	3.606	109.09	45.6
C9	2.642	122.4	46.5
C10	2.779	135.24	48.3
C11	2.083	151.42	48.3
C12+	17.14	313.02	54.5

Table A2: Well B-3 Molecular Weight and Composition Data

Component	Reservoir Fluid	MW	Std. Density
	mole %	lb/lbmol	lb/ft^3
N2	0.147	28.01	
CO2	1.926	44.01	
H2S	0	34.08	
C1	31.734	16.04	
C2	7.349	30.07	
C3	7.206	44.1	
i-C4	1.98	58.12	
n-C4	4.897	58.12	
i-C5	2.41	72.15	38.5
n-C5	5.068	72.15	38.8
n-C6	3.904	85.58	41.5
C7	4.95	94.9	44.6
C8	4.052	109.09	45.6
C9	2.949	122.4	46.5
C10	3.104	135.24	48.3
C11	2.294	151.42	48.3
C12+	16.03	313.02	54.5

Table A3: Well A-1 Molecular Weight and Composition Data

Component	Reservoir Fluid	MW	Std. Density
	mole %	lb/lbmol	lb/ft^3
N2	0.51	28.013	
CO2	5.12	44.01	
H2S	1.7	34.08	
C1	28.13	16.043	
C2	9.65	30.07	
C3	6.78	44.097	
i-C4	0.91	58.124	
n-C4	3.46	58.124	
i-C5	1.22	72.151	38.5
n-C5	2.22	72.151	38.8
n-C6	3.65	86.178	41.5
C7	3.83	100.205	44.6
C8	4.13	128.259	45.6
C9	3.92	114.232	46.5
C10	3.34	142.286	48.3
C11	2.15	151.42	48.3
C12+	19.3	309	54.5

Table A4: Well A-2 Molecular Weight and Composition Data

Component	Reservoir Fluid	MW	Std. Density
	mole %	lb/lbmol	lb/ft^3
N2	0.4	28.013	
CO2	4.6	44.01	
H2S	1.04	34.08	
C1	24.23	16.043	
C2	9.25	30.07	
C3	7.52	44.097	
i-C4	0.98	58.124	
n-C4	3.79	58.124	
i-C5	1.27	72.151	38.5
n-C5	2.33	72.151	38.8
n-C6	3.54	86.178	41.5
C7	3.65	100.205	44.6
C8	3.78	128.259	45.6
C9	3.48	114.232	46.5
C10	2.74	142.286	48.3
C11	1.64	151.42	48.3
C12+	25.76	320	54.5

Table A5: Onset of Asphaltene Precipitation Data for Well B-2 and B-3

Onset of Asphaltene Precipitation	
Pressure	**Temperature**
psig	F
2419	254

Table A6: Saturation Data for Well B-2 and B-3

Saturation Data	
Pressure	**Temperature**
psig	F
2179	254

Table A7: Molecular Weight and Composition Data for Well A-1

Onset of Asphaltene Precipitation	
Pressure	**Temperature**
psig	F
3100	212

Table A8: Saturation Data for Well A-1

Saturation Data	
Pressure	**Temperature**
psig	F
2156	212

Table A9: Molecular Weight and Composition Data for Well A-2

Onset of Asphaltene Precipitation	
Pressure	**Temperature**
psig	F
3200	212

Table A10: Saturation Data for Well A-2

Saturation Data	
Pressure	**Temperature**
psig	F
1669	212

Table A11: Reservoir Fluid Data After Lumping of Components for Phase Behavior Study

Component Name	Mole Fractions	Pc (atm)	Tc (K)	Acentric Factor	Molecular Weight	Volume shifts	Parachor	Viscosity	SG
N2	0.0016	33.5	126.2	0.04	28.01	0	41	0.0895	0.809
CO2	0.020002	72.8	304.2	0.225	44.01	0	78	0.094	0.818
H2S	0	88.2	373.2	0.1	34.08	0	80	0.0985	0.801
C1	0.333633	45.4	190.6	0.008	16.04	0	77	0.099	0.3
C2	0.077107	48.2	305.4	0.098	30.07	0	108	0.148	0.356
C3	0.073907	41.9	369.8	0.152	44.10	0	150	0.203	0.507
HC1	0.118313	34.9	442.7	0.230269	64.10	0	187	0.2819	0.60095
HC2	0.112112	28.9	539.4	0.302689	96.52	0	280	0.4022	0.70511
HC3	0.083608	23.4	620.5	0.408786	134.56	0	383	0.5485	0.76365
HC4	0.138178	14.2	768.1	0.722373	245.56	0	649	0.9992	0.83611
HC5	0.021569	9.1	914.7	1.129618	433.54	0	975	1.5873	0.90576
C36+	0.019655	7.2	1025.6	1.340256	649.64	0	1159	1.9562	0.96071
ASPH	0.000316	7.2	1025.6	1.340256	649.64	0	1159	1.9562	0.96071

APPENDIX B

Sample UTCOMP Input File for Asphaltene Precipitation Simulation

```
CC*********************************************************************
CC                                                                    *
CC     Hydrocarbon Data and Flash Calculation Options                 *
CC                                                                    *
CC*********************************************************************
CC
CC..+....1....+....2....+....3....+....4....+....5....+....6...+...7..
CC CASE NAME WITH FORMAT (17A4, A2) OF TOTAL 70 COLUMNS.
*----HEADER
ABU DHABI PROJECT-CASE (1)
CC
CC NUMBER OF COMPONENTS.
*--------NC
       11
CC COMPONENT NAMES WITH FORMAT ( 1X, A8 ), NC CARDS.
CC..+..8
*----NAME
  N2
  CO2
  C1
  C2
  C3
  HC1
  HC2
  HC3
  HC4
  HC5
  C36+
CC
CC BLACK OIL OPTION; AQUIFER SALINITY (ppm); AQUIFER OPTION
*-----IBOST     SLNTY    IAQUIF
         0       0.         0
CC CRITICAL PRESS. (PSI), TEMP. (R) AND VOL. (CU FT/LB-MOLE),
CC MOLECULAR WT. (LB/LB-MOLE), ACENTRIC FACTOR, PARACHOR. NC CARDS.
*--------PC       TC         VC         MW       OM     PARACH VSP
492.314325      227.16         1.43365431      28.013  0.04    41      0
1069.86516      547.56         1.505737488     44.01   0.225   78      0
667.19613       343.08         1.585829907     16.043  0.008   77      0
708.34479       549.72         2.370735619     30.07   0.098   108     0
615.760305      665.64         3.251752234     44.097  0.152   150.3   0
513.0650064     796.8618     4.515610615     64.1    0.23027 186.6   0
424.8011307     970.9884     6.442634229     96.52   0.30269 279.9   0
343.7382705     1116.891     8.786138425     134.556 0.40879 383.4   0
209.2115442     1382.634       16.00566912     245.556 0.72237 649.1   0
133.2922665     1646.541       25.42613951     433.542 1.12962 975.4   0
105.1348263     1846.0458       31.33535823     649.644 1.34026 1158.5  0
CC EOS parameters (Ac and Bc)
CC NC CARDS.
```

```
*----PARAA              PARAB
  0.457235529       0.077796074
  0.457235529       0.077796074
  0.457235529       0.077796074
  0.457235529       0.077796074
  0.457235529       0.077796074
  0.457235529       0.077796074
  0.457235529       0.077796074
  0.457235529       0.077796074
  0.365790000       0.077796074
  0.365790000       0.077796074
  0.457235529       0.077796074
CC
CC BINARY INTERACTION COEFFICIENTS, CIJ. NC CARDS.
*-----DELTA
0
-0.02   0
0.031   0.103   0
0.042   0.13    0.00269 0
0.091   0.135   0.00854 0.00166 0
0.095   0.13    0.01799 0.00688 0.00179 0
0.12    0.15    0.03194 0.01644 0.00774 0.0021  0
0.12    0.15    0.04706 0.02798 0.01626 0.00734 0.0016  0
0.12    0.15    0.08328 0.05803 0.04098 0.02614 0.01366 0.00597 0
0.12    0.15    0.11661 0.08741 0.06682 0.04792 0.03066 0.01855 0.00356 0
0.12    0.15    0.13292 0.1022  0.08019 0.05964 0.04039 0.02639 0.00748 0.00073 0
CC
CC BINARY INTERACTION COEFFICIENTS, DIJ. NC CARDS.
*-------DIJ
0
0       0
0       0       0
0       0       0       0
0       0       0       0       0
0       0       0       0       0       0
0       0       0       0       0       0       0
0       0       0       0       0       0       0       0
0       0       0       0       0       0       0       0       0
0       0       0       0       0       0       0       0       0       0
0       0       0       0       0       0       0       0       0       0       0
CC
CC MAXIMUM NUMBER OF PHASES ( 3 OR 4 )
*--------NP     IVISC     ISINGL   ISOLU
         3       1       1       0
CC
CC COEFFICIENT FOR LOHRENZ-BRAY-CLARK (LBC)
*----- COEF1,COEF2,COEF3,COEF4,COEF5
    0.1023  0.023364   0.058533  -0.040758  0.0093324
CC IEOS: 1,    IPEM: 0 OR 1
CC ISTAM: -1, 0 OR 1, IEST: 0 OR 1  KI: 0, 1 OR 2
*---IEOS   IPEM     ISTAM   IEST  IVSP   KI   INI2
     1      1        -1      0     0     0    0
CC
```

```
CC ITERATION TOLERANCES FOR PERSCHKE'S FLASH ROUTINES.
*----TOLFLA    TOLFLM    TOLPD    TOLSAM    TOLSAS    TOLSUM
    1.0E-07   1.0E-07    1.0E-07  1.0E-07  1.0E-07   1.0E-05
CC
CC MAXIMUM NUMBER OF ITERATIONS FOR PERSCHKE'S FLASH ROUTINES.
*----MAXFLA    MAXFLM    MAXPD    MAXSAM    MAXSAS
   500       500       500      500       500
CC
CC VECTOR FLASH OPTION
*-----IVCFL    TOLVFL    MAXVFL
        0     1.E-8        20
CC
CC SWITCHING PARAMETERS FOR PERSCHKE'S FLASH ROUTINES.
*----SWIPCC    SWIPSA
     .01        1
CC
CC PHASE IDENTIFICATION PARAMETERS FOR PERSCHKE'S FLASH ROUTINES.
*------IOIL      ITRK   DMSLIM
        1        1      20
CC
CC IFLAGT ( 0 : OFF,   1 : ON )
*------IFLAGT    IASPR
        0    1
CC
CC PERMEABILITY MODEL USED FOR ASPHALTENE PRECIPITATION
*------1: SOLID: 2: RELATIVE; 3: RELATIVE WITH ADJUSTABLE PARAMETER
        4     2209      16.01848391
CC
CC
*
0.1
CC
CC BINARY INTERACTION COEFFICIENT OF THE PRECIPITATED COMPONENT
*------ DELTA
 0.14   0.2     0.14825 0.11422 0.08975 0.06684 0.04039 0.02639 0.00748 0.00073 0       0
CC
CC*********************************************************************
CC                                                  *
CC OUTPUT OPTIONS                                           *
CC                                                  *
CC*********************************************************************
CC
CC
CC HISTORY PRINTING PARAMETER FOR <<HISTORY.CPR>>.
*---NHSSKIP   NSTSKIP     IPV
    10        100         0
CC
CC REFERENCE CONCENTRATION, CONC0, USED FOR EFFLUENT CONCENTRATION.
*-----CONC0
  1.0   1.0   1.0   1.0   1.0   1.0  1.0   1.0   1.0   1.0   1.0   1.0   1.0   1.0   1.0   1.0   1.0   1.0  1.0   1.0   1.0   1.0
CC
CC NUMBER OF PRINTS FOR <<.TAB>> (ALSO FOR TRAPPING & ASPHALTENE DATA)
*-------NPR
```

```
      13
CC
CC TIME(DAYS) AND FLAGS ( 0 OR 1 ) NPR CARDS.
*------TPR     MPRP   MPRSAT   MPROMFR   MPRPMFR    MPRPRO   MPRATES
     10.    1      1       1       1        1        1
     30.    1      0       0       0        0        1
     69.    1      0       0       0        0        1
     260    1      0       0       0        0        1
     390    1      0       0       0        0        1
     620    1      0       0       0        0        1
     730    1      0       0       0        0        1
     980    1      0       0       0        0        1
     1210   1      0       0       0        0        1
     1460   1      1       1       1        1        1
     2000   1      1       1       1        1        1
     2500   1      1       1       1        1        1
     3000   1      1       1       1        1        1
CC
CC NUMBER OF PRINTS FOR <<PROFILE.CPR>>.
*-------NPF
      1
CC
CC TIME(DAYS) AND FLAGS ( 0 OR 1 ) NPF CARDS.
*-------TPF    MPFSAT   MPFOMFR   MPFPMFR   MPFPROP
     50     1       1       1       1
CC
CC NUMBER OF PRINTS FOR <<CONTOUR.CPR>>.
*-------NCT
      8
CC
CC TIME(DAYS) AND FLAGS ( 0 OR 1 ) NCT CARDS.
*-------TCT     MCTP   MCTSAT   MCTOMFR   MCTPMFR    MCTPRO
      20.0    1       1       0       0       0
      50.0    1       1       0       0       0
      100.    1       1       0       0       0
      200.    1       1       0       0       0
      365.    1       1       0       0       0
      400.    1       1       0       0       0
      600.    1       1       0       0       0
      900.    1       1       0       0       0
CC
CC*********************************************************************
CC                                                  *
CC RESERVOIR AND WELL DATA                                  *
CC                                                  *
CC*********************************************************************
CC
CC A FLAG FOR RESERVOIR GEOMETRY:
CC 2-D: 11(Y), 12(X), 13(Z), 2-D: 21(XY), 22(YZ), 23(XZ), 3-D: 31
*-----IGEOM      INUG
      12       0
CC
CC NUMBER OF GRID BLOCKS IN X, Y, AND Z.
```

```
*--------NX        NY        NZ
      100         1         1
CC
CC NUMBER OF WELLS
*--------NW       IWM
         2         1
CC
CC WELLBORE RATIUS (FT). NW NUMBERS.
*--------RW: (NW)
      0.25      0.25
CC
CC WELL LOCATIONS. NW CARDS.
*-------LXW       LYW    IDIR   LZWF      LZWL
         1         1        3      1         1
         100       1        3      1         1
CC
CC A FLAG ( 0 OR 1 ) FOR GRID BLOCK SIZE IN X-DIRECTION.
*-------MDX
        0
CC
CC CONSTANT GRID BLOCK SIZE IN X-DIRECTION (FT).
*--------DX
       80.
CC
CC A FLAG ( 0 OR 1 ) FOR GRID BLOCK SIZE IN Y-DIRECTION.
*-------MDY
        0
CC
CC CONSTANT GRID BLOCK SIZE IN Y-DIRECTION (FT).
*--------DY
       80.
CC
CC A FLAG ( 0 OR 1 ) FOR GRID BLOCK SIZE IN Z-DIRECTION.
*-------MDZ
        1
CC
CC CONSTANT GRID BLOCK SIZE IN Z-DIRECTION (FT).
*--------DZ
       20.
CC
CC A FLAG ( 0 OR 1 ) FOR FORMATION DEPTH.
*--------MD
        0
CC
CC DEPTH (FT) OF THE MOST UPPER LAYER.
*---------D
      7500
CC
CC A FLAG ( 0 OR 1 ) FOR FORMATION POROSITY.
*------MPOR
      0
CC
CC HOMOGENEOUS POROSITY (FRACTION) AT PF.
```

```
*----PORSTD
    0.3
CC
CC A FLAG ( 0 OR 1 ) FOR PERMEABILITY IN X-DIRECTION.
*----MPERMX
      0
CC
CC HOMOGENEOUS PERMEABILITY (MD) IN X-DIRECTION.
*-----PERMX
      800.
CC
CC A FLAG ( 0 OR 1 ) FOR PERMEABILITY IN Y-DIRECTION.
*----MPERMY
      0
CC
CC HOMOGENEOUS PERMEABILITY (MD) IN Y-DIRECTION.
*-----PERMY
      800.
CC
CC FLAG ( 0 OR 1 ) FOR PERMEABILITY IN Z-DIRECTION.
*----MPERMZ
      0
CC
CC HOMOGENEOUS PERMEABILITY (MD) IN Z-DIRECTION.
*-----PERMZ
     800.
CC
CC FORMATION COMPRESSIBILITY (1/PSI) AND REFERENCE PRESSURE (PSI).
*--------CF          PF
        5.e-6       14.7
CC H2O COMPRESSIBILITY (1/PSI), REFERENCE PRESSURE (PSI) AND
CC MOLAR DENSITY (LB-MOLE/CU FT).
*--------CW       PW     DENMWS
       3.3e-6    14.7      3.467
CC
CC WATER MOLECULAR WT. (LBM/LBM-MOLE) AND VISCOSITY (CP).
*-------WTW     VISCW
       18.       0.7
CC
CC FORMATION TEMPERATURE (F).
*-----TEMPF
      250.0
CC
CC STANDARD TEMPERATURE (F) AND STANDARD PRESSURE (PSI).
*-----TFSTD      PSTD
       60.      14.7
CC
CC A FLAG ( 1, 2, 3 OR 4 ) FOR NUMERICAL DISPERSION CONTROL.
*----IUPSTW
        1
CC
CC ITC ( 0 : NO 2ND ORDER TIME,   1 : 2ND ORDER TIME ON )
*----ITC
```

```
     0
CC RESTART OPTIONS.
CC ISTART ( 1 OR 2 ), ISTORE ( 0 OR 1 ).
*----ISTART    ISTORE
       1        0
CC
CC A FLAG ( 0 OR 1 ) FOR AUTOMATIC TIME-STEP SELECTION ( = 1 ).
*-------MDT
       1
CC
CC A FLAG ( 0 OR 1 ) FOR PHYSICAL DISPERSION CALCULATION.
*-----MDISP
       0
CC FLAGS FOR RELATIVE PERMEABILITY MODEL AND CAPILLARY PRESSURE.
CC IPERM ( 1 OR 2 ), ICPRES ( 0 OR 1 ).
*-----IPERM    ICPRES      ICAP    IRPERM  IRSFFT
       8       0         0         0     0
CC CAPILLARY PRESSURE PARAMETERS AND
CC WATER/OIL INTERFACIAL TENSION (DYNES/CM).
*-------EPC       CPC    RIFTWO    RIFTWG    RIFTWL
       2.       1.0    20.       20.       20.
CC
CC HIGH IFT RESIDUAL SATURATIONS.
*------S1RW     S2RW1     S2RW2      S3RW     S4RW1     S4RW2
       0.3      .68       .3         0.0      0.0      0.0
CC
CC LOW IFT RESIDUAL SATURATIONS.
*------S1RC     S2RC1     S2RC2      S3RC     S4RC1     S4RC2
       0.3      .68       .3       0.0      0.0      0.0
CC
CC HIGH IFT END POINT RELATIVE PERMEABILITY.
*------P1RW      P2RW      P3RW      P4RW
       0.0       1.0       1.0       1.0
CC
CC LOW IFT END POINT RELATIVE PERMEABILITY.
*------P1RC          P2RC       P3RC     P4RC
       0.0         1.0         1.0      1.0
CC
CC HIGH IFT EXPONENT OF RELATIVE PERMEABILITY.
*-------E1W      E2W1      E2W2       E3W      E4W1      E4W2
       1        1      1       1.0      1.0       1.0
CC
CC LOW IFT EXPONENT OF RELATIVE PERMEABILITY.
*-------E1C      E2C1      E2C2       E3C      E4C1      E4C2
       1        1      1       1.0       1.0       1.0
CC
CC WATER AND L1 PHASE CAPILLARY DESATURATION PARAMETERS.
*-------T11       T12      T211      T221      T212      T222
        0.4       1.6      -0.5       2.2       -0.4      1.6
CC
CC GAS AND L2 PHASE CAPILLARY DESATURATION PARAMETERS.
*-------T31       T32      T411      T421      T412      T422
        -0.5       1.6      -0.5       2.2       -0.4      1.6
```

```
C
CC A FLAG FOR PRESSURE EQUATION SOLVER ( 1, 2, 3, 4 OR 5 ).
*----IPRESS    IPREC   METHSL   OMEGA
       3      3       1       1.0
CC
CC ITERATIVE PRESSURE SOLVER PARAMETERS.
*-----ITMAX  LEVLIT  IDGTS   NS1       NS2      ZETA
     100      1      1      5      1000000   1.E-07
CC
CC INITIAL TIME (DAYS).
*---------T
        0
CC
CC A FLAG ( 0 OR 1 ) FOR INITIAL PRESSURE.
*--------MP
       0
CC
CC CONSTANT INITIAL PRESSURE (PSIA).
*---------P
      2500.0
CC
CC A FLAG ( 0 OR 1 ) FOR INITIAL WATER SATURATION.
*------MSAT
      0
CC
CC CONSTANT INITIAL WATER SATURATION (FRACTION).
*-------SAT
       .2
CC
CC A FLAG ( 0 OR 1 ) FOR INITIAL OVERALL COMPOSITION.
*-----MOMFR
      0
CC
CC CONSTANT INITIAL COMPOSITION (MOLE FRACTION).
*------OMFR
0.0016  0.020002 0.333633 0.077107 0.073907 0.118313 0.112112 0.083608 0.138178 0.021569 0.019655
0.000316
CC
CC**********************************************************************
CC                                                  *
CC RECURRENT DATA                                          *
CC                                                  *
CC**********************************************************************
CC
CC
CC MAXIMUM TIME (DAYS), TIME STEP (DAYS) AND WELL DATA.
*----TM           DT       NWELLS    GORLIM    WORLIM
    1827       0.0002        2          -1.E+20        -1.E+10
CC
CC PARAMETERS FOR TIME STEP SELECTORS.
*-----DTMAX     DTMIN     DSLIM     DPLIM      DVLIM     DMFACT
      5.      0.001         0.5       0.5     .5      .5
CC
```

```
CC WELL NO. AND WELL TYPE.
*--------LW    IQTYPE
       1      4
CC
CC  TOTAL MOLAR FLOW RATE (LB-,OLES/DAYS)
*----QTML    FWMLC   NCOMP    ISWITCH   PBHC
    200       0       0         1      4000
CC
CC WELL NO. AND WELL TYPE.
*--------LW    IQTYPE
       2      -2
CC
CC   Constant BHP
*----  PBHC
       1000
CC
CC MAXIMUM TIME (DAYS), TIME STEP (DAYS) AND WELL DATA.
*----TM            DT       NWELLS    GORLIM    WORLIM
   2500          0.002        2     -1.E+20    -1.E+10
CC
CC PARAMETERS FOR TIME STEP SELECTORS.
*-----DTMAX     DTMIN     DSLIM     DPLIM      DVLIM    DMFACT
      1.      0.00001         0.01       0.01     .01      .01
CC
CC WELL NO. AND WELL TYPE.
*--------LW    IQTYPE
       1      4
CC
CC   (STB/D)  (MSCF/D)
*----QPSVC(1)   QPSVC(3)   NCOMP   ISWITCH   PBHC
      0.       2000         2       1   4000
CC
CC OVERALL COMPONENT
*-------KC     Z1
      1    0.000001
      2    0.999999
CC
CC WELL NO. AND WELL TYPE.
*--------LW    IQTYPE
       2      -2
CC
CC CONSTANT BHP PRODUCER
*--------PBHC
       1000
CC
CC END OF INPUT.
*--------TM DT    NWELLS    GORLIM    WORLIM ----------------
       -1.  -1.  -1       -1.E10    -1.E10
```

APPENDIX C

Sample ECLIPSE Input File for Asphaltene Precipitation Simulation

```
RUNSPEC ============================================================
TITLE
Asphaltene PRECIPITATION for WATER Flooding

START
1 JAN 2000 /

FIELD

GAS
OIL
WATER

DIMENS
100 1 1 /

COMPS
12 /

EQLDIMS
1 200 /

TABDIMS
1 1 2* 2 /

--AIM
FULLIMP

--NOSIM
UNIFIN
UNIFOUT

NOECHO

-- Switch on Asphaltene deposition model

ASPHALTE
WEIGHT /

GRID  ==============================================================
--Basic grid block sizes
EQUALS
DX 80/
DY 80 /
DZ 20 /
PORO 0.3 /
PERMX 800 /
PERMY 800 /
PERMZ 800 /
```

```
TOPS 7500 4* 1 1 /
/

-- Increase PV to provide pressure buffer and keep pres > psat

--EQUALS
--MULTPV 2/


-- Remove cells from "sump" of model

-- EQUALS

-- array value I1 I2 J1 J2 K1 K2
-- ACTNUM 0 2 10 1 1 2 3 /


--Properties section------------------------------------------------

PROPS
--Water saturation functions

--LBCCOEF
--0.1023  0.023364  0.058533  -0.040758 0.0093324 /

Pedersen

SWOF
-- Sw        Krw         Krow         Pcow
0.200000000  0.000000000  0.900000000  0.000000000
0.231250000  0.001562500  0.791015625  0.000000000
0.262500000  0.006250000  0.689062500  0.000000000
0.293750000  0.014062500  0.594140625  0.000000000
0.325000000  0.025000000  0.506250000  0.000000000
0.356250000  0.039062500  0.425390625  0.000000000
0.387500000  0.056250000  0.351562500  0.000000000
0.418750000  0.076562500  0.284765625  0.000000000
0.450000000  0.100000000  0.225000000  0.000000000
0.481250000  0.126562500  0.172265625  0.000000000
0.512500000  0.156250000  0.126562500  0.000000000
0.543750000  0.189062500  0.087890625  0.000000000
0.575000000  0.225000000  0.056250000  0.000000000
0.606250000  0.264062500  0.031640625  0.000000000
0.637500000  0.306250000  0.014062500  0.000000000
0.668750000  0.351562500  0.003515625  0.000000000
0.700000000  0.400000000  0.000000000  0.000000000
/

--Gas saturation functions

SGOF
-- Sg        Krg         Krog         Pcgo
0.0000000    0.0000000   0.9000000    0.0000000
```

```
0.0375000       0.0007813       0.7910156       0.0000000
0.0750000       0.0031250       0.6890625       0.0000000
0.1125000       0.0070313       0.5941406       0.0000000
0.1500000       0.0125000       0.5062500       0.0000000
0.1875000       0.0195313       0.4253906       0.0000000
0.2250000       0.0281250       0.3515625       0.0000000
0.2625000       0.0382813       0.2847656       0.0000000
0.3000000       0.0500000       0.2250000       0.0000000
0.3375000       0.0632813       0.1722656       0.0000000
0.3750000       0.0781250       0.1265625       0.0000000
0.4125000       0.0945313       0.0878906       0.0000000
0.4500000       0.1125000       0.0562500       0.0000000
0.4875000       0.1320313       0.0316406       0.0000000
0.5250000       0.1531250       0.0140625       0.0000000
0.5625000       0.1757813       0.0035156       0.0000000
0.6000000       0.2000000       0.0000000       0.0000000
/

--Rock properties

ROCK
-- pres cw
14.7 5.0E-6 /

-- Water properties
PVTW

-- pres bw cw vw
14.7 1.0 3.3E-6 0.7 /

-- Standard conditions
STCOND

--Temp Pressure
60 14.7 /

-- Reservoir temperature (deg F)
RTEMP

250 /

-- Equation of State
EOS
PR /

-- Modified Peng-Robinson EoS
-- PRCORR

-- Component names
CNAMES
      N2   CO2    C1   C2   C3
    HC1   HC2   HC3   HC4
    HC5   C36+   Asph
```

```
  /

-- Reservoir EoS properties

-- ... molecular weights

MW
            28.013          44.01     16.043   30.07
            44.097          64.1      96.52    134.556
            245.556         433.542 649.644 649.644    /

-- ... critical temperatures (R)

TCRIT
             227.16              547.56        343.08              549.72
             665.64              796.8618      970.9884          1116.891
             1382.634     1646.541 1846.0458          1846.0458
  /

-- ... critical pressures (psia)

PCRIT
            492.314325    1069.86516       667.19613        708.34479
            615.760305    513.0650064      424.8011307      343.7382705
             209.2115442  133.2922665      105.1348263      105.1348263
  /

ZCRIT
      0.290   0.277   0.264    0.257
      0.245    0.235   0.235   0.236
      0.290   0.277   0.264    0.257    /

--  ... accentric factors

ACF
           0.04     0.225    0.008    0.098
           0.152    0.23027 0.30269 0.40879
           0.72237 1.12962 1.34026 1.34026   /

-- ... binary interaction coefficients

BIC
0.0
-0.02    0.0
0.031    0.103    0.0
0.042    0.13     0.0027   0.0
0.091    0.135    0.0085   0.0017   0.0
0.095    0.13     0.018    0.0069   0.0018   0.0
0.12     0.15     0.0319   0.0164   0.0077   0.0021   0.0
0.12     0.15     0.0471   0.028    0.0163   0.0073   0.0016   0.0
0.12     0.15     0.0833   0.058    0.041    0.0261   0.0137   0.006    0.0
0.12     0.15     0.1166   0.0874   0.0668   0.0479   0.0307   0.0186   0.0036   0.0
0.12     0.15     0.1329   0.1022   0.0802   0.0596   0.0404   0.0264   0.0075   0.0007   0.0 /
```

```
-- Specify initial liquid composition

ZMFVD
1000.0   0.0016 0.020002 0.333633 0.077107 0.073907  0.118313 0.112112 0.083608 0.138178 0.021569
         0.019654968 0.000316
 7500.0  0.0016 0.020002 0.333633 0.077107 0.073907  0.118313 0.112112 0.083608 0.138178 0.021569
         0.019654968 0.000316
/
 -- Asphaltene parameters

ASPFLOC
-- first last floc
   11   11   12 /
--ASPP1P
--'P' /
ASPREWG
-- pres %_wt
1000.0    0.0
2209   0.21 /
-- 2000.0    5.0
--  3900.0   15.0
 --10000.0  100.0
    ... ashphaltene floc rates
-- (set here to cause faster floc degradation than formation)

ASPFLRT
-- CMP6
  0.0000
  0.000  /

-- ... asphaltene deposition

--ASPDEPO
-- adsorp   plug  entrain   Vcr
-- 5.0E-4  1.0E-6  1.0E-4   2500  /

-- ... asphaltene damage ratio

--ASPKDAM
-- deposit  mult
    0.0     1.0
    1.0E-5  0.99
    1.0E-4  0.90
    1.0E-3  0.80
  --  1.0E-2  0.50  /

-- ... asphaltene viscosity change

--ASPVISO
-- vfrac    mult
   0.0     1.0
   0.01    1.2
```

```
   0.12     1.7
   1.0    10.0 /


SOLUTION ============================================================

EQUIL
-- zdat pdat owc pcow goc pcog dummy dummy Ninit

7500 2500 10000 0 4000 0 1 1 1* /
RPTRST

PRESSURE SOIL SGAS SWAT XMF YMF RPORV
ASPADS ASPDOT ASPEN ASPFL ASPKDM ASPLU ASPREW ASPVOM ASPLIM ASPFRD /
SUMMARY ============================================================
FGOR
FWCT
FOPR
FGPR
FWPR
FOPT
FGPT
FWPT
FPR
FOSAT
FGSAT
FLPR
FLPT
PRES
PRESSURE
WPAVE
--BPR
FOVIS
PROD WINJ /
TCPU
ELAPSED
NEWTON

-- Asphaltene grid block parameters
----Asphaltene precipitation fraction (no flocs)
BASPREW
/
----Asphaltene precipitation fraction including flocs
BASPRET
----Asphaltene fraction precipitated and dissolved
BASPFRD
/
RUNSUM
SCHEDULE ============================================================
--Define injection and production wells
WELSPECS
-- Well Group I0 J0 depth phase
WATINJ FIELD 1 1 7500 WAT /
```

```
PROD FIELD 100 1 7500 OIL/
GASINJ FIELD 1 1 7500 GAS /
/
COMPDAT
-- Well I J K1 K2 Status
WATINJ 1 1 1 1 /
PROD 100 1 1 1 /
GASINJ 1 1 1 1 /
/

-- Composition of injected fluid (native oil)
WELLSTRE
-- name N2  CO2  C1  C2  C3  HC1  HC2  HC3  HC4  HC5  C36+  Asph
COMPINJ 0.0 1.0 0.0 0.0 0.0 0.0 0.0 0.0 0.0 0.0 0.0 0.0/
/
WCONPROD
-- Well Status Mode Orat Wrat Grat Lrat Resv BHP
PROD OPEN BHP 1* 1* 1* 1* 1* 1000 /
/
WINJGAS
GASINJ STREAM COMPINJ /
/
WCONINJE
-- Well Type Status Mode Surf Resv BHP
WATINJ WAT OPEN RATE 200 1* 4000/
GASINJ GAS SHUT RATE 2000 1* 1*/
/
TSTEP
1827 /
--TSTEP
1827*1/
--RPTPRINT
1 1 0 0 0 1
TSTEP
0.01 /

-- Switch off producer and start injecting to re-pressurise
WELOPEN
-- Well Status
GASINJ OPEN /
WATINJ SHUT /
PROD OPEN/
/
TSTEP
1200/
--RPTPRINT
1 1 0 0 0 1
TSTEP
0.01 /

END
```

APPENDIX D

Sample CMG/GEM Input File for Asphaltene Precipitation Simulation

```
**-----------------------------------------------------------------------------------------------------------**
*RESULTS *SIMULATOR *GEM
FILENAMES OUTPUT SRFOUT RESTARTOUT INDEXOUT MAINRESULTSOUT
*TITLE1 'Water Flooding'
*TITLE2 'Water injection'
*INUNIT *field

*DIM MDDD 10000
*WRST 0
*WPRN *WELL 1
*WPRN *GRID *TIME
*WSRF *WELL *TIME
*WSRF *GRID *TIME
*OUTPRN *WELL *ALL
*OUTPRN *GRID *PRES *SO *SG *SW *Z 'C36+' *Z 'Asph' *DENO *DENG *SOLID
*OUTSRF *GRID *PRES *SO *SG *SW *Z 'C36+' *Z 'Asph' *DENO *DENG *SOLID *VISO  *VISW
*VISG
*OUTSRF *WELL *PAVG
*SUMMARY
*DIARY *WELL-INFO

**-------------------------------------RESERVOIR & GRID DATA------------
*GRID *CART 100 1 1
*DI *CON 80
*DJ *CON 80
*DK *CON 20
**$ Property: NULL Blocks  Max: 1  Min: 1
**$  0 = null block, 1 = active block
NULL CON           1
*POR *CON 0.3
*PERMI *CON 800
*PERMJ *CON 800
*PERMK *CON 800
*DEPTH  *TOP 1 1 1  7500
**$ Property: Pinchout Array  Max: 1  Min: 1
**$  0 = pinched block, 1 = active block
PINCHOUTARRAY CON           1
*PRPOR *MATRIX 14.7
*CPOR *MATRIX 5.0E-6
**-------------------------------------FLUID PROPERTY DATA--------------
*MODEL *PR
*NC 12 12
*COMPNAME
'N2'   'CO2'   'C1'   'C2'   'C3'
'HC1'   'HC2'   'HC3'   'HC4'
'HC5'  'C36+'  'Asph'
**NUMBER_OF_PVC3_GROUPS     2
*PVC3     0.0
*HCFLAG     0           0           0           0
          0           0           0           0
```

```
        0           0           0           0
*SG       8.0900000E-01  8.1800000E-01   3.0000000E-01
        3.5600000E-01  5.0700000E-01  6.0095000E-01  7.0511000E-01
        7.6365000E-01  8.3611000E-01  9.0576000E-01  9.6071000E-01
        9.6071000E-01
*TB     -3.2035000E+02 -1.0921000E+02  -2.5861000E+02 -1.2757000E+02
        -4.3690000E+01  5.9889000E+01   1.9701900E+02   3.2853600E+02
         6.0960000E+02  9.1233400E+02  1.1358750E+03   1.1358750E+03
*PCRIT     33.5000017     72.8000037       45.40000231      48.20000245
             41.90000213   34.91200177      28.90600147      23.39000119
            14.23600072    9.070000461      7.154000363      7.154000363
*VCRIT     8.9500000E-02  9.4000000E-02    9.9000000E-02
        1.4800000E-01  2.0300000E-01  2.8190000E-01  4.0220000E-01
        5.4850000E-01  9.9920000E-01  1.5873000E+00  1.9562000E+00
        1.9562000E+00
*TCRIT     126.2304.2     190.6     305.4
             369.8          442.701 539.438 620.495
             768.13         914.745 1025.581          1025.581
*AC       0.04     0.225     0.008     0.098
          0.152    0.23027 0.30269 0.40879
          0.72237 1.12962 1.34026 1.34026
*MW        28.013          44.01     16.043   30.07
             44.097        64.1      96.52    134.556
             245.556       433.542 649.644 649.644
*VSHIFT    0.0000000E+00  0.0000000E+00   0.0000000E+00
        0.0000000E+00  0.0000000E+00  0.0000000E+00  0.0000000E+00
        0.0000000E+00  0.0000000E+00  0.0000000E+00 -3.2371946E-13
        7.5124659E-11
*BIN
0.0
-0.02     0.0
0.031     0.103     0.0
0.042     0.13      0.0027   0.0
0.091     0.135     0.0085   0.0017   0.0
0.095     0.13      0.018    0.0069   0.0018   0.0
0.12      0.15      0.0319   0.0164   0.0077   0.0021   0.0
0.12      0.15      0.0471   0.028    0.0163   0.0073   0.0016   0.0
0.12      0.15      0.0833   0.058    0.041    0.0261   0.0137   0.006    0.0
0.12      0.15      0.1166   0.0874   0.0668   0.0479   0.0307   0.0186   0.0036   0.0
0.12      0.15      0.1329   0.1022   0.0802   0.0596   0.0404   0.0264   0.0075   0.0007   0.0
*CW     3.3E-06
*REFPW   14.6960
*ENTHCOEF
        -6.8925000E-01  2.5366400E-01 -1.4549000E-05  1.2544000E-08
        -1.7106000E-12 -8.2390000E-17
         4.7780500E+00  1.1443300E-01  1.0113200E-04 -2.6494000E-08
         3.4706000E-12 -1.3140000E-16
        -5.5811400E+00  5.6483400E-01 -2.8297300E-04  4.1739900E-07
        -1.5255760E-10  1.9588570E-14
        -7.6005000E-01  2.7308800E-01 -4.2956000E-05  3.1281500E-07
        -1.3898900E-10  2.0070230E-14
        -1.2230100E+00  1.7973300E-01  6.6458000E-05  2.5099800E-07
        -1.2474610E-10  1.8935090E-14
```

```
        0.0000000E+00  3.1788100E-02  4.0106200E-04 -5.1310000E-08
        0.0000000E+00  0.0000000E+00
        0.0000000E+00 -1.0912500E-02  4.0732400E-04 -5.6377600E-08
        0.0000000E+00  0.0000000E+00
        0.0000000E+00 -2.5963500E-02  4.1529700E-04 -5.9736400E-08
        0.0000000E+00  0.0000000E+00
        0.0000000E+00 -1.1357500E-02  4.0312700E-04 -5.6066400E-08
        0.0000000E+00  0.0000000E+00
        0.0000000E+00 -5.3676500E-03  3.9727200E-04 -5.4494600E-08
        0.0000000E+00  0.0000000E+00
        0.0000000E+00 -6.9233800E-03  3.9409000E-04 -5.4487700E-08
        0.0000000E+00  0.0000000E+00
        0.0000000E+00 -6.9233800E-03  3.9409000E-04 -5.4487700E-08
        0.0000000E+00  0.0000000E+00

*AQUEOUS-DENSITY  *LINEAR
*OMEGA     0.457235529          0.457235529      0.457235529      0.457235529
           0.457235529          0.457235529      0.457235529      0.457235529
           0.36579      0.36579          0.457235529      0.457235529
*OMEGB     0.077796074          0.077796074      0.077796074      0.077796074
           0.077796074          0.077796074      0.077796074      0.077796074
           0.077796074          0.077796074      0.077796074      0.077796074
*PCHOR     41    78         77         108
           150.3          186.6    279.9    383.4
           649.1          975.4    1158.5   1158.5

**VISCOR **PEDERSEN
*VISCOR *HZYT
*VISVC     8.9500000E-02  9.4000000E-02    9.9000000E-02
        1.4800000E-01  2.0300000E-01  2.8190000E-01  4.0220000E-01
        5.4850000E-01  9.9920000E-01  1.5873000E+00  1.9562000E+00
        1.9562000E+00
**VISCOEFF  0.291 1.0 7.747E-05 4.265 0.8579
*VISCOEFF    0.1023 0.023364 0.058533 -0.040758 0.0093324

**MIXINGRULE  1
*TRES  250
**PHASEID *DEN
**VISCOR *HZYT
**MIXVC     1.0000000E+00
**DERIVATIVEMETHOD *NUMERALL
*VISW  0.7

*SOLIDMODEL
-9.060 1 30000.0 1

**SOLID-CONV-RATE
**10 10

*SOLID_ALPHA   10
*SOLID_BETA    10
*SOLID_GAMMA   10
*SOLID_SIGMA   10
```

**DENROCK 2650.0
**RFMAX 5.0
**WSLMAX 5.0E-04
**ADSCST 0.012
**----------ROCK FLUID DATA----------
*ROCKFLUID
*RPT
*SGT
0.0000000 0.0000000 0.9000000 0.0000000
0.0375000 0.0007813 0.7910156 0.0000000
0.0750000 0.0031250 0.6890625 0.0000000
0.1125000 0.0070313 0.5941406 0.0000000
0.1500000 0.0125000 0.5062500 0.0000000
0.1875000 0.0195313 0.4253906 0.0000000
0.2250000 0.0281250 0.3515625 0.0000000
0.2625000 0.0382813 0.2847656 0.0000000
0.3000000 0.0500000 0.2250000 0.0000000
0.3375000 0.0632813 0.1722656 0.0000000
0.3750000 0.0781250 0.1265625 0.0000000
0.4125000 0.0945313 0.0878906 0.0000000
0.4500000 0.1125000 0.0562500 0.0000000
0.4875000 0.1320313 0.0316406 0.0000000
0.5250000 0.1531250 0.0140625 0.0000000
0.5625000 0.1757813 0.0035156 0.0000000
0.6000000 0.2000000 0.0000000 0.0000000

*SWT
0.200000000 0.000000000 0.900000000 0.000000000
0.231250000 0.001562500 0.791015625 0.000000000
0.262500000 0.006250000 0.689062500 0.000000000
0.293750000 0.014062500 0.594140625 0.000000000
0.325000000 0.025000000 0.506250000 0.000000000
0.356250000 0.039062500 0.425390625 0.000000000
0.387500000 0.056250000 0.351562500 0.000000000
0.418750000 0.076562500 0.284765625 0.000000000
0.450000000 0.100000000 0.225000000 0.000000000
0.481250000 0.126562500 0.172265625 0.000000000
0.512500000 0.156250000 0.126562500 0.000000000
0.543750000 0.189062500 0.087890625 0.000000000
0.575000000 0.225000000 0.056250000 0.000000000
0.606250000 0.264062500 0.031640625 0.000000000
0.637500000 0.306250000 0.014062500 0.000000000
0.668750000 0.351562500 0.003515625 0.000000000
0.700000000 0.400000000 0.000000000 0.000000000
**ROCK DENSITY [LB/CUFT]
**ROCKDEN *CON 2649.999
**----------INITIAL RESERVOIR CONDITION------
*INITIAL
*VERTICAL *ON
*DWOC 10000
*REFDEPTH 7500
*REFPRES 2500

```
**PRES *CON 2500
**SW   *CON 0.2
*ZGLOBALC 'N2' CON      0.0016
*ZGLOBALC 'CO2' CON   0.020002
*ZGLOBALC 'C1' CON      0.333633
*ZGLOBALC 'C2' CON      0.077107
*ZGLOBALC 'C3' CON      0.073907
*ZGLOBALC 'HC1' CON   0.118313
*ZGLOBALC 'HC2' CON   0.112112
*ZGLOBALC 'HC3' CON   0.083608
*ZGLOBALC 'HC4' CON   0.138178
*ZGLOBALC 'HC5' CON   0.021569
*ZGLOBALC 'C36+' CON              0.019654968
*ZGLOBALC 'Asph' CON          0.000316

**SWOC 1
**--------------------------------------NUMERICAL METHOD-----------------
*NUMERICAL        ** Use defaults
**--------------------------------------WELL DATA------------------------
*RUN
*DATE 2000 1 1
DTWELL 0.001
DTMIN 0.01
     *DTMAX 1
**       *WELL 1 'INJ'
**$
WELL  'INJ'
        **    INJECTION AT 250 F
INJECTOR 'INJ'
IWELLBORE  MODEL
**$ wdepth  wlength  rel_rough  whtemp  bhtemp  wradius
   7500.  7500.  0.0001  15.  20.  0.25
INCOMP  WATER
*OPERATE  MAX  STW  200.  CONT
*OPERATE MAX BHP 4000
**       *WELL 2 'PROD'
**$
WELL  'PROD'
PRODUCER 'PROD'
PWELLBORE  MODEL
**$ wdepth  wlength  rel_rough  whtemp  bhtemp  wradius
   7500.  7500.  0.0008  16.  36.  0.25
OPERATE  MIN  BHP  1000.  CONT
AIMWELL WELLN
**$          rad  geofac  wfrac  skin
GEOMETRY  K  0.5  0.64  0.25  0.
PERF  GEO  'INJ'
**$ UBA    ff  Status  Connection
   1 1 1  1.  OPEN    FLOW-FROM  'SURFACE'
**$ UBA     ff  Status  Connection
**$          rad  geofac  wfrac  skin
GEOMETRY  K  0.25  0.64  0.25  0.
PERF  GEO  'PROD'
```

```
**$ UBA      ff  Status  Connection
   100 1 1  1.  OPEN    FLOW-TO  'SURFACE'
*DATE 2000 1   2
*DATE 2002 1   1
*DATE 2003 1   1
*DATE 2004 1   1
*DATE 2004 1   2
*DATE 2005 1   1
*SHUTIN 1
WELL  'INJE'
       **    INJECTION AT 250 F
INJECTOR 'INJE'
IWELLBORE  MODEL
**$ wdepth  wlength  rel_rough  whtemp  bhtemp  wradius
   7500.  7500.  0.0001  15.  20.  0.0762
INCOMP  SOLVENT  0  1.0  0  0  0  0  0  0  0  0  0  0
OPERATE  MAX  STG  2000000.0  CONT
**OPERATE  MAX  BHP 3100
PERF  GEO  'INJE'
**$ UBA    ff  Status  Connection
   1 1 1  1.  OPEN    FLOW-FROM  'SURFACE'
**$ UBA     ff  Status  Connection
**$          rad  geofac  wfrac  skin
*DATE 2005 1   2
*DATE 2006 1   1
*DATE 2007 1   1
*DATE 2008 1   1
     *STOP
```

APPENDIX E

Well A-1 Case Study

The three-dimensional compositional heterogeneous reservoir simulation model for well B-1 was used to model and investigate the impact of asphaltene precipitation, flocculation, and deposition during the primary recovery (pressure depletion), secondary recovery (waterflooding), and tertiary recovery (CO_2 injection) stages on Well A-1. The model was built using the same grid dimension of well B-1, 50 columns × 50 rows × 5 layers, however, 22 hydrocarbon components constituting the crude composition of well A-1 were use instead, the 22 components assumed to remain constant throughout the life of the reservoir. Well A-1 reservoir fluid data are summarized in **Table A3** in Appendix A**.** The injector and producer were positioned in grid 50, 50, 1 and 50, 50, 5, respectively. The initial injection and production plan was based on flooding and draining the reservoir from the five layers. The final base model comprised a total of 12500 grid blocks. The reservoir pressure and temperature are 2500 and 212 ^{o}F, respectively with initial bottomhole pressure of 2200 psi. The asphaltene onset pressure (AOP) used in modeling well A-1 is 2050 psi. Based on the sensitivity analysis applied to well A-1, it was found that the optimum operating production strategy for well A-1 is to deplete the reservoir for one year followed by a six years of waterflooding and finally CO_2 injection for 7 years. The original oil in place is 3.1 million barrels and the oil recovery for each case is shown in **Table E1.**

Table E1: Comparison of Oil Recovery for Well A-1

Cumulative Oil Recovery (STB)	
Without Asphaltene	15.8×10^5 (48%)
With Asphaltene	17×10^5 (55%)

The results of asphaltene deposited mass distributions of the throughout the CO_2 injection stage for the most permeable layer (layer 1) in the reservoir using the 2300 psi BHP. As can be seen that asphaltene deposited mass in the case of CO_2 injection is much higher than the primary recovery and waterflooding stages. **Figure E1** shows the comparison of cumulative oil recovery with and without asphaltene deposition .The recovery factor during CO_2 injection stage has decreased from 27% in the case without precipitation to 12% in the case with precipitation. The reason for this considerable drop in the recovery is attributed to the amount of deposited mass (lb) occurred during the CO_2 injection stage as shown in **Figure E2**. This amount of deposition will induce pore throat plugging, which causes permeability reduction associated with formation damage.

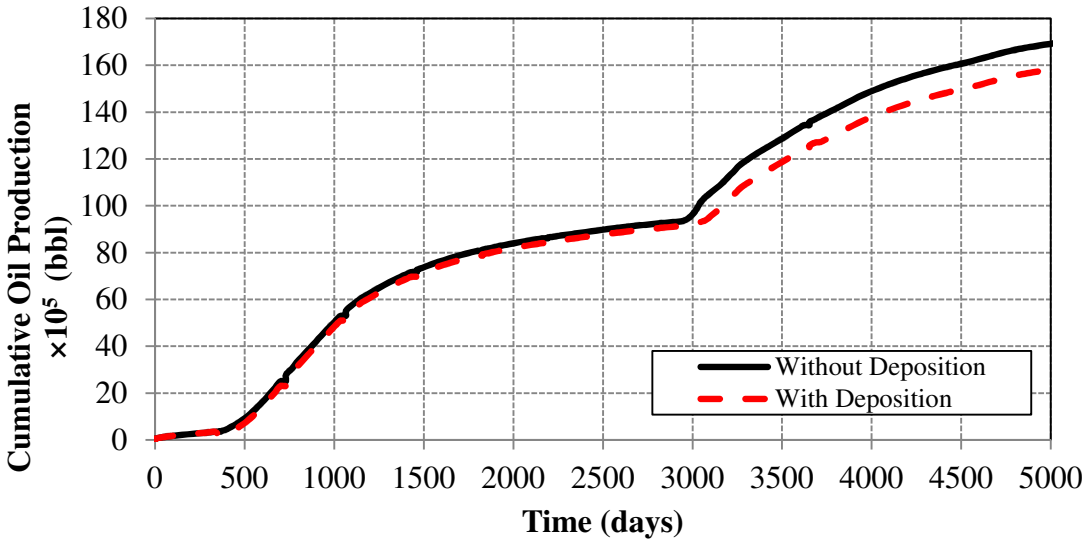

Figure E1: Comparison of Cumulative Oil Recovery With and Without the Deposition Option

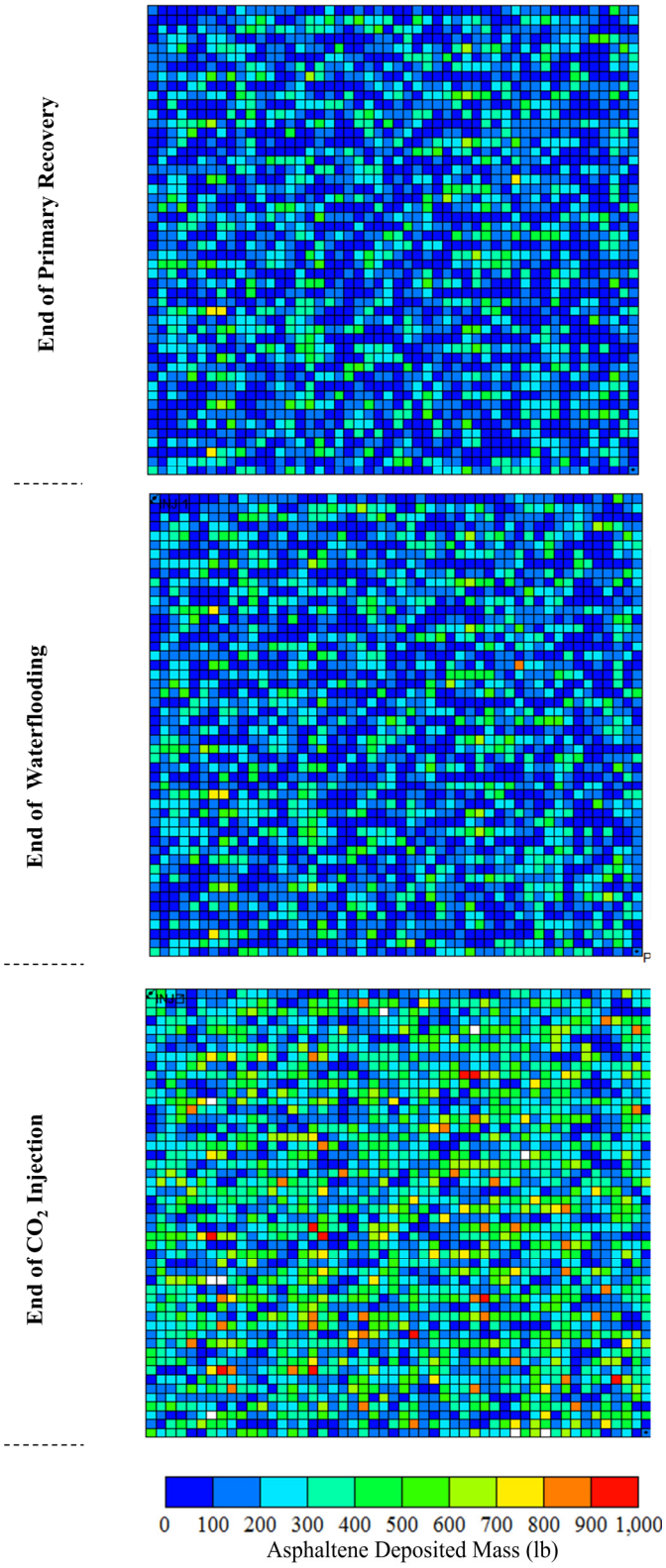

Figure E2: Two-Dimensional View of Asphaltene Deposited Mass (lb) During All Stages

REFERENCES

Abraham, H., "Asphalts and Allied Substances," Van Nostrand, Princeton, NJ, Vol. 1, p. 370, 6th Edition, 1960.

Adewumi, Michael, "https,//www.e-education.psu.edu/png520/m11_p2.html," Petroleum and Natural Gas Engineering, the Pennsylvania State University, 2011.

Adialalis, S.,"Investigation of Physical and Chemical Criteria as Related to the Prevention of Asphalt Deposition in Oil Well Tubing," Ph.D. Thesis, Imperial College, 1982.

Afshari, S., Kharrat, R., and Ghazanfari, M. H., "Asphaltene Precipitation Study During Natural Depletion at Reservoir Conditions," Beijing, China, 8 – 10 June, 2010.

Agarwal, R., Li, Y. K., and Nghiem, L., "A Regression Technique with Dynamic-Parameter Selection for Phase Behavior Matching," SPE 16343, California Regional Meeting, Ventura, California, April 8 – 10, 1987.

Albrecht, C. Von, Salathiel, W. M., and Nierode, D. E., "Stimulation of Asphaltic Deep Wells and Shallow Wells in Lake Maracaibo," Venezuela, 1979.

Allenson, Stephan J., Walsh, Marjorie A., "A Novel Way to Treat Asphaltene Deposition Problems Found in Oil Production," SPE 37286, Oilfield Chemistry Symposium, Houston, February 18 – 21, 1997.

Andrews, A. B., Guerra, R. E., Mullins, O. C., and Sen, P. N., "Diffusivity of Asphaltene Molecules by Fluorescence Correlation Spectroscopy," Journal of Physical Chemistry A 110, No. 26, 8093 – 8097, July 6, 2006.

Asomaning, S. and Watkinson, A. P., "Petroleum Stability and Heteroatom Species Effects in Fouling of Heat Exchangers by Asphaltenes," AICHE Spring National Meeting, 1998.

ASTM D2007-80 Standard Test Method for Characteristic Groups in Rubber Extender and Processing Oils by the Clay-Gel Adsorption Chromatographic Method, ASTM, 1980.

Binshan J., Xiaofeng Q., Jishun Q., and Xinglong C., "Asphaltene Deposition and Its Effects on Production Performances in the Development of Oil Field by CO2 Flooding, A Numerical Simulation Assessment," Barcelona, Spain, 14 – 17 June 2010.

Boduszynski, M. W., "Asphaltenes in Petroleum Asphalts, Composition and Formation," in Bunger JW and Li NC (Eds), Chemistry of Asphaltenes. Washington, DC, American Chemical Society, p.p. 119 – 135, 1981.

Boussingault, M., "MCmoire sur la Composition des Bitumens," Ann. Chemi. Phys., 64, 141, 1837.

Burke, N. E., Hobbs, R. E., and Kashon, S. F., "Measurement and Modeling of Asphaltene Precipitation," Journal of Petroleum Technology, 42, p.p. 1440 – 1446, 1990.

Chilingarian, G. V. and Yen, T. F., "Bitumens, Asphalts and Tar Sands," Elsevier, Amsterdam, Vol. 7. p.p. 153 – 190, 1978

Chukwudeme, E. A., and Hamouda, A. A., "Oil Recovery from Polar Components (Asphaltene and SA) Treated Chalk Rocks by Low Salinity Water and Water

Containing SO_{42-} and Mg_{2+} at Different Temperatures," Colloids and Surfaces A, p.p. 174 –182, 2009.

Chung, T. H., "Thermodynamic Modeling for Organic Solid Precipitation," Presented at the 1992 SPE Annual Technical Conference and Exhibition, SPE 24851,Washington, DC, Oct 4 – 7, 1992.

Cimino, R., Correra S., and Sacomani P.A., "Thermodynamic Modeling for Prediction of Asphaltene Deposition in Live Oil," International Symposium on Oilfield Chemistry, San Antonio, TX, Feb 14 – 17, 1995.

Coats, K. H. and Smart, G. T., "Application of a Regression-Based EOS PVT Program to Laboratory Data," SPE Reservoir Eng., Vol. 1, No. 3, p.p. 277 – 299, May 1986.

Computer Modeling Group, "Win Prop and GEM Manual," 2009.

Creek, J. L., Energy and Fuels, Vol. 19, 1212 – 1224, 2005.

De Boer, R. B., Leerlooyer, K., Engler, M. R. P., and Bergen, A. R. D., "Screening of Crude Oils for Asphaltene Precipitation, Theory, Practice and the Selection of Inhibitors," SPE 24987, Production and Facilities, 1995.

De Pedroza, T. M., Calderon, G., and Rico, A., "Impact of Asphaltene Presence in Some Rock Properties," SPE 27069, Advanced Technology Series, Vol. 4, No. 1, 185 – 191.

Dennis Jr, J. E., Gay, D. M., and Welsch, R. E., "An Adaptive Nonlinear Least-Squares Algorithm," ACM Trans. Math. Software, Vol. 7, No. 3, p.p. 348 – 368, September 1981.

Diallo, M. S., Cagin, T., Faulon, J. L., Goddard, W. A., "Thermodynamic Properties of Asphaltenes, A Predictive Approach Based on Computer Assisted Structure Elucidation and Atomistic Simulation, Asphalts and Asphaltenes II, Development in Petroleum Science," Amsterdam, 2000.

Dykstra, H., Beu, K., and Katz, D. L., "Precipitation of Asphalt from Crude Oil by Flow Through Silica," the Oil and Gas Journal, 79 – 104, Sept. 30, 1944.

ECLIPSE Technical Description, "The Asphaltene Option," p.p. 89 – 102, 2009.

Ellison, B. T. and Gallagher, C. T., "The Physical Chemistry of Wax, Hydrates, and Asphaltene," Houston, Texas, 1 – 4 May, 2000.

Farouq Ali, S.M. and Thomas, S., "Enhanced Oil Recovery," November, 2007.

Figuera, L., Marin, M., Lpoez, L., and Marin, E., "Characterization and Modeling of Asphaltene Precipitation and Deposition in a Compositional Reservoir," SPE 133180, Florence, Italy, 19 – 22 September, 2010.

Flory, P. J., "Thermodynamics of High Polymer Solutions," J. Chem. Phys. 10, 51, 1942.

Freed, D. M, Lisitza N. V., Sen, P. N., and Song, Y. Q., "Molecular Composition and Dynamics of Oils from Diffusion Measurements," Mullins et al., Reference 2, 279 – 300.

Garcia-Hernandez, F. and Sobre, E., "El Control de la Depositacion Organica en Pozos del Area Cretacica Chiapas-Tabasco," Petroleum Engineering Journal, No.7, p. 39, 1989.

Groenzin H., and Mullins O. C., "Molecular Size and Structure of Asphaltenes from Various Sources," Energy & Fuels 14, No. 3, 677 – 684, May, 2000.

Hammami, A., Phelps, C. H., Monger-McClure, T., and Little, T. M., "Energy Fuels," 14(1), 14 – 18, 2000.

Hamouda, A. A., Chukwudeme, E. A. and Alipour Tabrizy, V., "Influence of Temperature on Water and CO_2 Flooding of Asphaltenic Chalk Reservoirs, Experimental and Simulation Case Study," Barcelona, Spain, 14–17 June 2010.

Harin, G. H. and Sage, R. C., "Crude Split Figured by Computer," Hydro. Proc., p.p. 143 –148, April 1969.

Hassan S. Naji., "Feasible C_{7+} Splitting Methods: An Object-Oriented Approach," King Abdulaziz University, Jeddah, Saudi Arabia, International Journal of Engineering and Technology, Vol., 10, No. 1, 2010.

Hirschberg, A., DeJong, L. N. J., Schipper, B. A., and Meijer, J. G., "Influence of Temperature and Pressure on Asphaltene Flocculation," Petroleum Engineering Journal, p.p. 283, June, 1984.

Hortal A. R, Martínez-Haya, B., Lobato, M. D., Pedrosa, J. M., and Lago, S., "On the Determination of Molecular Weight Distributions of Asphaltenes and Their Aggregates in Laser Desorption Ionization Experiments," Journal of Mass Spectrometry 41, No. 7, 960 – 968, July, 2006.

Hutton, A., Bharati, S., and Robl, T., "Chemical and Petrographic Classification of Kerogen/Macerals," Energy and Fuels, Vol. 8, p.p. 1478 – 1488, 1994.

IPIMS, "International Human Resources Development Corporation Website," http://ipims.com/welcome_/portal.asp , 2011.

IPIMS, “International Human Resources Development Corporation Website” From Waples 1981, reprinted with permission of Burgess Publishing Co.

JL, Du and Zhang, “A Thermodynamic Model for the Prediction of Asphaltene Precipitation,” Petroleum Science and Technology 22, No. 7 and 8, p.p. 1023 – 1033, 2004.

Johansson, B., Friman, R., Hakanpää-Laitinen, H., and Rosenholm, J. B., “Solubility and Interaction Parameters as References for Solution Properties II. Precipitation and Aggregation of Asphaltene in Organic Solvents,” Adv. Colloid Interf. Sci. 147 – 148, 2009.

Juan H. and Mansoori, G.A., “Prediction of the Phase Behavior of Asphaltene Micelle and Aromatic Hydrocarbon Systems,” Vol. 16, No. 3 and 4, p.p. 377 – 394, 1998.

Ju, B., China U. of Geosciences; Dai, S., Shengli Oil Field Dongsheng Jinggong Petroleum Development Group Co. Ltd.; Fan,T., China U. of Geosciences; and Wu, H., Li, S. and Zhang, M. Shengli Oil Field Dongsheng Jinggong Petroleum Development Group Co. Ltd. Source SPE Europec/EAGE Annual Conference and Exhibition, Vienna 12 – 15 June, Austria, 2006.

Kawanaka, S., Park, S. J. and Mansoori, G. A., “The Role of Asphaltene Deposition in EOR Gas Flooding,” presented at the SPE/DOE Symposium on Enhanced Oil Recovery, Richardson, TX, February 15 – 17, 1988.

Kennicutt, M. E., Brooks, J. M., and Burke Jr, R. A., “Hydrocarbon Seepage, Gas Hydrates, and Authigenic Carbonate in the Northwestern Gulf of Mexico,” Houston, Texas, May 1 – 4, 1989.

Kokal Sunil, Dawood Naseem, Fontanilla Jerry, Al-Ghamdi Abdullah, Nasr-El-Din Hisham, Al-Rufaie Yousef, "Productivity Decline in Oil Wells Related to Asphaltene Precipitation and Emulsion Blocks," SPE 77767 Presented at the Annual Technical Conference and Exhibition held in San Antonio September 29, 2002.

Koots, J. A. and Speight, J. G., "Relation of Petroleum Resin to Asphaltenes," Fuel, Vol. 54, 79 – 184, July 1975.

Laux, V. H. and Rahimian, I., "Density Investigation of Asphaltenes, Coke Precursors, and Solid Deposits," 116(1), 15 – 17, 2000.

Lee, B. I. and Kesler, M. G., "A Generalized Thermodynamic Correlation Based on Three-Parameter Corresponding States," AICHE J., Vol. 21, p.p. 510 – 527, May 1975.

Leontaritis, K. J., "The Asphaltene and Wax Deposition Envelopes," Fuel Science and Technology International, Vol. 14, No. 1 and 2, 13 – 39, 1996.

Leontaritis. K. J. and Mansoori, G.A, "Asphaltene Flocculation During Oil Production and Processing, A Thermodynamic Colloidal Model," Paper SPE 16258, Proceedings SPE International Symposium on Oil Field Chemistry, San Antonio, Texas, February 4 – 6. 1987.

Marcusson, J., Die Narurlichen and Kunstlichen, "Asphaltene ," Engelmann, Leipzig, 1931.

Merdrignac, I., Desmazières, B., Terrier, P., Delobel, A., and Laprévote, O., "Analysis of Raw and Hydro-treated Asphaltenes Using Off-Line and On-Line SEC/MS

Coupling," Presented at the International Conference on Heavy Organics Deposition, Los Cabos, Baja California, Mexico, November 14 – 19, 2004.

Moore, E. W., Crowe, C. W., and Hendrickson, A. R., "Formation, Effect, and Prevention of Asphaltene Sludges During Stimulation Treatments," JPT, September, 1965.

Mousavi-Dehghani, S. A, Riazi, M. R., Vafaie-Sefti, M., and Mansoori, G. A., "An Analysis of Methods for Determination of Onsets of Asphaltene Phase Separations," Journal of Petroleum Science and Engineering, Vol. 42, p.p. 145 – 156, 2004.

Ngheim, L. X., Kohse, B. F., Ali, Farouq S. M., and Doan, Q., "Asphaltene Precipitation, Phase Behavior Modeling and Compositional Simulation," SPE 59432, Asia Pacific Conference on Integrated Modeling for Asset Management, Yokohama, Japan, 25 – 26 April, 2000.

Particle Engineering Research Center (PERC), University of Florida, 2010

Peng, D. Y. and Robinson, D. B., "A New Two-Constant Equation of State," Ind. Eng. Chem. Fundam., Vol. 15, p.p. 59 – 64, 1976.

Pfeiffer, J. P., "The Properties of Asphaltic Bitumen," Elsevier's publishing Co., New York, 1950.

Prechshot, G. W., Dehisle, N. G., Cottrell, C. E., and Katz, D. L., "Asphaltic Substances In Crude Oil," AIME, Vol. 1, 188-205, 1943.

Qian K., Edwards, K. E., Siskin, M., Olmstead, W. N., Mennito, A. S., Dechert, G. J. and Hoosain, N. E., "Desorption and Ionization of Heavy Petroleum Molecules and

Measurement of Molecular Weight Distributions," Energy and Fuels 21, No. 2, 1042 –1047, March, 2007.

Ray, B. R., Witherspoon, P. A., and Grim, R. E., "A Study of the Colloidal Characteristics of Petroleum Using the Ultracentrifuge," Journal of Physical Chemistry, Vol. 61, 1296 –1302, October, 1957.

Rezaian, A., Kordestany, A. Jamialahmadi, M. and Moghadasi, J., "Modeling Formation Damage Due to Flocculated Asphaltene Deposition Through Dynamic Displacement," China, Beijing, China, 8 – 10 June, 2010.

Rogel, E. and Carbognani L., "Density Estimation of Asphaltenes Using Molecular Dynamics Simulations," Caracas, Venezuela, Energy & Fuels Vol. 717, p.p. 378 – 386, 2003.

Riazi, M. R., and Daubert, T. E., "Simplify Property Predictions," Hydrocarbon Processing, p.p. 115 – 116, March, 1980.

Rodgers, R. P. and Marshall, A. G., "Petroleomics, Advanced Characterization of Petroleum-Derived Materials by Fourier-Transform Ion Cyclotron Resonance Mass Spectrometry," Mullins et al., Reference 2, 63–94.

SOCAR Journal Proceedings, "Remediation of Asphaltene and Other Heavy Organic Deposits in Oil Wells and in Pipelines," April, 2000

Sachanen A. N., "The Chemical Constituents of Petroleum," Reinhold Publishing Co., 1945.

Sanchez, J. H. P. and Mansoori G. A., "Modeling the Behavior of Asphaltene Micelle in Petroleum Fluids," Proceedings of the Second International Symposium on Colloid Chemistry in Oil Production, Brazil, Rio de Janeiro, 1997.

Sanchez, J. H. P. and Mansoori, G. A., "In Situ Remediation of Heavy Organic Deposits Using Aromatic Solvents," Proceedings 5th Latin American and Caribbean Petroleum Engineering Conference and Exhibition, SPE 38966, 1998.

Satou, M., Nakamura, T., Hattori, H., Chiba, T., "Fuel" 79, 1057, 2000.

Schlumberger Oilfield Review, 2007.

Shelton, J. L. and Yarborough, L., "Multiple Phase Behavior in Porous Media During CO_2 or Rich-Gas Flooding," Journal of Petroleum Technology, 1171 – 1178, September, 1977.

Soave, G., "Equilibrium Constants from a Modified Redlich-Kwong Equation of State," Chem. Eng. Sci. 27, 1197, 1972.

Speight, James G. and Moschopedis, Speros E., "On the Molecular Nature of Petroleum Asphaltenes," American Chemical Society, p. 3, 1981.

The National High Magnetic Field Laboratory at Florida State University in Tallahassee "Asphaltene Mass Spectrometry," p. 26.

Thomas, D.C., Becker. H.L. and Del Real Soria, R.A., "Controlling Asphaltene Deposition in Oil Wells," SPE 25483, 679 – 687, 1993.

Ting, D. L., "Thermodynamic Stability and Phase Behavior of Asphaltenes in Oil and of Other Highly Asymmetric Mixtures," Ph.D. Thesis, Rice University, Houston, Texas, 2003.

Tuttle R. N., "High Pour-Point and Asphaltic Crude Oils in Condensates," Journal of Petroleum Technology, No. 6, p.p. 1192 – 1196, 1983.

Twu, C. H., "An Internally Consistent Correlation for Predicting the Critical Properties and Molecular Weights of Petroleum and Coal-Tar Liquids," Fluid Phase Equilibrium. Vol. 16, p.p. 137 – 150, 1984.

Van Gunsteren, W. F., Berendsen, H. J. and Angew, C.,

Vafaie-Sefti, M. and Mousavi-Dehghani, S. A., "Application of Association Theory to the Prediction of Asphaltene Deposition, Deposition Due to Natural Depletion and Miscible Gas," Chem., Int. Ed. Engl. 29, 992, 2006.

Vafaie-Sefti, M., Mousavi-Dehghani, S., and Zadeh, M., "A Simple Model for Asphaltene Deposition in Petroleum Mixtures," Fluid Phase Equilibria. 206, 1 – 11, 2003.

Wang, X., "Simulation of Asphaltene Deposition in Petroleum Reservoir During Primary Oil Recovery," Ph.D. dissertation Thesis, The University of Oklahoma, 2000.

Wang, J. X., Buckley, J. S., Burke, N. E., and Creek, J. L., "A Practical Method for Anticipating Asphaltene Problems," 19 (3), 152 – 160, 2004.

Wargadalam V. J., Norinaga K., and Iino, M., "Size and Shape of a Coal Asphaltene Studied by Viscosity and Diffusion Coefficient Measurements," Fuel 81, No. 11 – 12, P.P. 1403 – 1407, July, 2002.

Watson, A. T., and Lee, W. J., "A New Algorithm for Automatic History Matching Production Data," SPE 15228, the Unconventional Gas Technology Symposium, Louisville, Kentucky, May 18 – 21, 1986.

Yarranton, H. W. and Masliyah, J. H., AICHE J. 41, 3533, 1996.

Yen, T. F., Chilingarian, G. V., "Asphaltenes and Asphalts," Elsevier Science, Vol. 2, 1994.

Yi, T., Fadili, A. and Ibrahim, M., "Modeling the Effect of Asphaltene on the Development of the Marrat Field," SPE 120988, European Formation Damage Conference held in Scheveningen, The Netherlands, 27 – 29, May, 2009.

VITA

Abdulaziz Salem Al-Qasim was born in AlHafouf City, Eastern Province, Saudi Arabia on the 21st of July, 1984. He is the son of Mr. Salem A. Al-Qasim and Mrs. Nadia A. Al-Aqeel. After completing his high school education at Al-Shoqaiq Secondary school. in 2002, he entered King Fahd University of Petroleum & Minerals (KFUPM), Dhahran, Saudi Arabia. He received the degree of Bachelor of Science (B.S.) from KFUPM in June 2007. Between August 2007 and January 2008, he engaged in several ongoing EOR (CO_2 and chemical) projects in the EXPEC ARC Department at Saudi Aramco. Also, between February 2008 and February 2009, he worked as a reservoir engineer for the Southern Area Reservoir Management Department (SARMD) in the Mubarraz area, one of the very mature areas in Ghawar field (the largest oil field in the world). In September 2009, he entered graduate school at The University of Texas at Austin. Abdulaziz was the co-author and presenter of the SPE paper titled, "The Effect of Injected-Water Temperature on Relative Permeability to Oil and Residual Oil Saturation" in the local Young Professional Symposium in March, 2008. He was elected as a member of the Young Professional Regional Steering Committee of 2008, and co-chairperson of the Regional Young Professional Workshop in the Middle East, North Africa and India, 2008 – 2009. He coordinated the Student Outreach Program in SPE Saudi Section, Dhahran, Saudi Arabia, 2008-2009. Abdulaziz is married to Arwa A. Al-Aqeel and has two daughters: Alia (Born July 28, 2008) and Nadia (Born September 6, 2009) and one son: Fahad (Born March 23, 2011)

Permanent Address:

P.O. Box 9616
Dhahran 31311, Saudi Arabia
Email: Qasimas@mail.utexas.edu